Status of thesis

Title of thesis | SYNTHESIS AND CHARACTERIZATION OF CARBON AEROGELS FOR CHROMIUM ION REMOVAL

I, DHALLIA MAMOUN BESHIR MOHAMED

hereby allow my thesis to be placed at the Information Resources Center (IRC) of Universiti Teknologi PETRONAS (UTP) with the following conditions:

1. The thesis becomes the property of UTP.
2. The IRC of UTP may make copies of the thesis for academic purposes only.
3. This thesis is classified as

☐ Confidential

☑ Non – confidential

If this thesis is confidential, please state the reason:

_____

The contents of this thesis will remain confidential for _____ years.

Remarks on disclosure:

_____

Endorsed by

_____
Signature of Author
Permanent Address:
Faculty of Engineering
University of Khartoum
Khartoum, Sudan

Date: _____

_____
Signature of Supervisor
Name of Supervisor:
Dr. Azmi Mohd Shariff

_____
Signature of Co-Supervisor
Name of Co-Supervisor:
Dr. Mohamad Azmi Bustam

Date: _____

UNIVERSITI TEKNOLOGI PETRONAS

Approval by supervisor(s)

The undersigned certify that they have read, and recommend to the postgraduate studies programme for acceptance, a thesis entitled

SYNTHESIS AND CHARACTERIZATION OF CARBON AEROGELS FOR CHROMIUM ION REMOVAL

submitted by

DHALLIA MAMOUN BESHIR MOHAMED

for the fulfillment of the requirements for the degree of

MASTERS OF SCIENCE IN CHEMICAL ENGINEERING

_____

Date

Signature : _____

Main supervisor : AP. Dr. Azmi Mohd Sheriff

Date : _____

Co-Supervisor : AP. Dr. Mohd Azmi Bustam

TITLE PAGE

UNIVERSITI TEKNOLOGI PETRONAS

SYNTHESIS AND CHARACTERIZATION OF CARBON AEROGELS FOR CHROMIUM ION REMOVAL

By

DHALLIA MAMOUN BESHIR MOHAMED

A THESIS

SUBMITTED TO THE POSTGRADUATE STUDIES PROGRAMME

AS A REQUIREMENT FOR THE
DEGREE OF MASTERS OF SCIENCE

CHEMICAL ENGINEERING PROGRAMME

BANDAR SERI ISKANDAR,
PERAK

JUNE, 2009

DECLARATION

I hereby declare that the thesis is based on my original work except for quotations and citations which have been duly acknowledged. I also declare that it has not been previously or concurrently submitted for any other degree at UTP or other institutions.

Signature: _____

Name : DHALLIA MAMOUN BESHIR MOHAMED

Date : _____

DEDICATION

To my mother soul

ACKNOWLEDGEMENT

First and foremost, I would like to thank God the almighty, for without his consent, it would be impossible to achieve what had been done in this work. And I would like to thank my parents and all my family members for their love and support from a distance to go on.

Special acknowledgement goes for my supervisors, AP. Dr. Azmi Mohd Shariff and AP. Dr. Mohamad Azmi Bustam those who pushed me hard to overcome the complications of this project with all of their knowledge, experience and critical thinking.

Thanks and gratitude must be given to the members of Chemical Engineering Department whom contributed their ideas, expertise and advices. Special thanks for Mr. Yousof, Mr. Firdose, Mr. Asnizam, Mr. Tazli, and Mr. Anoar laboratory technologists at Universiti Teknologi PETRONAS Chemical Engineering Department for their great contribution and assistance during all th e experimental part. Thanks are extended for the members of Post Graduate Studies Office for their invaluable help.

The author would like to express her gratefulness to her beloved family, Prof. Mamoun Beshir Mohamed, Sommaya Alnoar Mustaffa, and her sister Mayada Mamoun Beshir, and her brothers, Hani Mamoun Beshir and Beshir Mamoun Beshir, who have never ceased encouraging and supporting her whenever she faced difficulties during the entire research study. Special thanks also go Dr. Abobker Khidir Ziada for his support and help. Thanks also go to my colleagues and friends, whom support and comfort me through the good and bad times.

ABSTRACT

Chromium is one of the heavy metals (HMs) that may cause lung cancer, irritation or damage to nose, throat, eyes and skin at high concentrations. One of the effective separation methods of HMs from aqueous solution is adsorption using carbon aerogels (CAs). These CAs are known to have the potential ability to remove HMs; but to date there is no documented scientific literature on justification, methodologies and practices of chromium removal. Since CAs specific to remove chromium are not commercially available, and CAs development is still in its infancy at the research stage, therefore it is of critical importance to synthesize these CAs before hand in order to satisfy the commercial needs. This is scientifically attainable since CAs work is well developed in many other applications, for instance in the fields of capacitors, insulators, and medical applications.

In this work CAs were synthesized and characterized in order to obtain the best material for the removal of chromium. CAs development is influenced by many factors; one of the most important factors is the catalyst. Three types of catalyst were normally used to synthesis CAs namely sodium carbonate, sodium hydroxide, and acetic acid. In this work CAs were developed by stirring resorcinol, formaldehyde, and water with the selected catalysts. The solutions were then cured in an oven at $85\pm5^{0}C$ for three hours followed by supercritical drying, and finally carbonization at $800^{0}C$ in inert environment. The materials were then characterized in order to understand the parameters affecting the sorption process using x-ray diffraction (XRD) for degree of crystallinity, scanning electron microscope (SEM) for porous surface morphology, nitrogen adsorption tests to obtain Brunauer-Emmett-Teller (BET) surface area and pore size distribution, and Fourier transform infra-red (FTIR) spectroscope for functional group. The results showed that the developed CAs have high surface area and they are porous, amorphous, and have a hydroxyl group which is known to strongly bind metal cations in aqueous solution. The sorption system was found to be affected by the sorbent dose, initial chromium concentration, and the pH of the solution. The kinetic data showed that the sorption

capacity of the three types of carbon aerogels for the chromium increased with increasing initial chromium concentration, while a reverse trend was observed when the effect of sorbent dosage was studied. Analysis of the data obtained from the different sorption studies for the three types of carbon aerogels revealed that the data fitted better to the pseudo-second order model than the first order kinetic model. The results showed that the CA prepared by acetic acid has the highest removal percentage followed by those prepared using sodium hydroxide and finally sodium carbonate. The CAs removal performance was analyzed using two different known isotherm models for solid-liquid interference (Langmuir, and Freundlich). The highest values of linearity error (R^2) were obtained when the experimental data were fitted into Langmuir model.

ABSTRAK

Kromium adalah satu daripada logam berat yang pada kepekatan yang tinggi mampu menyebabkan barah paru-paru, kerengsaan atau kerosakan kepada deria bau, deria penglihatan dan kulit. Satu daripada kaedah penyingkiran logam berat daripada larutan berair yang berkesan adalah dengan menggunakan bahan penyerapan daripada Karbon Aerogel (CA). CA telah dikenali dengan kemampuan dan potensinya sebagai penyingkir logam berat; tetapi sehingga kini masih tiada lagi dokumen ilmiah tentang justifikasi, kaedah-kaedah dan amalan-amalan penyingkiran kromium. Oleh kerana penggunaan CA khusus bagi membuang kromium tidak boleh didapati secara komersial, dan proses memajukan CA masih di peringkat awal penyelidikan, oleh itu adalah sangat penting untuk mensintesis CA bagi memenuhi keperluan pasaran. Ini merupakan kaedah saintifik yang boleh digunakan kerana kerja penghasilan CA boleh dilakukan dengan baik menggunakan banyak aplikasi lain, misalnya dalam bidang kapasitor, penebat-penebat, dan penggunaan perubatan.

Dalam kajian ini CA telah disintesiskan dan dicirikan bagi mendapatkan bahan terbaik untuk penyingkiran kromium. Penghasilan CA dipengaruhi oleh banyak faktor; satu daripada faktor-faktor terpenting adalah pemangkin. Tiga jenis pemangkin yang biasanya digunakan untuk sintesis CA adalah natrium karbonat, natrium hidroksida, dan asid asetik. Dalam kerja ini CA telah dihasilkan dengan mengacau resorsinol, formaldehid, air dan juga dengan memasukkan pemangkin terpilih. Larutan itu kemudiannya dirawat di dalam satu ketuhar pada suhu 85 ± 5^{0}C selama tiga jam diikuti dengan pengeringan kuat, dan akhirnya pengkarbonan pada 8000C dalam persekitaran lengai. Bahan-bahan itu kemudiannya dicirikan bagi mendapatkan parameter yang mempengaruhi seperti proses penyerapan menggunakan x-ray belauan (XRD) bagi darjah penghabluran, mikroskop elektron pengimbas (SEM) untuk morfologi permukaan berliang, ujian penjerapan nitrogen untuk mendapatkan luas permukaan dan taburan saiz liang Brunauer-Emmett-Teller (BET) dan Fourier transform infra-red (FTIR) spektroskop untuk kumpulan berfungsi. Keputusan menunjukkan bahawa CA yang dihasilkan mempunyai luas

permukaan yang besar dan berliang, bersifat amorfus, dan mempunyai satu kumpulan hidroksil yang dipercayai mampu mengikat kation dengan kuat dalam larutan berair.

Sistem penyerapan didapati memberi kesan kepada dos bahan penyerap, kepekatan awal kromium dan pH larutan. Data kinetik menunjukkan bahawa kemampuan penyerapan kromium bagi tiga jenis karbon aerogel bertambah apabila kepekatan kromium bertambah, manakala satu aliran songsang diperolehi daripada kajian kesan dos bahan penyerap. Analisis data yang diperolehi daripada kajian penyerapan tiga jenis karbon aerogel yang berbeza mendedahkan bahawa data lebih serasi kepada model kinetik pseudo-kedua daripada model kinetic pseudo-pertama. Keputusan tersebut menunjukkan bahawa CA yang disediakan oleh asid asetik mempunyai kadar peratusan penyingkiran tertinggi diikuti oleh yang disediakan menggunakan natrium hidroksida dan akhirnya natrium karbonat. Prestasi penyingkiran CA dianalisis menggunakan dua model isoterm yang biasa digunakan untuk campuran pepejal-cecair (Langmuir, dan Freundlich). Nilai tertinggi bagi ralat kelinearan (R^2) telah diperolehi apabila data dimuatkan ke dalam model Langmuir.

TABLE OF CONTENT

LIST OF TABLES

LIST OF FIGURES

NOMENCLATURE

AAS	Atomic Absorption Spectrometer.
BET	Brunauer-Emmett-Teller .
CA	Carbon Aerogel.
C_i	Initial concentration of the metal solutio [mg/L].
C_e	Concentration of the sorbate at equilibrium [mg/l].
C_t	Concentration of the sorbate at time t [mg/l].
CDT	Capacitive deionization technology.
EPA	Enviromental Protection Agency.
FBAU	Fixed bed activation unit.
FTIR	Fourier Transform Infrared.
h	Initial sorption rate.
HM	Heavy metals.
IUPAC	International Union of Pure and Applied Chemistry.
k	Langmuir equilibrium constant [l/mg].
k_l	Freundlich coefficient.
KBr	Potassium bromide.
k_f	Rate constant of pseudo-first order adsorption.
k_s	The overall rate constants of pseudo-second order sorption [(g/mg)/min].
m	Mass of adsorbent [mg].
n	Freundlich coefficient.
P_c	Critical pressure.
q_e	Amount of sorbate sorbed at equilibrium per unit mass of sorbent [mg/g].
q_m	Monolayer sorption capacity at equilibrium [mg/g].
q_t	Amount of sorbate sorbed at time t per unit mass of sorbent [mg/g].
R^2	The linear correlation coefficient of determinations
r_{peak}	Peak radius.
SAXS	Small angel x-ray scattering.
SEM	Scanning Electron Microscopy.
SFE	Supercritical Fluid Extraction.
T	Temperature.
T_c	Critical temperature.

TRI	Toxics Release Inventory
V	Solution volume [ml].
V_{mes}	Mesopore volumes.
XRD	X-ray diffraction.

Chapter 1

INTRODUCTION

1.1 Background

Water is essential to life. Without water, plants and animals will not be able to absorb food substances for their metabolic processes. Without water, it is impossible for most chemical and biochemical processes to occur. Water on earth is mainly produced as a result of atmospheric precipitation. After the water reaches the earth surface, some of the water enters the soil, while the rest may run off the surface. Unfortunately, water from both surface and under-ground sources are susceptible to contamination by heavy metals (HMs). These HMs are mainly released from industrial activities. In the United States, as is the case in most industrialized countries, the greatest source of pollution is the industrial community. According to the 2000 Toxics Release Inventory (TRI) of the U.S. Environmental Protection Agency (EPA), over 6.5 billion pounds of toxic chemicals from about 2,000 industrial facilities are annually released into the environment, including nearly 100 million pounds of recognized carcinogens [www.pollutionissues.com, 2009].

As a result of increasing industrialization, HMs are continuously being released to the environment. As a consequence, wastewater discharged by industrial activities is often contaminated by a variety of toxic and harmful HMs, such as chromium. Chromium is primarily released from process chemical industries like electroplating, leather tanning (chromium sulfate), metal alloys such as stainless steel, cement, and textile industries. Even though chromium occurs in nature mostly as chrome iron ore and is widely found in soils and plants, it is rarely found in natural water. Production of the most water soluble forms of chromium, chromate and dichromates, was in the range of 250,000 tons in 1992. From 1987 to 1993, according to the TRI of the EPA, chromium complex released to land

and water are nearly 200 million pounds [www.epa.gov, 2009]. The increasing presence of chromium in rivers and streams is very problematic due to its high level of toxicity**.** Chromium has been considered as one of the top 16 toxic pollutants [Nameni *et al*., 2008]. Chromium is a threat to human health, where at high concentrations it causes irritation or damage to the nose, throat, eyes and skin and even lung cancer. This has prompted environmental engineers and scientists to concentrate their efforts on analytically studying this problem and develop practical solutions for removal or reduction of the resultant HMs contaminants. The Environmental Protection Agency (EPA) of the United States of America and Enviromental Quality Act 1974 has set permissible contaminant level of 0.05 mg/L for total chromium ion concentration in water [Xu and Zhao, 2007; http://www.lenntech.com, 2009], and of 0.05 mg/L in potable water [Demirbas *et al*., 2004]. According to the European Community Directive 80/778/EEC, L229/20, D48, the maximum allowable concentration of Cr (VI) in industrial wastewater is 0.2 mg/L [Melaku *et al*., 2005]. From the toxicity point of view; and in order to meet the regulatory safe discharge standards, it is essential for industrial complexes to remove HMs from wastewater streams before it is released into the environment.

There are several technologies available to reduce metal ions from wastewater. Some of the most important technologies include filtration, chemical precipitation, ion exchange, adsorption, electrode position, and membrane systems [Pradhan, 2001]. Amongst these technologies, the adsorption process is currently considered to be an attractive option for the removal of HMs from wastewater because of the ease and efficiency with which it can be applied in the treatment of wastewater containing HMs [Goel, 2006]. Adsorption is a process whereby substances (e.g. dissolved solids) are transferred from the liquid phase to the surface of a solid (e.g. adsorbent) and become bounded by physical and/or chemical interactions [Pehlivan, 2008].
Thus in this study, the removal of metal ions from aqueous solutions using activated carbon by the adsorption process is of great interest.

A new form of activated carbon, Carbon Aerogel (CA) has been invented. However, its use for the removal of inorganic (and specifically metal ions) is yet to be widely studied. CAs are unique porous materials with controllable pore size distribution (≤50nm) [Goel *et*

al., 2005; Rana *et al*., 2004], high surface areas (400-900m^2/g) [Tamon *et al*., 1997, 1998, 2000], and high pore volume (1-3 cm^3/g). They are prepared through three different steps: the initial sol-gel chemical reaction where the cross-linked polymer and the wet resorcinol-formaldehyde gel are formed, the drying of the gel and finally the pyrolysis of the organic gel to a carbon aerogel. Every step in the process influences the final structure of the material.

1.2 Problem statement

Wastewater discharge from chemical industrial activities is often contaminated by a variety of toxic and harmful HMs. Most of these metals exert harmful effects on many forms of life. Chromium is one of the HMs that at high concentrations may cause severe damage to human health. One of the effective separation methods of HMs from aqueous solutions is the adsorption method using CA. Although CA is known to have the potential ability to remove HMs, there is no documented scientific literature on the justification, methodologies and practices of its use in chromium removal to date. Considering that CA, which is specific in the removal of chromium is not commercially available, and that the stage of research efforts to develop such material is still in its lab stage, it is of critical importance for the purposes of this study to synthesize CA. This is scientifically attainable since CA is well developed in other applications, such as in the fields of capacitors, insulators and medical applications.

1.3 Objective

The objectives of this study are:

1- To synthesis carbon aerogels suitable for Cr (VI) removal.
2- To characterize these carbon aerogels.
3- To investigate the performance of synthesized CAs for the removal of chromium.
4- To investigate the adsorption isotherm and kinetic behavior of chromium adsorption on the synthesized CAs.

1.4 Scope of the study

The goal of this research is to develop CAs that give the best performance in removing chromium from aqueous solution. To achieve this goal, the following four tasks were carried out:

- CAs were synthesized using three main steps; curing in oven, drying and carbonization;

- physical characterization of synthesized CAs using, x-ray diffraction, scanning electron microscopy, Brunauer−Emmer−Teller and Fourier Transform Infrared to determine crystallinity, functional groups, surface area, pore volume and pore size;

- investigation of chromium adsorption from aqueous solution by the CAs was carried out by studying the influence of contact time, initial chromium concentration, adsorbent dose and pH level on adsorption process performance, and;

- determination of appropriate adsorption isotherm and kinetic parameters of chromium adsorption on these CAs.

Chapter 2

LITERATURE REVIEW

2.1 Introduction

The following is a discussion of previous research and studies that have been conducted on removal techniques, adsorption, adsorbents used in chromium removal as well as CA synthesis and applications. This review is important as the first step in starting this project and in assisting with the setting up of experiments.

2.2 Heavy metal removal techniques

HMs are often found in industrial wastewater and its discharge to the environment poses a serious problem due to its acute toxicity to aquatic and terrestrial life, which includes humans. As a result of industrialization, HMs are continually being released into the environment. In Malaysia there are lots of industries that released chromium in their effluents. According to a statistic study done by Federation of Malaysian Manufactures till 2000, it is found that only in Malcca state there are 13 factories of Textile which are releasing chromium in their effluent [Malaysia environmental quality report, 2004]. In order to protect human health, the Environment Protection Agency (EPA) of The United States of America [http://www.lenntech.com, 2009] as well as Interim National Water Quality Standard (INQWS) and Environmental Quality Act (EQA) 1974 regulations 1979 for Malaysia [Alkarkhi *et* al., 2008] established maximum permissible HMs concentrations in natural waters, these concentrations are listed in Table 2.1. This has provoked environmental engineers and scientists to develop and construct methods for HM removal from wastewater effluents before they are released into the environment in order to meet the set standard regulatory concentrations.

Table 2.1: Maximum permissible concentrations of several HMs in natural waters for the protection of human health [Alkarkhi *et* al., 2008; http://www.lenntech.com, 2009].

Metal	Chemical Symbol	EPA standard, mg/L	Malaysia standard, EQA 1974 (mg/L)	
			Standard A[1]	Standard B[2]
Mercury	Hg	0.000144	0.01	0.05
Lead	Pb	0.05	0.05	0.1
Cadmium	Cd	0.01	0.01	0.02
Chromium	Cr	0.05	0.05	0.05

Many techniques for the removal of HMs from wastewaters are now available. Chemical precipitation, membrane filtration, ion exchange, and adsorption are amongst the most widely used treatment methods for HMs removal. Although some of these methods are successful in removing HMs from wastewaters, they have several disadvantages. The following paragraphs will briefly describe some of these methods with examples.

Chemical precipitation involves the addition of reagents, which will react with dissolved metals and form insoluble or hardly soluble compounds. The more insoluble the compound, the less metal will remain in the solution. Inorganic HMs are removed from aqueous streams by chemical precipitation in various forms such as carbonates, hydroxides and sulfide [Hua *et al*., 2007; Tadesse *et al*., 2006; Guyer, 1998]. It is generally observed that free ions are predominant at low pH levels. At high pH levels however, the complex compounds become more stable due to their low solubility. Therefore, by increasing the pH, HMs will precipitate from solutions in the form of complex compounds. At low metal concentrations, the removal of toxic HMs by precipitation from diluted effluents is economically unviable [Meena *et al*., 2005]. Amongst the problems associated with the use of the precipitation process are; HMs may dissolve in the precipitate formed by change in the environmental conditions such as the pH of the sludge [Kuyucak *et al*., 1995] and also large quantities of sludge are generated causing the precipitate difficult to dewater [Noyes, 1991]. For low metal concentrations, the precipitation process results in incomplete metal removal. This requires high dosage

[1] Standard A: is the limit allowed for effluent to be safely released in to any catchment area.
[2] Standard B: is for effluent to be released in to terrestrial water system.

of chemicals and disposal of the excessive amounts of toxic sludge which adds to the process cost [Volesky, 1990].

The membrane separation method is another technology that seems promising in HMs removal. This method saves energy which is used up in the separation process because of its selective tendency to separate HM ions when they are present at high concentrations [Matheichal and Yu, 1999; Okushita and Shimidzu, 1996]. This process involves the application of a pressure difference through a semi permeable membrane in order to separate a solution into two portions; a concentrated solution and a more diluted one. Cheryan and Rajagopalan (1998) reported some advantages of membrane separation processes which include; no need for addition of chemicals, low energy costs and the plants used in the process can be highly automated without the need of highly skilled operators. Some disadvantages have been reported such as fouling, which occurs due to clogging of the membrane, requiring frequent cleaning operations. Fluctuation in concentration is also not handled well by the membrane, while temperature and pH effects on diffusivity can also cause some setback [http://vienna.bioengr.uic.edu, 2009]. These disadvantages cause some concern and must be addressed entirety when using membrane processes for HMs removal.

Another attractive removal method is the ion exchange technique, known to extract small amounts of impurities from dilute wastewater. This method also permits the recirculation of high quality water for reuse, thus saving on water consumption. However, due to the limited capacity of the ion exchange system, relatively large installation is necessary to provide the exchange capability needed between regeneration cycles. This in turn leads to high operating costs [Solmaz *et al*., 2007; Smith and Means, 1994].

The adsorption process is also one of the most recommended methods used in HM removal. It involves a mass transfer process by which a substance is transferred from the liquid phase to the surface of a solid and becomes bounded by physical and/or chemical interactions [Pehlivan, 2008]. Adsorption has been confirmed to be an excellent way to treat industrial waste effluents, offering significant advantages like low cost, availability, profitability, no difficulty of operation and efficiency [Demirbas, 2008].The advantages of adsorption over other technologies are that no additional sludge is produced, no need

for additional reagents, and the pH of the discharged wastewater stays unchanged [http://www.nhm.ac.uk, 2009].

Out of these techniques the adsorption process is an attractive option for the removal of trace HMs from wastewater. This is due to the quickness, ease and efficiency with which the adsorption process can be applied in the treatment of wastewater containing HMs [Goel *et al*., 2006].

2.3 Adsorption

Adsorption may result from either physical adsorption or chemical interaction between adsorbate and surface of the adsorbent. Physical adsorption on solids is attributed to forces of interaction between the solid surface and adsorbate molecules that are similar to the van der Waals forces between molecules, while chemical adsorption (chemisorption) is a stronger interaction which involves ionic or covalent bonding between the adsorbate and the solid surface. The efficiency of the adsorption process is attributed to many factors related to adsorbent (surface area, particle size, pore structure, and chemistry of the surface) and related to adsorbate (solubility, molecular weight, molecular size, molecular polarity). Systems parameters such as temperature and pH can also influence the adsorption process to the extent that they affect one or more of the parameters mentioned above [Chuah, 2005; Faust *et al*., 1998].

Adsorption isotherms are used to explain the distribution of sorbate between the liquid and solid phase at equilibrium. The concept of 'equilibrium' is established when the amount of solute being adsorbed onto the adsorbent is equal to the amount being desorbed. The adsorption isotherm is significant in order to predict a model for analysis and design of adsorption systems. An isotherm may fit experimental data accurately under one set of conditions but fail totally under another condition. No single theory of adsorption has been put forward to explain all the systems; it mainly depends on the assumptions associated with their respective derivations [Allen *et al*., 2004]. The Langmuir and Fruendlich isotherm models are widely used to describe the adsorption phenomena at the solid–liquid interface [Oladoja, 2008; Aber *et al*., 2007; Rahman, 2007; Goel *et al*., 2006; Meena *et al*., 2005; Allen *et al*., 2004; Akinbayo, 2000].

The Langmuir isotherm (which fits the equation developed by Langmuir) assumes monolayer sorption on to the homogeneous surface with a specific number of equivalent sites. A basic hypothesis is that sorption takes place at specific homogeneous sites within the adsorbent. Once a molecule occupies a site, no more adsorption can take place at that site. This equation is thermodynamically following Henry's Law at low concentrations. The Freundlich isotherm model assumes that as the adsorbate concentration increases the concentration of adsorbate on the adsorbent surface increases resulting in multi-layer adsorption [Oladoja *et al*., 2008; Rahman, 2007; Allen *et al*., 2004]. The Freundlich equation agrees well with the Langmuir equation over moderate concentration ranges, but the Freundlich isotherm does not reduce to Henry's law at low concentration [Benmaamar and Bengueddach, 2007; Allen *et al*., 2004].

2.4 Adsorbent

The adsorption technique uses different types of adsorbent for the removal of HMs. Some of these adsorbents were applied for chromium removal such as wheat bran, sugarcane bagasse, saw dust, dead fungal biomass, formaldehyde condensate coated silica gel, activated alumina, activated charcoal and activated carbons. The paragraphs below will briefly report the main findings.

Nameni *et al*. (2008) studied the performance of wheat bran in chromium removal. The study found that the adsorption reached equilibrium after 60 min and after that a little change of chromium removal efficiency was observed. The higher chromium adsorption was observed at lower pH levels, and maximum chromium removal (87.8 %) was obtained at pH level of 2 and initial chromium concentration of 5 mg/l. The study also found that the adsorption of chromium by wheat bran decreased at the higher initial chromium concentration and lower adsorbent doses. The study showed that the adsorption follows Langmuir isotherm equation, and the kinetics of the adsorption process follows the pseudo second-order kinetics.

Khan and Mohamad (2007) used sugarcane bagasse in order to study the chromium removal. The study showed that the removal was effective at low pH values and low chromium (VI) concentrations. The removal efficiency was found to be 70.2 % at the initial chromium concentration of 10 mg/L, pH level 1 and 4 hours contact time, but when

the metal concentration was increased to 70 mg/L the removal efficiency dropped to 19 %. Their study also found that the adsorption data fitted well with Freundlich isotherm.

Baral *et al*. (2006) studied the performance of using sawdust in chromium removal. The study found that the percentage of adsorption increased with decrease in pH and showed maximum removal in the pH level range 4.5–6.5 for an initial concentration of 5 mg/L, adsorbent amount of 0.6 g and time of 1hr at 30 ^{o}C. Their study found that the adsorption data fitted well to the Langmuir adsorption isotherm and pseudo second order reaction model. Rice hull ash was also used as an adsorbent by Wang and Lin (2009). Their main finding was that the adsorption data followed Freundlich model better than Langmuir model.

Park *et al*. (2005) investigated the efficiency of dead fungal biomass in chromium removal. Their study found that the removal rate increased with a decrease in pH and with an increase in chromium concentration, biomass concentration and temperature. The study also found that the initial chromium removal rate exhibited pseudo first order dependence.

Kumara *et al*. (2007) used formaldehyde condensate coated silica gel for chromium removal; they found that the chromium adsorption followed Freundlich's isotherm with adsorption capacity of 65 mg/g at initial chromium concentration of 200 mg/L, and total chromium adsorption followed second order kinetics and the equilibrium was achieved within 90–120 min.

Mor *et al*. (2007) investigated the removal of chromium ions from aqueous solution under different conditions (adsorbent dose, contact time, pH, temperature and initial chromium concentration) using activated alumina and activated charcoal as adsorbents. The study found that the activated alumina had high percentage of removal at pH level of 4, whereas that of the activated charcoal was at pH level of 2. They also reported that the maximum adsorption was found at 25 ^{o}C for activated alumina, and at 40 ^{o}C for activated charcoal. The study also found that the percentage of removal increased with increasing adsorbents dose and decreasing the initial chromium concentration. Furthermore their study showed good fits to both Freundlich and Langmuir adsorption isotherms.

Activated carbons with their microporous character, large surface area, and the chemical nature of their surface have made them prospective adsorbents for the removal of HMs from wastewater. Many researchers discussed the performance of many types of activated carbons in chromium removal. Demirbas *et al*. (2004) investigated the performance of three types of activated carbons (cornelian, apricot stone and almond shell) in chromium ion removal. The study found that the adsorption of the chromium was highly pH-dependent and the results showed that the optimum pH level for the removal was found to be 1, and the kinetics of the chromium adsorption on the different adsorbents was found to follow pseudo second order rate equation. The study found that the activated carbon from almond shell was the most effective one with a removal percentage of 99.9 %. Okparanma and Ayotamuno (2008) used commercial activated carbon for chromium removal; the equilibrium was reached in a contact time of 60 min. The study found that the removal percentage at equilibrium was 78.6 % with using 10 g/L amount of adsorbent, and the adsorption data were found to be better fitted to Freundlich isotherm than Langmuir model. Karthikeyan and Ilango (2008) investigated the performance of three types of activated carbon prepared from indigenous materials. Their study found that the three types were a good adsorbent for chromium. The study also found that the removal percentage depended on the adsorbent dosage, contact time, co-ions, temperature and pH. The highest chromium adsorption was 96% at pH 3. The equilibrium data were found to have good agreement with Freundlich isotherms model. Acharya *et al*. (2008) studied the performance of activated carbon developed from Tamarind wood in chromium ion removal. Their main findings were that the percentage removal of chromium increased with increasing adsorbent dosage and decreased with increasing initial chromium concentration. Their experimental results were better fitted with Freundlich (R^2=0.996) adsorption isotherm model than Langmuir model (R^2=0.995), and the kinetics of the chromium adsorption on the activated carbon was found to follow pseudo second order equation. Table 2.2 summarizes the adsorbents used for chromium ion removal.

A new form of activated carbon, CAs, has invented but their use for the removal of inorganic (and specifically metal ions) has not widely been studied [Goel *et al*., 2005, 2006]. Adsorption using CAs is capable of removing some toxic species such as cadmium, lead, mercury, copper, nickel, manganese and zinc [Goel *et al*., 2005, 2006; Meena *et al*., 2005; Kadirvelu *et al*. 2008].

Table 2.2: A summary of the adsorbent used for chromium ion removal

Adsorbent	Authors	Remarks
Wheat bran	Nameni *et al*. (2008)	The study found that adsorption follows Langmuir isotherm equation. Kinetic showed the applicability of pseudo second-order model.
Bagasse	Khan and Mohamad (2007)	The removal percentage decreased with initial chromium concentration increased. And the removal was effective at low pH values and low chromium concentrations.
Sawdust	Baral *et al*. (2006)	The study showed a maximum removal in the pH level range 4.5–6.5 for an initial concentration of 5 mg/L, adsorbent amount of 0.6 g. Their study found that the adsorption data fitted well to the Langmuir adsorption isotherm and pseudo second order reaction model.
Rice hull ash	Wang and Lin (2009)	They found that the adsorption data followed Freundlich model better than Langmuir model.
Dead fungal biomass	Park *et al*. (2005)	Their study found that the removal rate increased with a decrease in pH and with an increase in chromium concentration, biomass concentration and temperature. The study also found that the initial chromium removal rate exhibited pseudo first order dependence.
Formaldehyde condensate coated silica gel	Kumara *et al*. (2007)	They found that the chromium adsorption followed Freundlich's isotherm. And the kinetic showed that the data were better fitted to second order model.
Activated alumina and activated charcoal	Mor *et al*. (2007)	They reported that the maximum adsorption was found at 25 ^{o}C for activated alumina, and at 40 ^{o}C for activated charcoal. The study also found that the percentage of removal increased with increasing adsorbents dose and decreasing the initial chromium concentration. Furthermore their study showed good fits to both Freundlich and Langmuir adsorption isotherms.
Activated carbon	Demirbas *et al*. (2004)	The kinetics of the chromium adsorption on the different adsorbents was found to follow pseudo second order rate equation.
	Okparanma and Ayotamuno (2008)	The study found that the removal percentage at equilibrium was 78.6 % with using 10 g/L amount of adsorbent, and the adsorption data were found to be better fitted to Freundlich isotherm than Langmuir model.
	Karthikeyan and Ilango (2008)	The study also found that the removal percentage depended on the adsorbent dosage, contact time, co-ions, temperature and pH. The equilibrium data were found to have good agreement with Freundlich isotherms model.
	Acharya *et al*. (2008)	Their main findings were that the percentage removal of chromium increased with increasing adsorbent dosage and decreased with increasing initial chromium concentration. Their experimental results were better fitted with Freundlich, adsorption isotherm model, and the kinetics of the chromium adsorption on the activated carbon was found to follow pseudo second order equation.

2.5 Carbon aerogels

CAs are organic aerogels that are usually prepared by a poly condensation reaction of two organic materials in an aqueous solution. Pekala was the first to develop CAs in the late 1980s using resorcinol and formaldehyde as main reactants and water as a solvent [Pekala, 1989].

Qin and Guo (2001) prepared organic aerogel based on resorcinol, formaldehyde and alcohol instead of water. The main purpose of their research was to eliminate the time spent in the solvent exchange step by using alcohol as a solvent. As a result, they found that both the products and their carbonized derivatives had typical nano porous structure with low density.

Li *et al*. (2002) synthesized CA using cresol, resorcinol, and formaldehyde as bases with sodium hydroxide (NaOH) as a basic catalyst. The CA that was produced had 0.92 g/cm^3 density and surface area of 400-700 m^2/g. The study found that both the shrinkage and mass loss upon pyrolysis of the mixed aerogels increased with increasing cresol content. Hwang and Hyun (2004) synthesized organic aerogel and CA using resorcinol, formaldehyde, water as solvent and sodium carbonate (Na_2CO_3) as catalyst. The CAs had high surface area (400–700 m^2/g), low density (0.40–1.16 g/cm^3) and fine pore size (<50nm). Zhang *et al*. (2002) explained the sol-gel process when resorcinol-formaldehyde was used as shown in Figure 2.1.

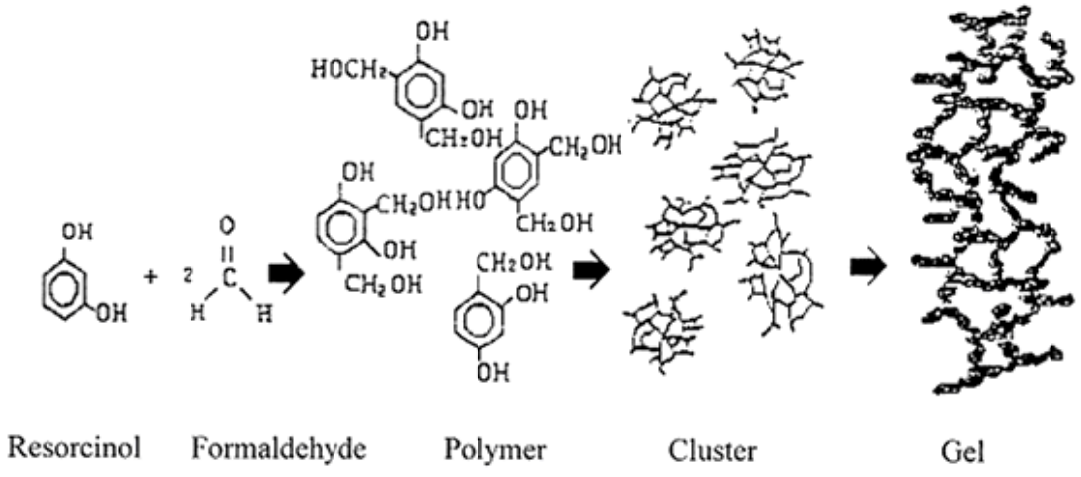

Figure 2.1: Typical sol gel process from Zhang *et al*. (2002).

Since the 1980s, vast amount of research has been carried out in the area of developing CA. It was found that CA could be produced from different precursors, such as phenol and furfural. According to Wu and Fu (2005), CA can be produced from phenol and furfural by adding hydrogen chloride (HCl) as a catalyst. The produced CA had high surface area of 507-561 m^2/g and large micro pore volumes and small mesopore volumes relative to their organic aerogel precursors.

Wu and Fu (2005) also established that the increase in the phenol-furfural concentration (10-70 wt %), and the HCl/phenol ratio (1.5-6 wt ratio) or the phenol/furfural ratio (1:1.5-1:3 wt ratio) helped to increase hydrogen ion (H-ions) concentration of the initiative reaction system. This accelerated the sol-gel poly condensation rate, which eventually led to an increase of the gelation ability of the phenol-furfural system. This study also showed that besides higher H-ions concentration, the increase in the phenol-furfural concentration (10-70 wt %) also led to a higher sol particle concentration and thus increased the colliding chance of the sol particles. This helped in reducing the required gelation time. The experimental results also reported that the most important factor for bulk density tailoring is the phenol-furfural concentration, where bulk density increases (0.23-0.63 cm^3/g) with the phenol-furfural concentration (40-70 wt %). Many other studies were also successful in producing CA using furfural and phenolic as the main reactants [Pekala *et al*., (1994); Zhang *et al*., (2003); Wu and Fu, (2006)].

Wu and Fu (2006) further improved the method of preparing phenol-furfural aerogels and related CAs. The sol gel polymerization is divided into two steps; the formation of gel precursors by pre polymerization of phenol-furfural with NaOH as a catalyst and subsequently the gelation of the precursors with HCl as a catalyst. It was found that a proper increase in the cross-link density of the gel precursors by pre polymerization with NaOH as a catalyst helped to increase the yield of CA. It also led to an increase of the mesoporosity, leading to an increase in the bulk density of CAs. This process however, showed a decrease in the particle size of the CA.

The reaction of formaldehyde with resorcinol can be similar to phenol but the reactivity is completely different and therefore the products formed from the reaction can be different. Durairaj (2005) conducted studies comparing the reactivity of resorcinol against various phenolic compounds. Table 2.2 summarizes the reaction rate of formaldehyde with

different phenolic derivatives including resorcinol. Assuming that the reactivity of phenol consists of one hydroxyl group and no presence of other substituents[3] in the benzene ring with formaldehyde equal to one, the reactivity of other phenol derivatives was compared.

Table 2.3: Relative reaction rates of phenolic compounds with formaldehyde from Durairaj (2005).

Phenolic compound	Comparative rate
Phenol	1
p-Methyl phenol	0.35
o-Methyl phenol	0.26
m-cresol	2.88
3,5-Dimethyl phenol	7.75
Resorcinol	12.2

From Table 2.2, it is observed that the resorcinol has high reactivity compared to phenol. Thus, resorcinol can undergo all the typical reactions of phenol at a much faster rate. This condition is due to the enhanced electron density at the 2-, 4-, and 6-positions. Based on the findings of this section, it can be concluded that the use of resorcinol is better than that of phenol in synthesizing CAs.

2.6 Carbon aerogel synthesis

Parameters such as catalyst, water, drying methods and gelation temperature may have some effects on the properties of the produced CA. This section will discuss these factors briefly.

2.6.1 Resorcinol to formaldehyde ratio

Tamon *et al*. (1997) studied the effect of resorcinol to formaldehyde ratio on the porous structure of CA by using resorcinol/catalyst = 200 and resorcinol/water= 0.11, and changed resorcinol/formaldehyde as 0.25, 0.29, 0.34, 0.40, 0.50, 0.67 and 1.0, but they

[3] A substituent is an atom or group of atoms substituted in place of a hydrogen atom on the parent chain of a hydrocarbon [http://dic.academic.ru/dic.nsf/enwiki/489938, 2009].

could not dry the aquagel for resorcinol/formaldehyde = 1.0 because the sol did not gel enough. The study found that the resorcinol/formaldehyde did not affect the BET surface area, but it affected the mesopore volumes (V_{mes}) and the peak radius (r_{peak}) of the pore size distribution. The study found that V_{mes} and r_{peak} were small for resorcinol/formaldehyde <0.34, and large for resorcinol/formaldehyde >0.40. They found that the mesoporous resorcinol-formaldehyde aerogels were produced under the conditions of resorcinol/formaldehyde =0.4-0.7.

2.6.2 Catalyst ratio

Saliger *et al*. (1998) investigated the effects of catalyst ratio on the porosity of CAs. The study used small-angle x-ray scattering and nitrogen adsorption to study the structure as a function of resorcinol/catalyst molar ratio, under conditions of high resorcinol/catalyst values of 1000 and 1500 molar ratio. The study reported that the amount of catalyst controls the size of the particles constituting the gel network. It was also found that particle growth could be further enhanced if the reaction temperature was kept low and gel time was increased. In another paper, Saliger *et al*. (1998) found that the average pore diameter increased from 20 nm to about 100 nm with increasing resorcinol/catalyst ratio. Despite some errors in the absolute values due to inaccessible pores, a tendency towards increasing pore sizes with rising resorcinol/catalyst ratio could have been clearly observed. If the high resorcinol/catalyst molar ratio was used, it could have influenced the particle size from a few nanometers up to micrometers (2μm) as was found by Bock *et al*. (1998).

With the catalyst ratio increased, the particles which make up the solid network become bigger [Saliger *et al*., 1998; Job *et al*., 2005; Bock *et al*., 1998; Tamon and Ishizaka, 1998; Shen *et al*., 2005]. This is due to the slow sol gel process, which gives enough time for the grains to grow larger [Zhang *et al*., 2002]. If the resorcinol/catalyst decreases, the carbon nano particles and the pore size will also decrease [Wu *et al*., 2005]. Tamon *et al*. (1998) reported that as the resorcinol/catalyst molar ratio increased the porous structure of the aerogel became more dispersed.

The pore size distribution becomes wider as the amount of catalyst decreases (resorcinol/catalyst ratio increases). The shape of the gyratory radii of the primary

particles increases with increasing catalyst ratio. While the form of the particles that constitute the resorcinol-formaldehyde hydrogel was spherical at the catalyst ratios of resorcinol/catalyst at 50 and 200, it was disc shaped at the catalyst ratio of resorcinol/catalyst at 1000 [Horikawa *et al*., 2004].

Jimenez *et al*. (2006) prepared different CAs resorcinol-formaldehyde base by using alkaline carbonates and organic acids. The study found that for the same resorcinol/water molar ratio CA samples prepared under acidic conditions were denser than those prepared using alkaline carbonates as a catalyst. Barndt *et al*. (2004) prepared CAs using acetic acid as a catalyst with different resorcinol/catalyst molar ratios (0.13, 0.3, 5, and 1300). The study found that the produced CAs had high densities (300-1000 kg/m^3). They compared CAs prepared by using base catalyst and acetic acid and found that CA produced by using acetic acid with resorcinol/catalyst=0.3 have larger mesopore surface area than the base-catalyzed one with resorcinol/catalyst=1300. However they had a comparable density (250–300 kg/m^3) and particle sizes (120 and 37 nm), respectively.

2.6.3 Gelation temperature

The gelation temperature of resorcinol-formaldehyde hydrogels does not greatly influence the mesoporous properties of resorcinol-formaldehyde aerogel [Tamon and Ishizaka, 1998]. According to Wiener *et al*. (2004), the pore diameters of resorcinol-formaldehyde aerogels decrease as the gelation temperature increases. Wu *et al*. (2004) found that if the gelation process was at first carried out at an ambient temperature of 303 K, and then at a higher temperature of 348 K, the resultant hydrogels would be more stable and could better resist shrinkage during the ambient pressure drying process. The gelation temperature widely used in literature ranged between 85 to 90 ^{o}C and the duration between 6 to 7 days [Liu *et al*., 2006; Fabry *et al*., 2004].

2.6.4 Drying methods

There are several methods to dry the resorcinol-formaldehyde hydrogel such as supercritical drying, freeze drying and evaporative drying. Supercritical drying leads to the highest pore volume and the widest texture range. Freeze drying leads to surface tensions and shrinkage because the gels with small pores do not remain frozen throughout

the drying period. Evaporative drying is suitable when dense carbons are needed or when the only selection criterion is pore size [Job *et al*., 2005]. Tonanon *et al*. (2006) used a microwave oven to dry CA. The study showed that drying using the microwave oven had several advantages including non-heating from the outside, faster drying rate and lower operational cost. Unfortunately, the CAs produced had poor porous properties.

Czakkel *et al*. (2005) prepared three types of aerogels by supercritical drying, freeze drying and evaporating drying. The gels produced from supercritical drying had an intermediate value of surface area 1000 m^2/g. The one produced from freeze drying had the highest surface area, but was not structurally stable. The measured surface area decreased with time. The gels produced from evaporative drying displayed the lowest specific surface area [Czakkel *et al*., 2005].

The properties of the CAs produced by supercritical drying were more sensitive to the synthesis and processing conditions [Zanto *et al*., 2002]. However, in order to preserve the skeleton of the gels and to minimize their shrinkage during drying, it was necessary to remove the solvent from the gels under supercritical conditions [Tamon *et al*., 1997]. The pore liquid, which was usually an alcohol or acetone according to the preparation conditions, was used as the supercritical fluid. A temperature and pressure of about 250 ^oC and 7 MPa respectively were needed to put these solvents in the supercritical state. Problems arose from the compensation of high temperature, high pressure and flammability of the solvents [Husing and Schubert 2005]. An alternative to drying in organic solvents is the use of liquid carbon dioxide (CO_2). This method has the advantage of a very low critical temperature (T_c=31 °C) at a moderate critical pressure (P_c=7.4 MPa). Another requirement is the miscibility of the pore liquid with carbon dioxide. For example, water and CO_2 are immiscible. Therefore, an intermediate solvent exchange (e.g. water against acetone) is necessary. Figure 2.2 below represents the supercritical drying bath, at the critical point (T_c, P_c) the density of the liquid and the gas are equal. Supercritical drying can be performed along path A or B [Husing and Schubert, 2005].

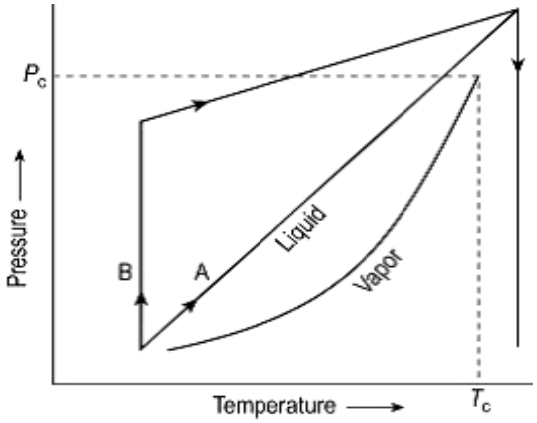

Figure 2.2: Schematic representation of the principle of supercritical drying [Husing and Schubert, 2005].

Liang *et al*. (2000) made a comparison on the basic physical properties between an RF aerogel from supercritical acetone drying and an resorcinol-formaldehyde aerogel from supercritical CO_2 drying. The study reported that the shrinkage and density of the RF aerogel from supercritical acetone drying were larger than those of the RF aerogel with supercritical CO_2 drying. The study also found that the examination of the materials obtained by scanning electron microscopy, transmission electron microscopy and FT-infrared spectroscopy showed similar data to those of the resorcinol-formaldehyde aerogel prepared by supercritical CO_2 drying. However, Horikawa *et al*. (2004) found that supercritical drying with CO_2 was very important for generating mesopores in the resorcinol-formaldehyde CAs.

On average, the CAs synthesized by supercritical drying exhibited the highest surface area compared to the ones synthesized by using freeze drying and evaporative drying. Using supercritical drying with CO_2 was considered to be better than using alcohol and acetone. This is due to the high temperature and pressure required for setting these two solvents (alcohol and acetone) into supercritical conditions.

2.6.5 Water

Job *et al*. (2005) conducted an experiment to study the influence of water on the characteristics of pores. The result of the experiment showed that whatever the resorcinol/catalyst value, the total pore volume increased with the increase in dilution

ratio[4]. The total pore volume of a sample with dilution=5.7 is 2.1 cm^3/g is twice smaller as in a sample with dilution=20 at 4.4 cm^3/g. When resorcinol-formaldehyde aerogel was prepared under the condition of low resorcinol to water ratio, its macro pore volume becomes larger [Tamon and Ishizaka, 1998].

Fabry *et al*. (2004) made a comparison between using acetone and water as a solvent in the production of resorcinol-formaldehyde gel. The study found that when acetone was used as a solvent, the solubility of the base catalyst was poor. This was because it was only soluble in the water coming from the formaldehyde solution. Therefore, the phenolate intermediate form was not stable and the formation of hydroxymethyl groups was slow. The gelation time in acetone was also much longer than in water because of the solubility problems mentioned above and the lower degree of the gelation temperature (50 °C in acetone instead of 85 °C in water).

2.7 Carbon aerogels techniques and analyses

CAs are mesoporous materials with high surface areas [Tamon *et al*., 1997], obtained by pyrolyzing the resorcinol-formaldehyde aerogels in an inert atmosphere [Tamon *et al*., 1998]. Nano porous solids are generally characterized by their surface area and/or by their pore volume [Dolle *et al*., 2005].

2.7.1 Surface morphology

The surface morphology of CAs is usually determined using the scanning electron microscope (SEM) [Czakkel *et al*. 2005; Wu *et al*. 2004; Hwang and Hyun 2004; Brandt *et al*. 2003; Merzbacher *et al*. 2001; Liang *et al*. 2000]. The surface chemistry is usually investigated by using infrared spectrum (IR) [Jirglov *et al*. 2009; Guilminot *et al* 2007; Brandt *et al*. 2003; Liang *et al*. 2000]. The CAs structure is determined by using x-ray diffraction (XRD) [Du *et al*. 2007; Wu and Fu 2005]. Pore structure is usually investigated by using gas adsorption isotherm as well as small angel x-ray scattering (SAXS).

[4] Dilution ratio is the ratio between water and resorcinol, formaldehyde, catalyst [Tamon and Ishizaka, 1998].

The analysis of gas adsorption isotherm helps in determining the micropore volume and pore size of CAs. The six IUPAC standard adsorption isotherms are shown in Figure 2.3; they differ because the systems demonstrate different gas/solid interactions.

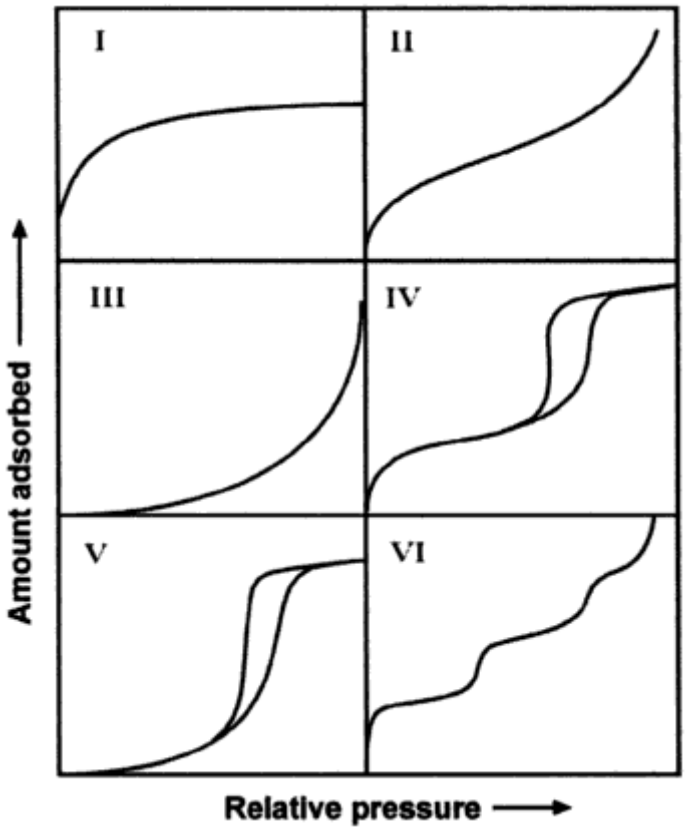

Figure 2.3: The IUPAC classification for adsorption isotherms [from Lowell *et al.*, 2004].

The Type I isotherm is typical of microporous solids and chemisorption isotherms. Types II and III are shown by finely divided macroporous adsorbents with strong and weak adsorbate-adsorbent interactions. Type III and type V are typical of vapor adsorption (i.e. water vapor on hydrophobic materials). Type IV and V present a hysteresis loop generated by the capillary condensation of the adsorbate in the mesopores of the solid. Finally, the rare type VI represents stepwise multilayer adsorption on a uniform surface [Lowell *et al., 2004*].

Reichenauer *et al*. (1998) prepared CA by pyrolysis of resorcinol-formaldehyde gels with a resorcinol/catalyst mole ratio of 200 and used them in order to study the effects of density (120-620 kg/m^3) and pyrolysis temperature (1050-2100 °C) on the CA

microporosity. The analysis was made using SAXS and CO_2 adsorption. They found that the micropore size and volume deduced from SAXS data were almost independent of bulk density, while adsorption of CO_2 was significantly smaller for higher aerogel densities. Upon increasing the pyrolysis temperature from 1050°C to 2100°C, a drastic enlargement of the structure on all the lengths of the scale was observed by SAXS. Simultaneously, the micro pore volume accessible to CO_2 almost vanished, indicating the evolution of closed micro pores. Hanzawa *et al.* (1998) measured the adsorption isotherms of nitrogen on CAs at 77 K. The study found that the predominant pores in the CAs were mesopores and the percentage of micropores was in the range of 5 to 10% of the total pore volume. Czakkel *et al.* (2005) synthesized three types of CAs by varying the drying method. The prepared CAs had different surface areas; these surface areas were calculated using Brunauer Emmett Teller (BET) model based on nitrogen adsorption isotherm data.

2.8 Carbon aerogels applications

CAs have attractive properties such as high porosity (80–98%), controllable pore structure, high surface area (400-900 m^2/g), remarkable electrical conductivity (25–100 S/cm), and thermal and mechanical properties [Tamon *et al.*, 1997; Wu *et al.*, 2006; Li *et al.* 2007]. All of these properties make them promising materials for application in adsorption and as catalysts [Castilla and Hodar, 2005]. Moreover, CAs can also be used in capacitive deionization technology (CDT) water treatment (Figure 2.4), hydrogen generation and oxygen generation

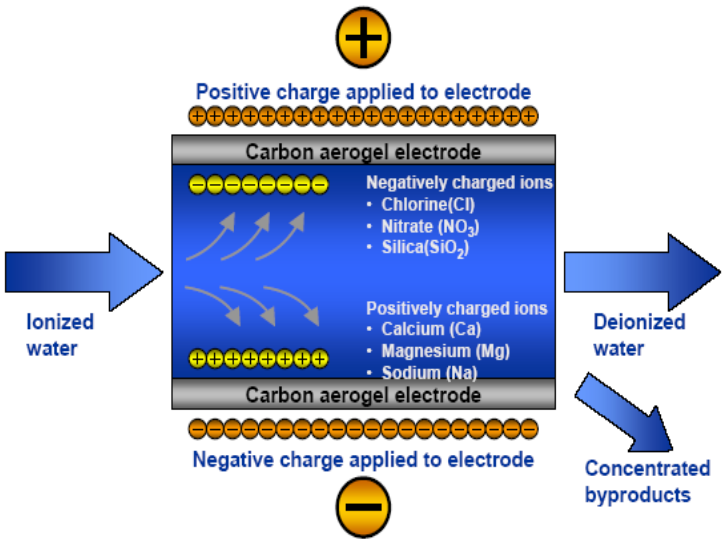

Figure 2.4: Use of CDT in water treatment **[**Source: www.cdtwater.com, 2008**]**

CAs can also be used as electric double layer capacitors and materials for chromatographic separation [Tamon and Ishizaka, 1998; Gavalda *et al*., 2002], medical applications (controlled drug delivery system and drug targeting) [Tonanon *et al*., 2006], supercapacitors electrodes with large inner surface areas [Saliger *et al*., 1998], high electrical conductivity [Saliger *et al*., 1998] and high specific volume capacitance [Li *et al*., 2002].

Guilminot *et al*. (2007) prepared cellulose-based CAs and used them as a catalyst to support polymeric electrolyte membrane (PEM) fuel cell electrodes applications. Aerogels have low thermal conductivity thus suitably used as thermal insulators, for example in refrigerators or heat storage devices [Gavalda *et al*., 2002]. Figure 2.5 below presents a comparison of the thermal insulation properties of aerogels with some commercially available insulating materials [Husing and Schubert, 2005].

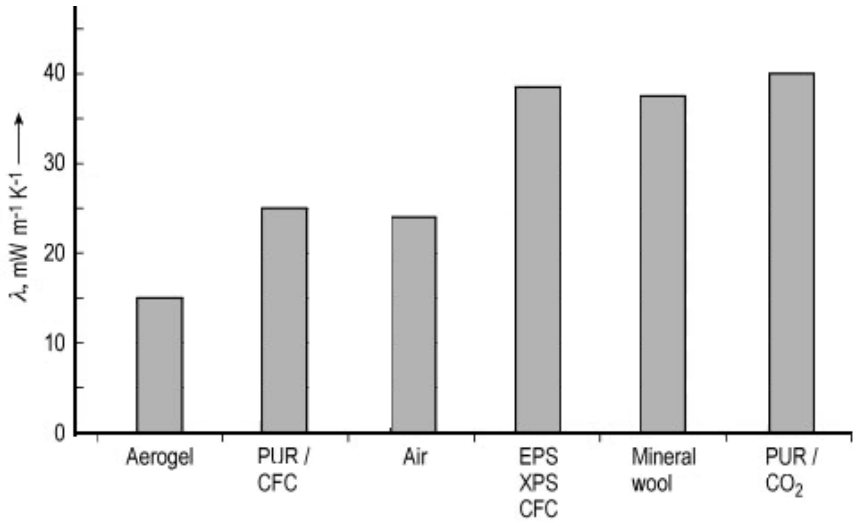

Figure 2. 5: Comparison of thermal insulation properties amongst commercially available insulating materials (PUR≡ polyurethane foam; CFC ≡ chlorofluorocarbons; EPS, XPS ≡ expanded and extruded polystyrene) [Husing and Schubert, 2005].

2.8.1 Carbon aerogel in HM removal

Currently, there have only been a few studies [Goel *et al*., 2005; Meena *et al*., 2005; Kadirvelu *et al*., 2008] on the use of CAs in adsorption of HMs from wastewater. These studies investigated the performance of CAs in removing mercury, cadmium, lead,

copper, nickel, manganese, and zinc. The following paragraphs summarize the parameters which affected the HMs performance using CAs.

2.8.1.1 Parameters which affect the performance of CAs in HM removal

Parameters like pH levels, HM concentrations, temperature, and CA dosages have some effects on the adsorption performance.

pH is one of the important parameters controlling uptake of HMs from aqueous solutions. The pH affects the hydrolysis of metal ions, resulting in the formation of metal hydroxide at high pH levels which precipitate and lead to low removal percentage [Yu, 1995; Meena *et al*., 2005; Rahman, 2007; Goel, 2006]. At lower pH levels, the metal is present predominantly as metal ions in the adsorptive solution; there is a competition between H^+ and metal ions for adsorption at the ion-exchangeable sites, leading to a low removal of metal. The optimum pH level was found to be varying from one metal to another [Goel *et al*., 2005; Meena *et al*., 2005; Rahman, 2007]. The HMs concentration also affects the adsorption performance where the percent removal of HMs depends on the initial metal ion concentration and decreases with increase in initial metal ions concentration; this is because at high concentrations the numbers of HM ions are relatively higher compared to availability of adsorption sites [Meena *et al*., 2005; Rahman, 2007]. The effect of temperature on the adsorption of HMs was found to be proportional, as the temperature increased the adsorption increased. That is because with the temperature being increased the thickness of the boundary layer surrounding the adsorbent decreased, so that the mass transfer resistance of the adsorbate in the boundary layer decreases [Meena *et al*., 2005]. CA dosages have a paramount effect on the HM removal. The amount of CA affects the available exchangeable sites and the surface area which in other words affects the adsorption performance [Meena *et al*., 2005; Yu, 1995].

Meena *et al*. (2005) studied the removal of mercury, cadmium, lead, copper, nickel, manganese, and zinc by using CA as an adsorbent material. The study reported that the percentage of HMs removal depended on the initial metal ion concentration, which decreased with the increase in the initial HM ion concentration. It also depended on the adsorbent dose where the removal of HMs increased rapidly with the increase in the dose of adsorbents. For the same initial concentration of HMs, their percentage removal was

increased with the increase of contact time until equilibrium was attained. This study also found that at a constant initial metal concentration of 3 mg/L, adsorbent dose of 10 g/L and agitation period of 48h for all HM ions at varying pH on CA, the percentage adsorption increased with pH. It attained a maximum level at pH 6 for copper, nickel and zinc, whereas, for lead at pH 7 and for cadmium at pH 4. And thereafter the percentage decreased with further increases in pH.

Goel *et al.* (2005) used CA in removing mercury from aqueous solutions. The studies found that the amount of Hg (II) adsorbed by CA increased from 65% to 90% with the increase in temperature from 20 to 70 °C. The optimum condition for maximum removal was found at pH = 5.0 - 7.0 and adsorbent mass = 0.1 g and temperature = 70 °C. Goel *et al.* (2005) further studied the removal of three metal ions, mercury, lead, and nickel, onto CA. They investigated the metal ions removal using different parameters such as agitation time, metal ions' concentration, adsorbent dose and pH. The study found that increasing the initial solution pH level (2-10) and carbon concentration (50-500 mg per 50 ml) increased the removal of all three metal ions. The kinetic study showed that the pseudo second order kinetic model correlated well with the experimental data and better than the pseudo-first order model, where the thermodynamics study showed that the sorption was significantly increased with increasing the temperature.

Goel *et al*. (2006) studied the efficiency of removing cadmium using CA. The main findings were that the isotherm adsorption of Cd (II) followed the Langmuir model and the adsorption kinetics studies showed that the pseudo second order equation was better able to describe the adsorption of the cadmium ion than the first order equation of Lagergren .The studies also reported that the adsorption capacity from the Langmuir model was 15.53 mg/g for Cd (II) at an initial solution pH of 5.0.

The removal of lead, mercury and cadmium in mono- and multi-component (binary and tertiary) systems were investigated by Kadirvelu *et al*. (2008). The study found that the perfect adsorption of these metals in a single system was in the order of Hg (II) > Pb (II) > Cd (II). However, in binary and tertiary systems the sorption was suppressed by the presence of other metal ions in aqueous solutions.

2.9 Conclusion

HMs from industrial complexes and other pollutants are very toxic to human and other forms of life and the ecological environment in general. It is of paramount importance to take all the necessary measures to reduce their concentration in the environment. Definite attention must be given and serious work must be embarked upon to take out or lessen the dangers of industrial wastewater and other polluted water threats. There have been many instances where HMs discharge in wastewater has caused serious problems to the environment such as in Yamuna River, a major tributary of the river Ganges in India, where many casualties of birds and fishes were reported due to the disposal of untreated wastewater [Rawat *et al*. 2003]. This and similar situations of uncontrollable presence of harmful and poisonous HMs in the environment threatened life and endangered all living species large or small and hence alarmed many scientists, public servants and the general public. However, this problem can be resolved by effective treatment prior to discharge of polluted water into the environment. To date, past studies generally concentrated on taking out the HMs via adsorption. Moreover, it is distinctly clear from the findings of this literature review that the work in the area of adsorption of HMs, including chromium, using CAs is insufficient. Apart from Goel *et al*. (2005), Meena *et al*. (2005), Goel *et al*. (2006) and Kadirvelu *et al*. (2008) there are no other studies relating to the removal of chromium using adsorption by CAs. Therefore, this project aims to study the performance of CAs in removing chromium using the adsorption process.

Chapter 3

METHODOLOGY

3.1 Introduction

Generally in the field of scientific experimentation it is important to describe in detail the experimental setup and the analytical methods followed up and used in all experiments. In this work and in order to achieve the objectives of this thesis, the methods, materials and experimental set ups can be divided into three main categories as follows; (1) The synthesis of carbon aerogels. (2) The kinetic study of chromium removal using the produced carbon aerogels. (3) The equilibrium isotherm study of chromium ions on the carbon aerogels. Materials, experimental set ups and procedures for each category were as follows:

3.2 Materials used in these experiments

The materials used throughout this experimental study were acquired from different sources. Resorcinol, formaldehyde, sodium hydroxide, acetic acid, and acetone were acquired from MERCK, whereas sodium carbonate was from R&M Chemicals and sodium dichromate 2-hydrate was from HmbG Chemicals.

3.3 The synthesis of carbon aerogels

Carbon aerogels in aqueous solution were prepared using resorcinol (C_6H_4 $(OH)_2$) and formaldehyde (HCHO) [Brandt *et al*., 2003; Merzbacher *et al*., 2001; Czakkel *et al*., 2005]. In order to prepare a porous CA acetic acid, sodium carbonate and sodium hydroxide were used. These CAs were prepared by following three consecutive main

steps; the first step was preparation of resorcinol-formaldehyde hydrogels (RF hydrogels), the second step was preparation of resorcinol-formaldehyde aerogels (RF aerogels), and the third step was preparation of carbon aerogels (CAs) (Figure 3.1). The procedure used here was following Tamon *et al*. (1997, 1998) recommendations.

3.3.1 The first step: Preparation of RF hydrogels

3.3.1.1 *Using sodium carbonate*

Stoichiometric ratio of resorcinol/formaldehyde=0.5, constant mole ratio of resorcinol /water=0.125 and resorcinol/catalyst=400 were used. First the resorcinol, water, and sodium carbonate were mixed and stirred in a beaker until the mixture became a homogeneous solution. The formaldehyde was then added and the solution stirred for 1hr. The synthesized solution was sealed and heated in an oven at 85 ± 3^{0}C for 7 days. Then RF hydrogels were produced.

3.3.1.2 *Using sodium hydroxide*

The mole ratios and the synthesis procedure were same as mentioned above, but with changing the catalyst from sodium carbonate to sodium hydroxide.

3.3.1.3 *Using acetic acid*

This one was prepared in an aqueous solution by using a resorcinol/formaldehyde=0.5, and resorcinol/catalyst=0.3. Then the solution was stirred and placed in an oven under the same conditions as the sodium carbonate samples.

3.3.2 The second step: Preparation of RF aerogels

The RF aerogels were prepared by leaving the RF hydrogels to cool at room temperature (23 ^{o}C) and replacing the water in the RF hydrogels with acetone. The RF hydrogels were left immersed in acetone for 3 days. The acetone was then extracted by supercritical drying with CO_2 using the Supercritical Fluid Extraction (SFE) unit.

3.3.3 The third step: Preparation of CAs

In this third step the RF aerogels were carbonized under nitrogen flow (30 ml/min) in a Fixed Bed Activation Unit (FBAU) to produce carbon aerogels. The samples were then heated up to 800°C and maintained at 800°C for 3 hrs after which they were cooled to room temperature. The FBAU is equipment used to carbonize the CAs and it is mentioned in details in section 3.6.2.

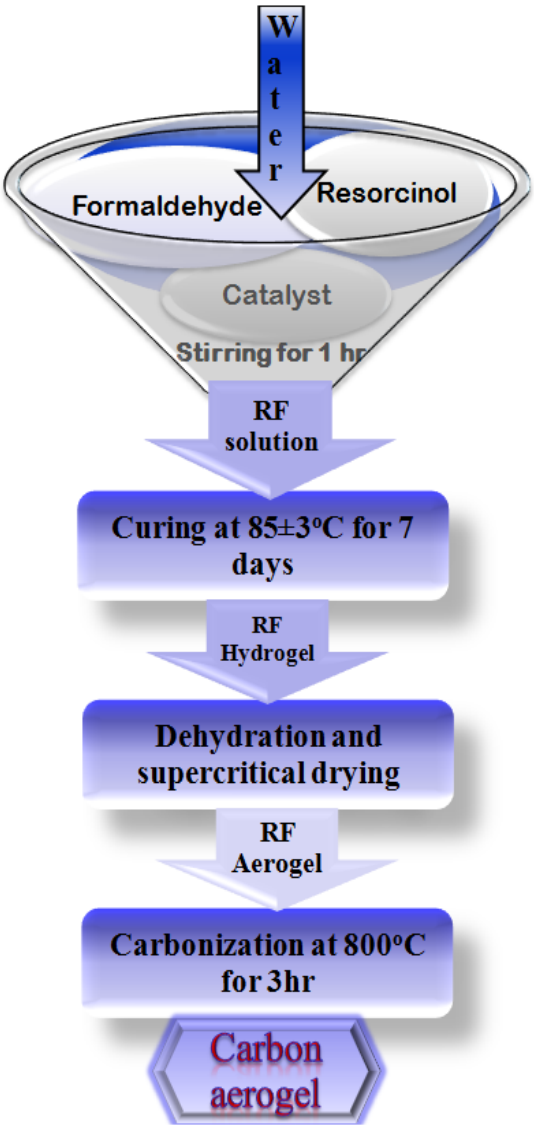

Figure 3.1: Flow chart of synthesis carbon aerogels

3.4 Kinetic study of chromium removal

In order to understand the variables that influence the sorption of solutes it is necessary to study the kinetics of sorption process. Batch kinetic experimental work was carried out to

study the effects of pH, initial chromium concentration, and loading of carbon aerogels versus time [Meena *et al*., 2005]. The summary of the kinetic study conducted in this research work is given in Figure 3.2. In each experiment 25 ml of metal ion solution was used (Figure 3.2). All experiments were executed at ambient room temperature (23 ^{o}C). The concentrations of chromium solutions before and after adsorption were measured by atomic adsorption spectrophotometer [Meena *et al*., 2005; Kadirvelu *et al*., 2008]. Fixed pH 5 was chosen since it gives the best removal percentage of chromium (section 4.5.3), whereby 30 ppm and 0.05 g were used throughout the kinetic study since they provide better presentation of chromium removal from aqueous solution.

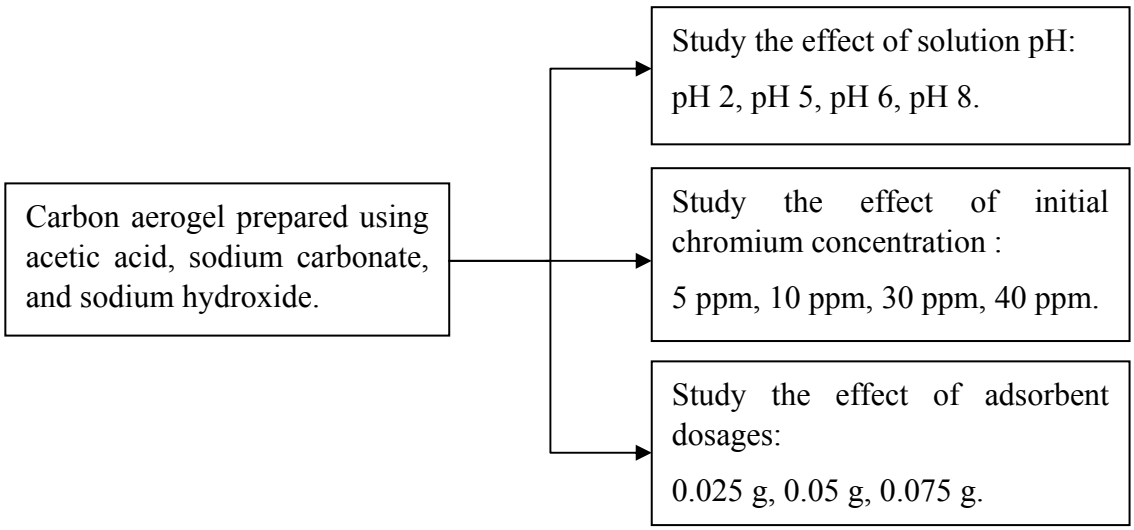

Figure 3.2: Summary of kinetic study using the three types of carbon aerogels

3.4.1 Effect of initial metal ion concentration on sorption process

Batch experiments were conducted under constant pH level (pH= 5), ambient temperature (T= 23 ^{o}C) and agitation rate (120 rpm) but with different initial chromium ion concentrations (5, 10, 30, 40 ppm). The samples were taken after 0, 2, 6, 16, 36, 60, and 120 min. The experiments were conducted under a fixed amount of adsorbent (0.05 g) using carbon aerogels (which were prepared using acetic acid, sodium carbonate, and sodium hydroxide).

3.4.2 Effect of adsorbent dose on sorption process

The dependence of chromium removal on the three types of carbon aerogels was studied at room temperature (23 ^{o}C) at a fixed pH level (pH= 5), initial chromium concentration (30 ppm) and agitation rate (120 rpm). Varying amounts of the sorbents (0.015, 0.025, 0.05 g) were used, while keeping the volume of the chromium solution constant (25 ml). Samples of chromium solution were then taken after 0, 2, 6, 16, 36, 60, and 120 min from the starting time of the experiments. These samples were then analyzed to determine the concentration of the remaining chromium solution using atomic adsorption spectroscopy.

3.4.3 Effect of pH on sorption process

One of the most important parameters controlling uptake of heavy metals from wastewater and aqueous solutions is the solution pH [Meena *et al*., 2005; Rahman, 2007]. This is because the adsorption process depends on the nature of the adsorbent surface and adsorbate species distribution of the ions in aqueous solution, both of which in turn mainly depend on the pH of the solution. These studies were conducted at a constant initial metal ions concentration of 30 ppm, adsorbent dose 0.05 g, agitation rate 120 rpm for all carbon aerogels at various solution pH levels (pH 2, 5, 6, and 8) and different time intervals (0, 2, 6, 16, 36, 60, and 120 min).

3.4.4 Stock and standards solutions

The standard solutions of chromium were prepared using a calibration standard solution (supplied from Fisher Scientific) at concentrations of 1, 2, 3, and 4 ppm. These standard solutions were used in obtaining the calibration curves.

3.4.5 Mathematical models for Kinetic study

In order to observe the sorption process of chromium onto the adsorbents under different experimental conditions, two mathematical models were proposed, pseudo- first and second order models.

The linearised form of the pseudo-first order equation is generally expressed as follows [Meena *et al*., 2005; Goel *et al*., 2006; Abdullah *et al*., 2006; Oladoja, 2008]:

$$\log(q_e - q_t) = \log q_e - \frac{k_f}{2.303} \times t \quad \text{..... (3.1)}$$

Where,

q_t ≡ Sorption capacity at time t (mg/g).

k_f ≡ Rate constant of pseudo-first order adsorption (min^{-1}).

q_e ≡ Sorption capacity at equilibrium (mg/g) and it can be calculated by equation 3.2.

t ≡ Time of adsorption (min).

$$q_e = \left(\frac{C_i - C_e}{m} \times V \right) \quad \text{..... (3.2)}$$

Where,

C_e ≡ Concentration of the sorbate at equilibrium (mg/l).

C_i ≡ Initial concentration of the sorbate (mg/l).

m ≡ Mass of adsorbent (g).

V ≡ Solution volume (l).

The pseudo-second order kinetics, represented by the linear equation presented below [Goel *et al*., 2006; Abdullah *et al*., 2006; Oladoja *et al*., 2008], was also used to test the experimental data.

$$\frac{t}{q_t} = \frac{1}{k_s q_e^2} + \left(\frac{1}{q_e} \right) \times t \quad \text{..... (3.3)}$$

Where,

k_s ≡ The overall rate constants of pseudo-second order sorption ([g/mg]/min).

The initial sorption rate can be obtained from the pseudo-second order linear plots, as q_t/t approaches zero using equation 3.4:

$$h = k_s q_e^2 \quad \text{..... (3.4)}$$

Where,

h ≡ Initial sorption rate.

k_s ≡ The overall rate constants of pseudo-second order sorption ([g/mg]/min).

3.5 The equilibrium isotherm study

In order to study the equilibrium relationship between the concentration of the chromium in the fluid phase and its concentration in the carbon aerogels at constant temperature, pH, and amount of adsorbent, equilibrium isotherm experiments were conducted. Isotherms were drawn by finding out the amount of metal ions adsorbed onto the carbon aerogels versus time in different initial metal concentrations. The initial metal ion concentrations for each adsorbent used were 5, 10, 30, and 40 ppm. The experiments were carried out at room temperature (23 ^{o}C). Initial experiment was found that the equilibrium was attained in 3 days and no significant change on the adsorption percentage was observed up to 5 days; hence 3 days were chosen for the equilibrium period. Agitation was provided by a shaker at a rate of 120 rpm for 3 days. After stirring, samples were filtered through a Whatman-filter paper and subsequent clear solutions were diluted to the range of the standard solutions; then they were taken for determination of the metal ion concentration using an atomic adsorption spectrometer. Two of the most widely used adsorption isotherms equations (i.e. Langmuir, and Freundlich isotherm equations) were employed to describe the observed sorption phenomena of these studies for each adsorbents solution [Akinbayo, 2000; Rahman, 2007; Meena *et al*., 2005; Oladoja, 2008; Goel *et al*., 2006].

3.5.1 Langmuir isotherm model

The Langmuir adsorption isotherm is derived from considerations based upon the assumption that the uptakes of metal ions occur on a homogenous surface by monolayer adsorption without any interaction between the adsorbed ions. The Langmuir adsorption isotherm equation is represented in equation 3.5 [Fabre *et* al., 2003; Jusoh *et al.*, 2005; Aber *et al*., 2007].

$$q_e = \frac{q_m k C_e}{1 + k C_e} \quad \text{(3.5)}$$

The linerized form is presented in equation 3.6.

$$\frac{1}{q_e} = \left[\frac{1}{k.q_m}\right]\frac{1}{C_e} + \left[\frac{1}{q_m}\right] \quad \text{(3.6)}$$

Where,

C_e ≡ Concentration of the sorbate at equilibrium (mg/l).

q_e ≡ Amount of sorbate sorbed at equilibrium per unit mass of sorbent (mg/g).

q_m ≡ Monolayer sorption capacity at equilibrium (mg/g).

k ≡ Langmuir equilibrium constant (l/mg).

3.5.2 Freundlich isotherm model

The Freundlich isotherm model describes a multi-layer adsorption with the assumption of presence of a heterogeneous surface. The model can be presented in equation 3.7 [Oladoja *et al.*, 2008; Rahman, 2007].

$$q = k.C_e^{1/n} \quad \text{(3.7)}$$

And the linearized form can be written as in equation 3.8.

$$\log q_e = \log k_l + \left(\frac{1}{n}\right)\log C_e \quad \text{(3.8)}$$

Where,

C_e ≡ Concentration of the sorbate at equilibrium (mg/l).

q_e ≡ Amount of sorbate sorbed at equilibrium per unit mass of sorbent (mg/g).

k_l, n ≡ Freundlich coefficients.

3.6 Experimental apparatus

This section will describe the analytical instruments which were used throughout this study in order to synthesize the carbon aerogels, study their surface morphology and crystallinity, determine the changes in the functional groups before and after removal studies, adjust the pH levels, and measure the chromium concentration in solutions. In

order to measure the liquids (formaldehyde, water) used throughout this study a micrometer pipette was used.

3.6.1 Supercritical Fluid Extraction (SFE)

The supercritical fluid extraction unit was used in order to dry the hydrogels supercritically to remove the acetone in a controlled way without causing the gel to collapse. This was done using CO_2 under 45 ^{0}C and 200 bars for 3 hours. This was performed by using ISCO SFX 220 SFE model (Figure 3.3).

Figure 3.3: The supercritical fluid extraction unit

3.6.2 Fixed bed activation unit (FBAU)

The fixed bed activation unit (Figure 3.4) was used to carbonize the RF aerogels in order to produce carbon aerogels. The carbonization step was performed using nitrogen gas (30 ml/min) at 800 ^{o}C for a period of three hours.

Figure 3.4: The fixed bed activation unit

3.6.3 pH Meter

A pH meter is an electronic instrument used to measure the pH (acidity or alkalinity) of a liquid. The concept of pH is a means of quantitatively expressing the degree of the hydrogen ion concentration in a solution. In these series of experiments the pH measurements of all aqueous samples were performed with MP230 pH meter (Figure 3.5). The pH meter was standardized using buffer solutions with the following pH values: pH 4.0, pH 7.0 and pH 10.0. Buffer solution is an aqueous solution consisting of a mixture of a week acid and its conjugate base or a week base and its conjugate acid. It has the property that the pH of the solution changes very little when a small amount of acid or base is added. The pH meter was used to adjust the pH levels in the metals ions solutions.

Figure 3.5: pH meter

3.6.4 Shaker

A laboratory shaker (Figure 3.6) was used for all the adsorption experiments. The speed of the shaker was manually controlled at 120 rpm.

Figure 3.6: Laboratory shaker

3.6.5 Scanning Electron Microscopy (SEM)

Scanning electron microscopy is the best known and most widely-used of the surface analytical techniques. Due to the manner in which the image is created, SEM images have a characteristic three-dimensional appearance and are useful for judging the surface morphology of the sample. The SEM analyses were recorded using an Oxford Instruments INCA-sight (model LEO 1430 VP), operated at 15 kV (Figure 3.7). The samples were loaded on a stub and coated with a gold-palladium film before scanning to avoid charge build-up.

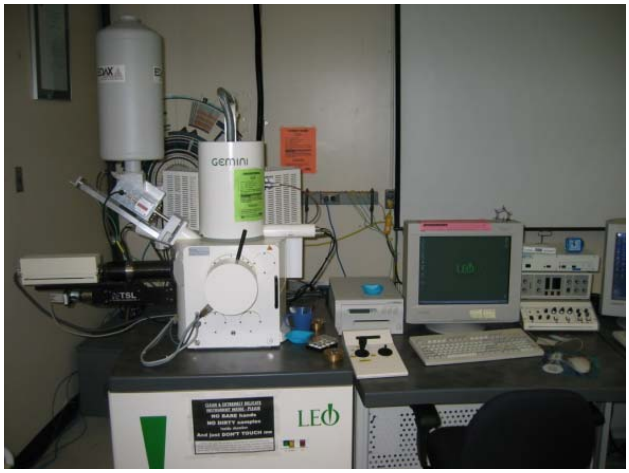

Figure 3.7: Scanning Electron Micrograph (SEM) Spectrometer**.**

3.6.6 Fourier Transform Infrared (FTIR) Spectroscopy

Fourier Transform Infrared (FTIR) spectroscopy has been used as a very valuable tool for studying the surface chemistry of materials. In this study, FTIR Spectrometer (Figure 3.8) was used to detect the vibration frequency changes for each of the functional groups present in carbon aerogels before and after the adsorption process. The spectra are collected by a spectrometer using KBr pellets. In each case, about 0.1%wt of carbon aerogel was homogenized with the KBr (Potassium bromide), thereafter pressed into a transparent tablet at 9000 psi. The pellets were analyzed using FTIR-8400S Shimadzu in the transmittance (%) mode with wave lengths in the range of 4000-400 cm^{-1}. KBr was used because it dosen't infuleunce the IR spectrum in the wave number range 4000 till 400 cm^{-1}.

Figure 3.8: FTIR Spectrometer.

3.6.7 Atomic Absorption Spectrometer (AAS)

Atomic absorption spectrometry (AAS) is a technique used to determine metal ions concentration. In a typical AA method, the sample is aspirated into a flame, where ions within the liquid are reduced to the atomic state, and then these metals in the atomic state can quantitatively absorb light at the wavelengths characteristic of their resonance frequencies (wave length for chromium is 357.9). Light was provided using hollow cathode lamps (made in England). The amount of radiation absorbed in the flame is proportional to the concentration of the element present in the flame and this principle is the basis of AAS. By this method several hundred samples can be analyzed within a working day if the samples were already prepared beforehand, so it is a time saving method. In this thesis research work, air-acetylene flame was utilized for the detection of

the chromium metal ions. All the experiments were performed using AA-6800 Shimadzu (Figure 3.9).

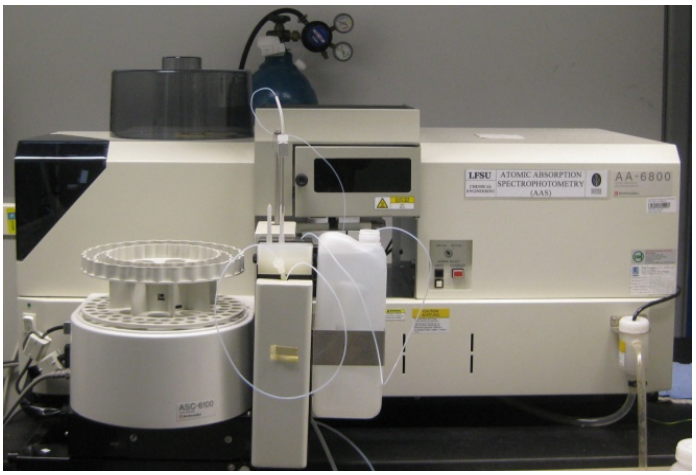

Figure 3.9: Atomic absorption spectrometer.

3.6.8 X-ray diffraction (XRD)

X-ray powder diffraction (XRD) analysis is a method for determining the degree of crystallinity. A typical XRD pattern is given in Figure 3.10. The XRD analyses were performed using a Bruker A&S D8 Advanced Diffractometer instrument equipped with a CuKα radiation source, at 40 kV and 30 m^2, in the scanning angle (2θ) range of 2–80^o at a scanning speed of 1.2^o/min (Figure 3.11).

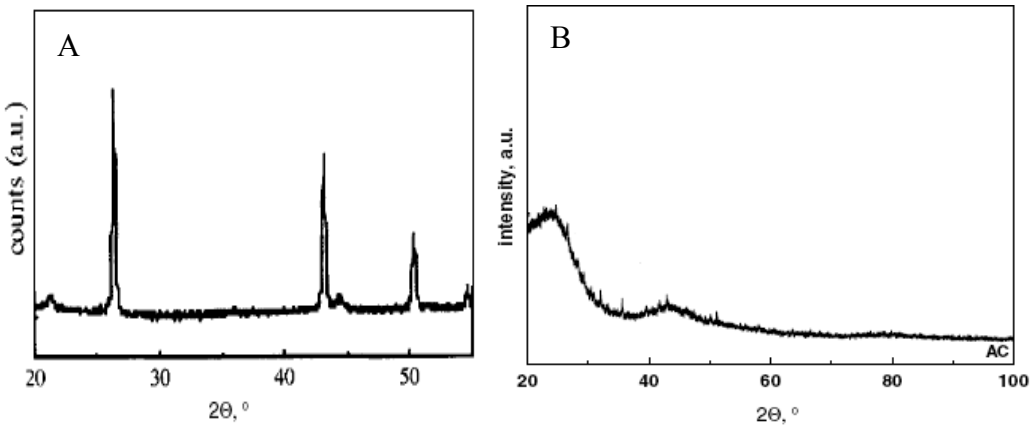

Figure 3.10: Typical XRD pattern for (A) crystalline graphite [Sandu *et al*., 2003], and (B) amorphous activated carbon [Zielinski *et al*., 2005].

Figure 3.11: X-ray powder diffraction.

3.6.9 Nitrogen Adsorption Analysis

Nitrogen adsorption tests were performed to obtain BET surface area and pore size distribution of the adsorbent using Micrometrics ASAP 2000 gas analyzer (Figure 3.12). This test was performed in Petronas Research and Services centre, PRSB, Bangi. The surface area and pore volume were calculated using the Brunauer-Emmett-Teller (BET) method.

Figure 3.12: Micrometrics ASAP 2000 surface area.

Chapter 4

RESULTS AND DISCUSSION

4.1 Introduction

This chapter presents the results and discussion of the experiments that were conducted in this study. These include the X-ray Diffraction (XRD), Scanning Electron Microscopy (SEM), nitrogen adsorption isotherm (BET) and Fourier Transformed Infrared (FTIR) characterization results. The efficiency of the prepared CAs in removing chromium is also discussed, as well as the kinetic and isotherm study of chromium ion removal.

4.2 Crystal structure of the synthesized CAs

To confirm and elucidate the crystal structure of the prepared CAs, x-ray diffraction (XRD) characterization was carried out as shown in Figure 4.1. Typical XRD peaks of CAs are at an angle of $2\theta=23^{o}$ and a small peak at $2\theta=43^{o}$ [Wu *et al*., 2005; Wu and Fu, 2005]. From the observation as shown in Figure 4.1, it is clear that the developed CAs are amorphous materials. There is no difference in the appearance structure of CAs prepared using sodium carbonate and sodium hydroxide after $2\theta=10^{o}$ as shown in Figure 4.1. The XRD pattern for the synthesized CAs in Figure 4.1 are in agreement with Wu *et al*. (2005) and Wu and Fu (2005) as shown in Figure 4.2.

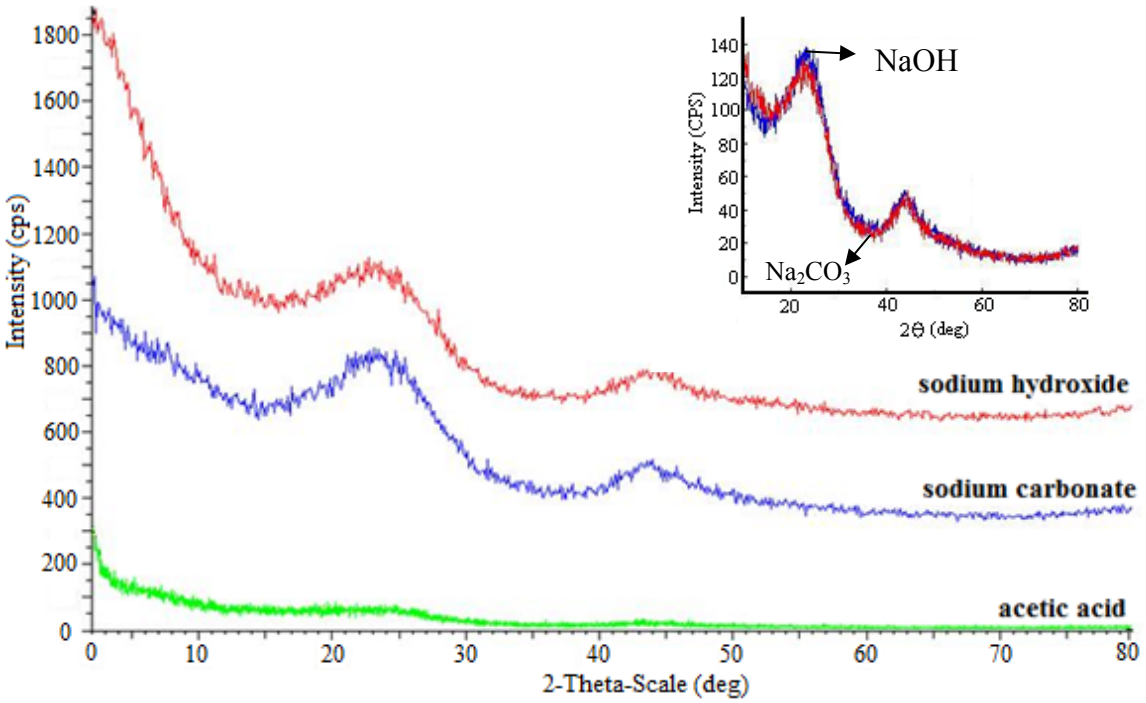

Figure 4.1: XRD pattern for CAs prepared by acetic acid, sodium carbonate, and sodium hydroxide (This study).

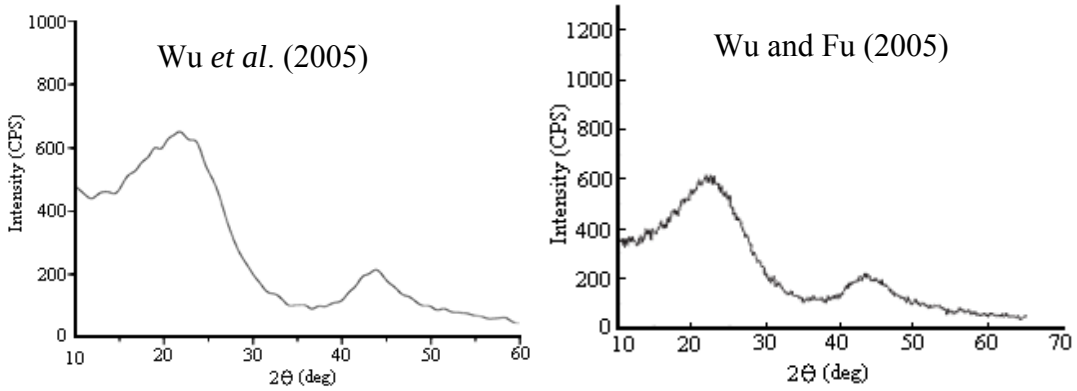

Figure 4.2: XRD pattern for CAs prepared by Wu *et al*. (2005) and Wu and Fu (2005).

The microcrtystallinye structure of the three types of CAs is attributed to the irregular arrange stacks of aromatic sheets. This irregularity resulted from the carbonization process, where most of noncarbon elements such as oxygen and hydrogen are eliminated as volatile gaseous species by the pyroltical decomposition of the starting material. After the pyroltical decomposition the carbon atoms group them self in stacks in a random manner.

4.3 Pore structure of the synthesized CAs

4.3.1 Scanning electron microscopy (SEM) analysis

SEM images of the surface morphology of CAs are shown in Figure 4.3. It is obvious that the three types of CAs have a porous surface, but the surface textures are different. At micrometer scale, the surface morphology of sample (a) was different to that of samples (b) and (c). Samples (b) and (c) showed open structures with large interconnected network of pores, whereas sample (a) showed a smoother surface, which is formed by small fused particles. On the other hand, the pore shape of sample (a) was smaller than that of samples (b) and (c).

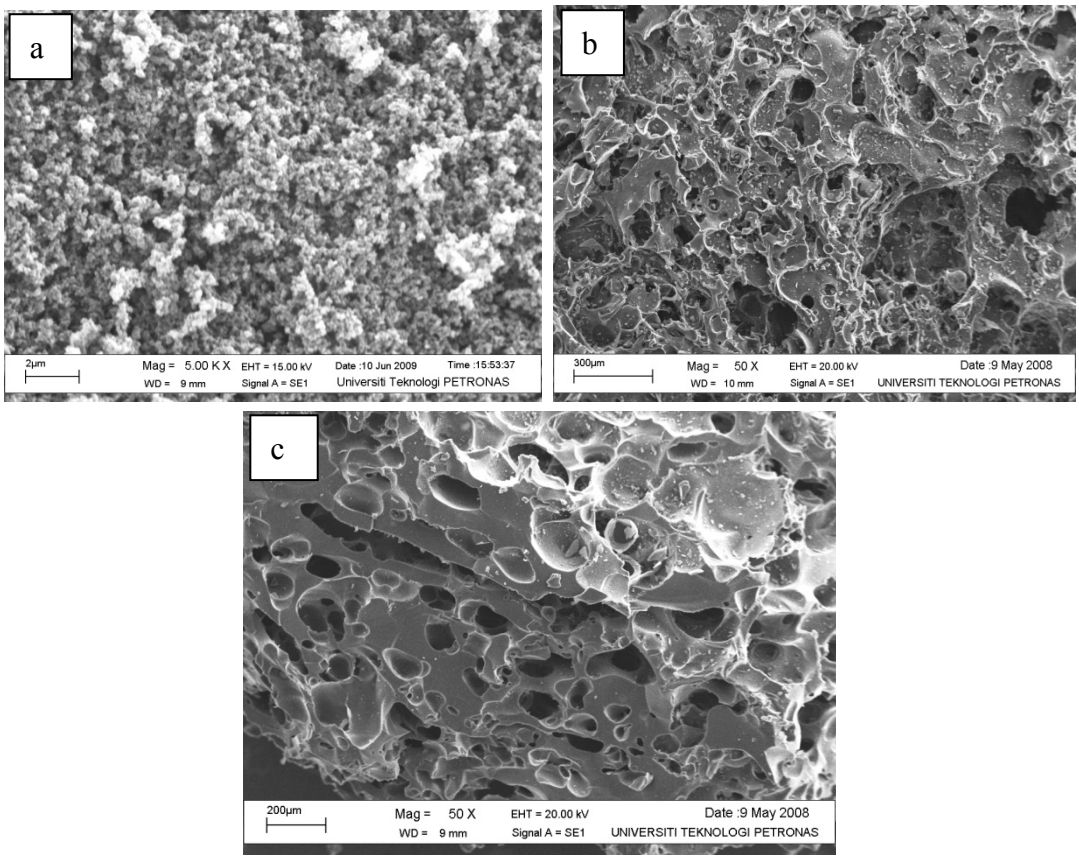

Figure 4.3: CAs prepared using (a) acetic acid, (b) sodium carbonate and (c) sodium hydroxide.

The porosity of these CAs is attributed to the pyrolytic decomposition. After the pyrolytic decomposition the aromatic sheets are irregularly arranged, which leaves free interstices. These interstices give rise to the pores.

By comparing these SEM results with those from other studies (Figure 4.4), it is clear that all of these CAs are porous but with different surface texture appearance.

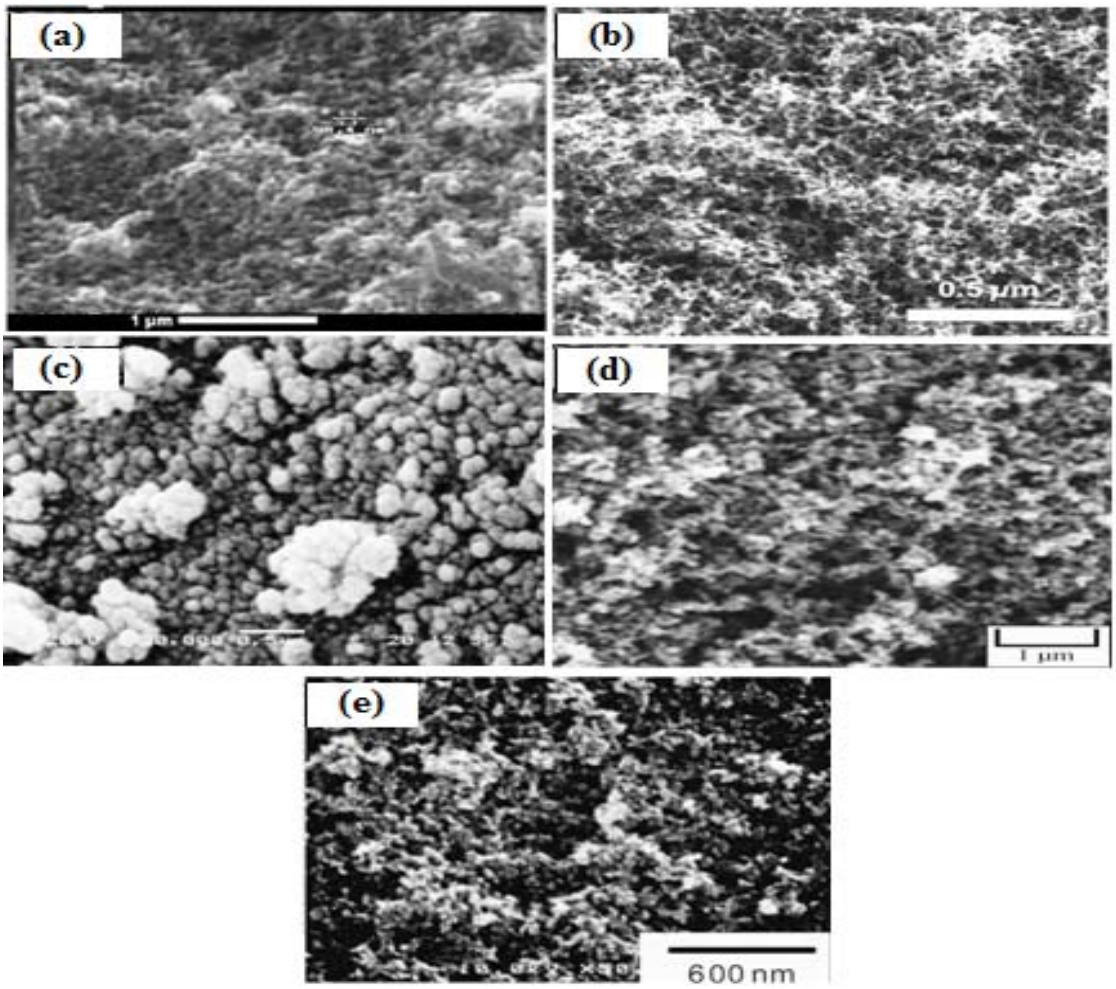

Figure 4.4: SEM images from other studies of CAs prepared by using (a) acetic acid [Brandt *et al*., 2003], (b) alkaline catalyst [Merzbacher *et al*., 2001], (c) sodium carbonate [Czakkel *et al*., 2005], (e) hexamethylenetetramine (HMTA) [Wu *et al*., 2004], and (c) sodium carbonate [Hwang *et al*., 2004].

4.3.2 BET surface area measurement

The results of adsorption and desorption isotherms of N_2 at 77 K on the CAs are shown in Table 4.1 and Figure 4.5 respectively. According to the IUPAC classification [Lowell *et al., 2004*], the isotherms of the CAs were Type II in the IUPAC classification. This type of isotherm is identified with unrestricted monolayer–multilayer adsorption, and is a characteristic of nonporous or macroporous adsorbents. According to the isotherms of the samples, the surface area, pore volume, and pore size of the samples were calculated, and

the results are shown in Table 4.1 and Figure 4.5. The data in Table 4.1 reveal that the CAs prepared using acetic acid had higher BET surface area value (619.26 m^2/g) and larger pore diameter and pore volume values (30.14 Å, and 0.47 cm^3/g) compared to CAs prepared using sodium carbonate and sodium hydroxide. Further investigation showed that the higher surface area helped in increasing the chromium removal percentage, which was consistent with the results from kinetic studies in section 4.5.

Table 4.1: Characteristic results using BET.

Adsorbent	BET surface area [m^2 /g]	Average pore diameter [Å]	Total pore volume	Micropore volume [cc/g]	Micropore volume / Total pore volume	Micro pore area [m^2 /g]
Acetic acid CA	619.26	30.14	0.47	0.21	0.45	527.83
Sodium hydroxide CA	362.27	17.09	0.15	0.14	0.91	358.96
Sodium carbonate CA	209	18.62	0.1	0.08	0.85	212.88
CA from literature (resorcinol/catalyst=500, dilution ratio=5.7) [Job *et al*., 2005]	575	40	2.1	-	-	-

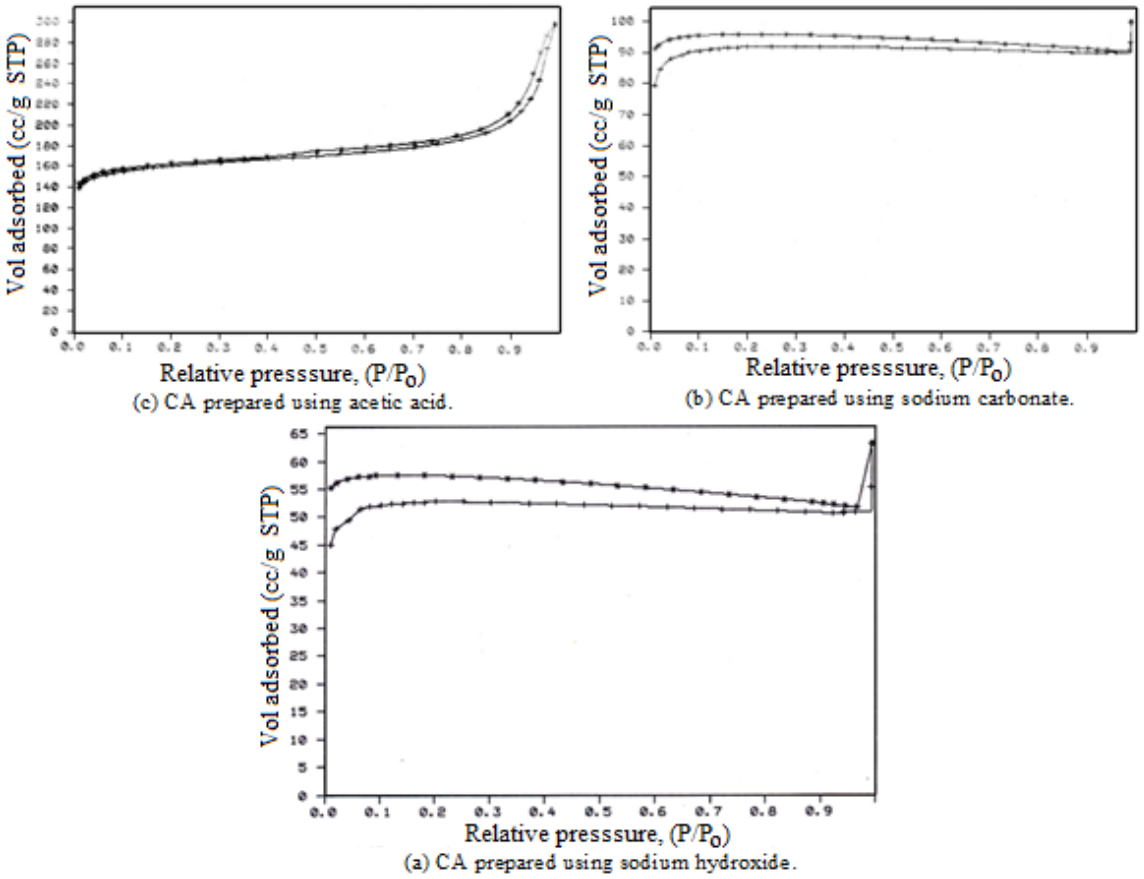

Figure 4.5: Nitrogen sorption isotherms of CAs.

4.4 FTIR spectroscopy

Many bands of functional groups are observed for the three types of CAs as shown in Figures 4.6, 4.7 and 4.8., which displays its important coverage by oxide groups. Functional groups are a chemically reactive group of atoms within a molecule. Each functional group has its characteristic reactivity, which may be modified by its position within the molecule or by the presence of other neighboring functional groups [Hanson, 2001]. These three types of CAs are rich in functional groups such as carboxylic and hydroxyl, and are known to strongly bind metal cations in aqueous solution [Pehlivan *et al*., 2008; Shukla and Pai, 2005; Xuan *et al*., 2006]. The functional groups are resulted from the unpaired electrons that appears from the pyrolytic composition.

The CAs are microcrystalline and this results from the random ordering of the aromatic sheets, which causes a variation in the arrangement of electron clouds in the carbon skeleton and results in creation of unpaired electrons and uncompleted saturated valencies.These unpaired electrons are resonance stabilized and trapped during the carbonization process, due to the breaking of bonds at the edges of the aromatic sheets, and, thus they create edge carbon atoms. These edge or aromatic sheets have unsaturated valncies and can interact with hetroatoms such as oxygen and hydrogen giving rise to different types of surface groups.

Peaks appearing in the FTIR spectrum of CAs were assigned to various groups and bonds in accordance with their respective wave numbers as reported in the literature [Hebalkar *et al*., 2005; Guilminot *et al*., 2007; Liang, 2000]. On the FTIR spectrum of CA prepared using acetic acid (Figure 4.6), the broad and intense peaks in the region of 3578.19, 3520.81, 3235.85, 3177.99, 3000.55, 2837.09, 2745.96, and 2700.16 cm^{-1} show presence of the hydroxyl groups. A hydroxyl group is a molecule consisting of an oxygen atom and a hydrogen atom connected by a covalent bond (O-H), due to inter and intra-molecular hydrogen bonding of polymeric compounds, such as resorcinol and acetic acid [Crews *et al*., 1998; Pavia *et al*., 2001]. The O-H stretching vibrations occur within a broad range of frequencies indicating the presence of free hydroxyl groups and bonded O-H bands of carboxylic acids [Crews *et al*., 1998; Pavia *et al*., 2001]. The carboxyl group where its structure is composed of one carbon atom attached to an oxygen atom by a double bond and to a hydroxyl group by a single bond (COOH), can be found in the range 3235.85,

3177.99, 3000.55, 2837.09, 2745.96, and 2700.16 cm^{-1} [Crews *et al*., 1998; Pavia *et al*., 2001]. The sharp peak at 2040.06 is an evidence of the carbonyl group (carbon atom double-bonded to an oxygen atom) [Aramata *et al*., 1991]. This group may be from the benzoquinone group (Benzoquinones are diketones and have molecular formula $C_6H_4O_2$), which is formed at the broken C-O-C linkages in the presence of oxygen [Hebalkar *et al*., 2005]. The range of 690-900 cm^{-1} is an evidence of C-H stretching vibration, which is a confirmation for the presence of a hydroxyl group [Pavia *et al*., 2001]. Because of the heating process, some of the CH_2-O-CH_2 linkages may have been broken to form -CH_2OH and =CH_2 groups attached to different resorcinol molecules [Hebalkar *et al*., 2005]. This is further supported by the sharp intense peaks observed at around 660 cm^{-1} due to the C=CH_2 [Hebalkar *et al*., 2005]. The peaks served in the 400-625 cm^{-1} region confirm the presence of C=C ring bend vibration [Crews *et al*., 1998].

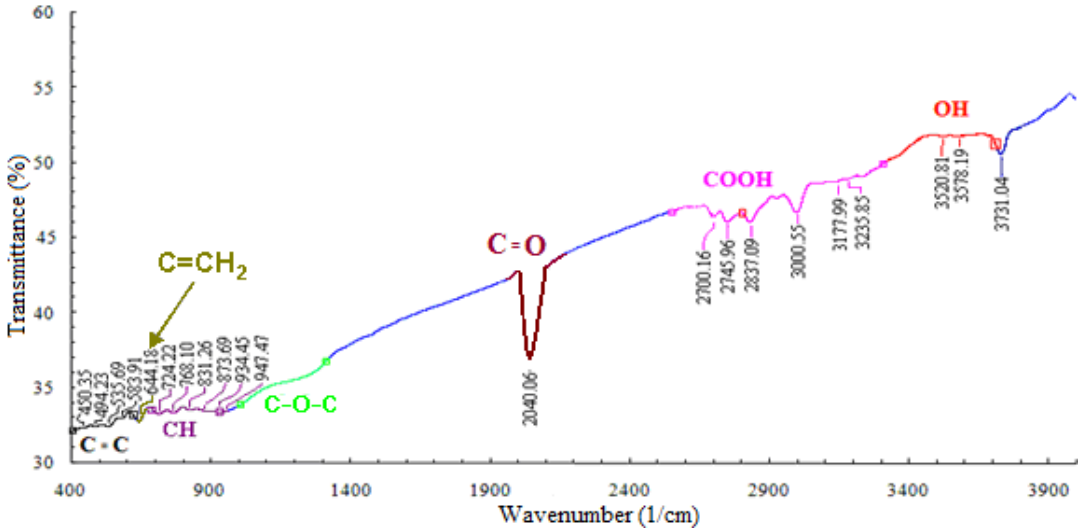

Figure 4.6: FTIR result for acetic acid CA.

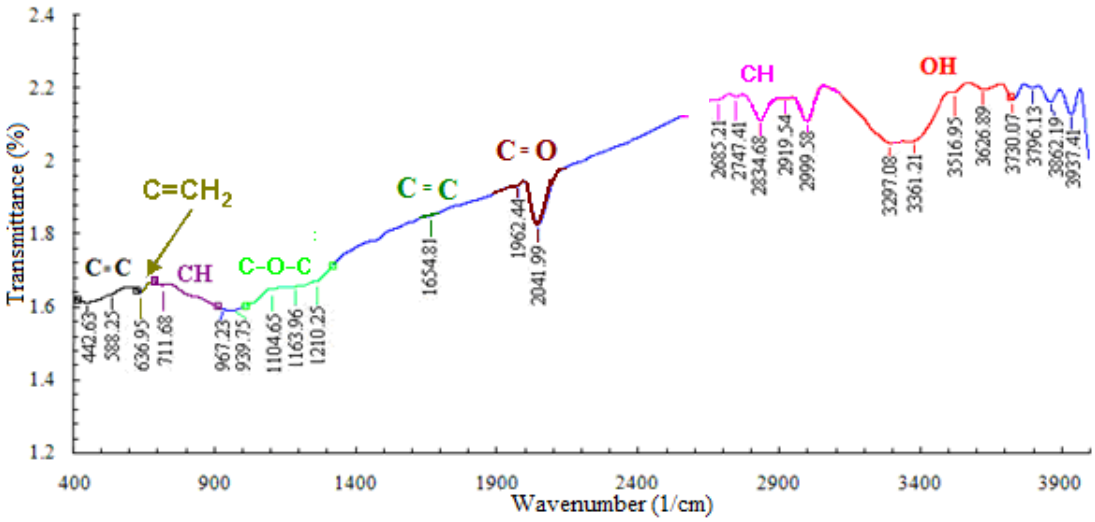

Figure 4.7: FTIR result for sodium carbonate CA.

The FTIR result of CA prepared using sodium carbonate is as shown in Figure 4.7. Various groups and bonds in accordance with their respective wave numbers were found. The peaks 3730.07, 3626.89, 3516.95, 3361.21, and 3297.08 cm^{-1} can be considered as evidence of presence of hydroxyl groups [Crews *et al*., 1998; Pavia *et al*., 2001], mainly due to the –OH groups bonded to the benzene ring [Pavia *et al*., 2001], but also may be due to $–CH_2OH$ groups connected to the resorcinol molecule [Hebalkar *et al*., 2005]. CH stretching vibration was represented by 2999.58, 2919.45, 2834.68 2747.41, and 2685.21 cm^{-1}. Intensity of band at 2041.99 cm^{-1} is related to the carbonyl group [Aramata *et al*., 1991]. As mentioned before, this group may be from the benzoquinone group. The peaks at 1210.25, 1163.96, 1104.65, 939.75 cm^{-1} region could represent C-O-C linkage stretching between two resorcinol molecules which is expected in the poly-condensation reaction between resorcinol and formaldehyde [Hebalkar *et al*., 2005]. The peak at 711.68 cm^{-1} refers to C-H groups, which is a confirmation for the presence of hydroxyl group [Pavia *et al*., 2001]. As before, due to the heating process, some of the CH_2-O-CH_2 linkages may have broken the sharp intense peaks observed at around 660 cm^{-1} due to the $C=CH_2$ [Hebalkar *et al*., 2005]. C=C stretching vibration was found at 1654.81, due meta substitute aromatic [Pavia *et al*., 2001]. The peaks served in 400-625 cm^{-1} region (636.95, 588.25, 442.63 cm^{-1}) could be evidence of C=C ring bend vibration [Crews *et al*., 1998].

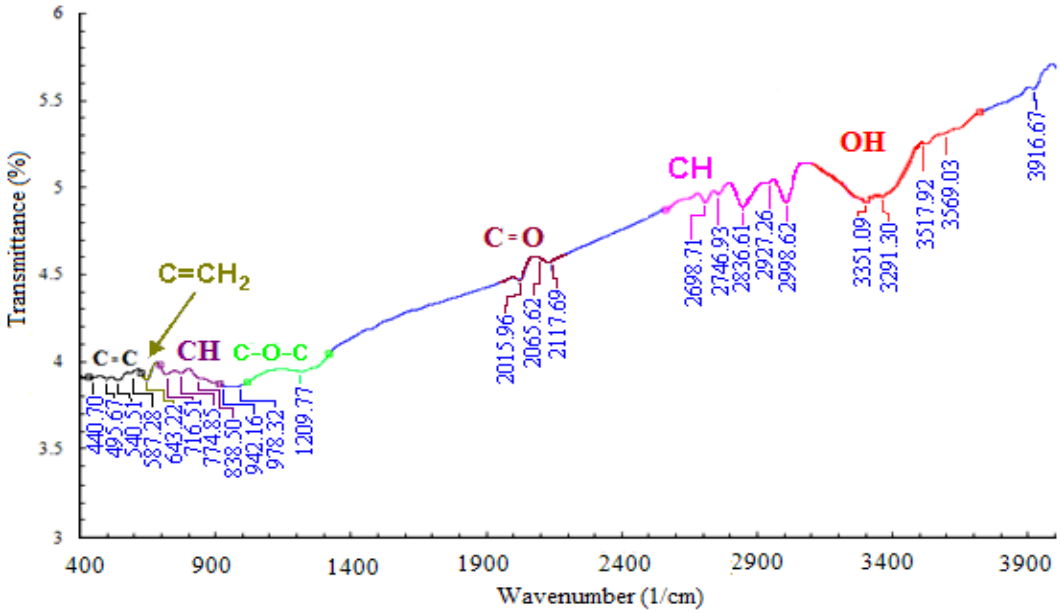

Figure 4.8: FTIR results for sodium hydroxide CA.

The spectrum of the CA prepared using sodium hydroxide is shown in Figure 4.8. The bands observed at 3569.03, 3517.92, 3351.09, and 3291.30 cm^{-1} could be assigned to hydroxyl groups (O–H) [Crews *et al*., 1998; Pavia *et al*., 2001], and that is due to inter- and intra-molecular hydrogen bonding of resorcinol [Kadirvelu *et al*., 2008; Pavia *et al*., 2001]. The peaks at 2015.96, 2065.62, and 2117.69 are an evidence of presence of carbonyl group. This group may also be from the benzoquinone group. The C-H stretching vibration can be represented by 2998.62, 2927.26, 2746.93, and 2698.71 cm^{-1} [Pavia *et al*., 2001. The peaks at 1209.77 cm^{-1} region could represent C-O-C linkage stretching between two resorcinol molecules. At area 690-900 cm^{-1} there are some peaks (838.50, 774.85, and 716.51 cm^{-1}), which show evidence of C-H groups confirming the presence of a hydroxyl group [Pavia *et al*., 2001]. Because of heating, some of the CH_2-O-CH_2 linkages may have broken to form -CH_2OH and =CH_2. The sharp intense peaks observed at around 660 cm^{-1} due to the C=CH_2 [Hebalkar *et al*., 2005]. C=C ring bend vibration were found in 400-625 cm^{-1} region [Crews *et al*., 1998].

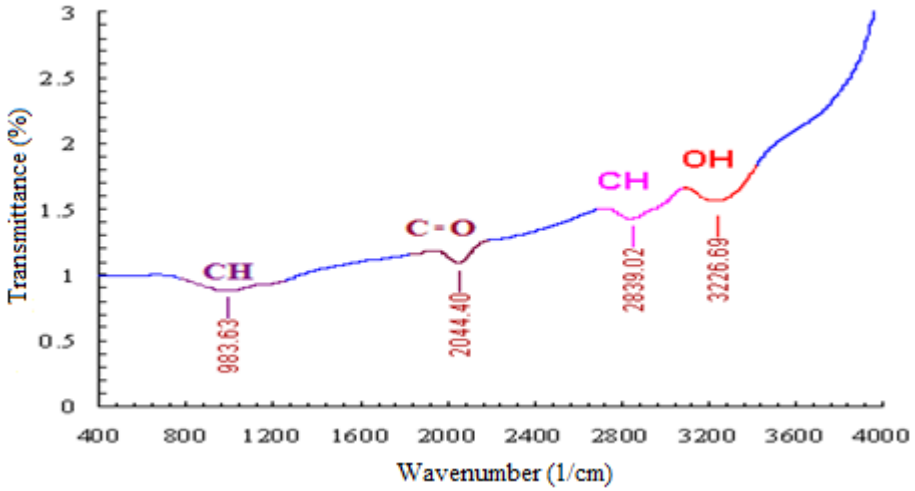

Figure 4.9: FTIR for activated carbon**.**

Figure 4.9 shows the FTIR result for commercial activated carbon supplied by Merck with surface area of 589.87 m^2/g, and molecular weight of 12.01 g/mol. As apparent in the FTIR result, it has an OH group which is represented by a 3226.69 peak, and as an evidence of the OH group presence is the appearance of a CH group at around 983.63 as reported in the literature [Pavia *et al*., 2001]. The peak at 2839.02 may be due to CH stretching vibration [Pavia *et al*., 2001]. The carbonyl group was represented by the 2044.40 peaks [Aramata *et al*., 1991].

It is well indicated from the FTIR spectrum of CAs and activated carbon that the hydroxyl groups were present in abundance. This group may function as proton donors; hence de-protonated hydroxyl group may be involved in coordination with metal ions.

Figure 4.10 shows the comparison of the FTIR spectrum for the three types of CAs. It is observed from Figure 4.10 that the CA prepared by using acetic contains carboxylic groups (COOH) whereas CAs produced using basic catalysts have none. Apart from that the acetic acid CA also contains more hydroxyl groups (OH) as appeared from the depth of the peaks compared to sodium carbonate and sodium hydroxide CAs, as shown by the depth of the peaks. When the FTIR results of CAs prepared using the two basic catalysts were compared, it was found that the depth of hydroxyl groups was deeper in the CA prepared using sodium hydroxide than in the one prepared using sodium carbonate, as shown in Figure 4.10.

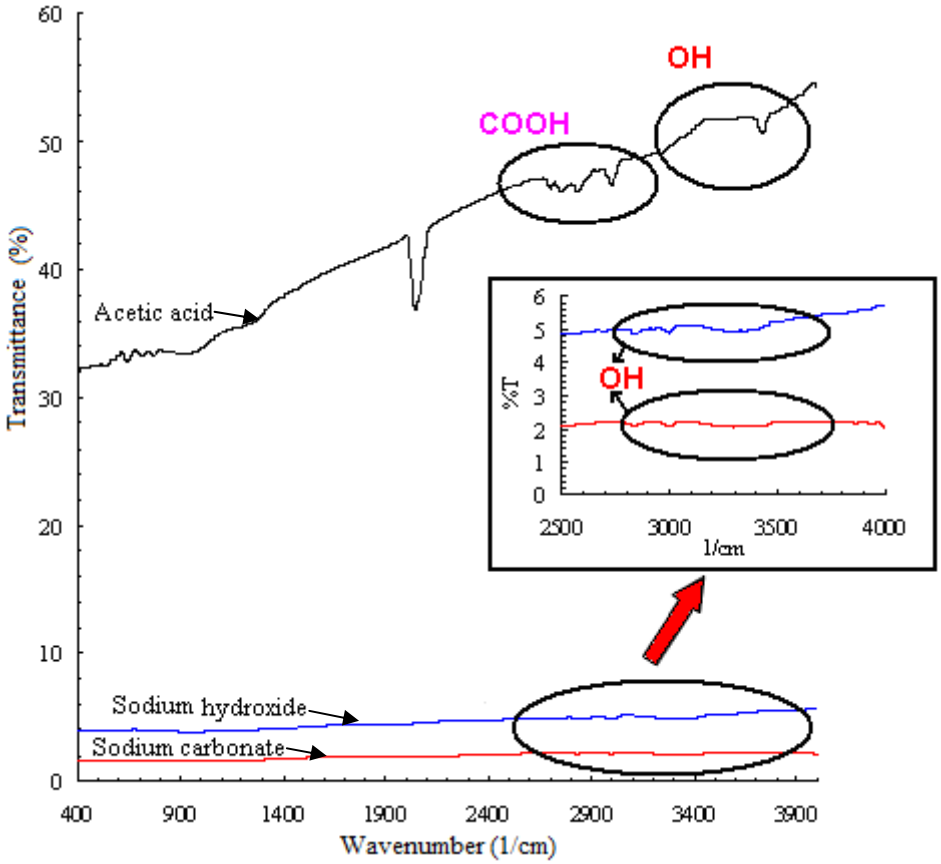

Figure 4.10: FTIR results of all types of CAs.

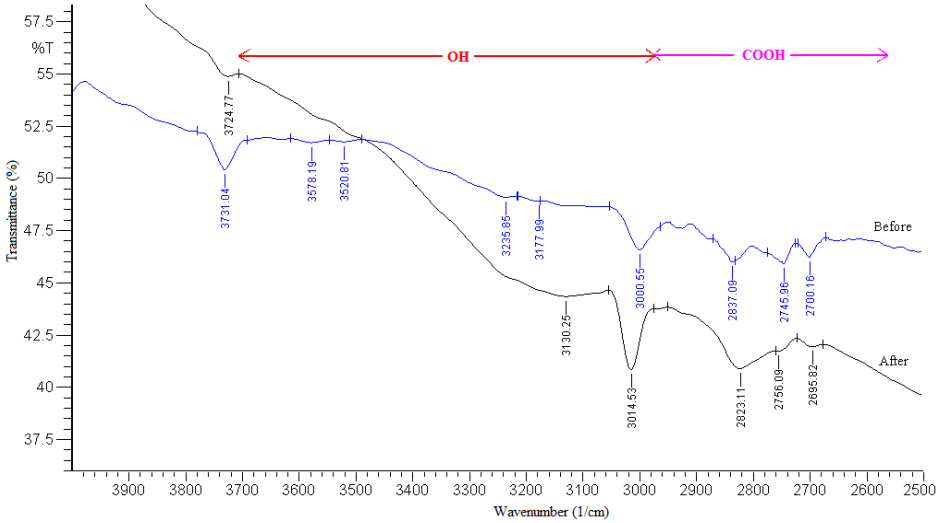

Figure 4.11: CA prepared by using acetic acid before and after adsorption of chromium.

Figures 4.11, 4.12, and 4.13 show a comparison between FTIR results of each adsorbent before and after the adsorption process. As shown from Figure 4.13; 3578.19, 3520.81, 3235.85, cm^{-1} had disappeared after adsorption and 3731.04, 3177.99, 3000,55, 2837.09, 2745.96, and 2700.16 cm^{-1} had shifted their initial positions to 3724.77, 3130.25, 3014.53, 2823.11, 2756.09, and 2695.82 cm^{-1} respectively. The changes are due to chromium adsorption.

As observed from Figure 4.11; 3796.13, 3730.07, and 3361.21 cm^{-1} had disappeared after adsorption and 3937.41, 3862.19, 3626.89, 3516.95, 3297.08, 2999.58, 2919.54, 2834.68, 2747.41, and 2685.21 cm^{-1} had shifted their initial positions to 3978.87, 3836.15, 3573.85, 3515.51, 3279.24, 3011.16, 2925.33, 2838.06, 2748.86, and 2642.78 cm^{-1} respectively. All of the changes are due to chromium adsorption.

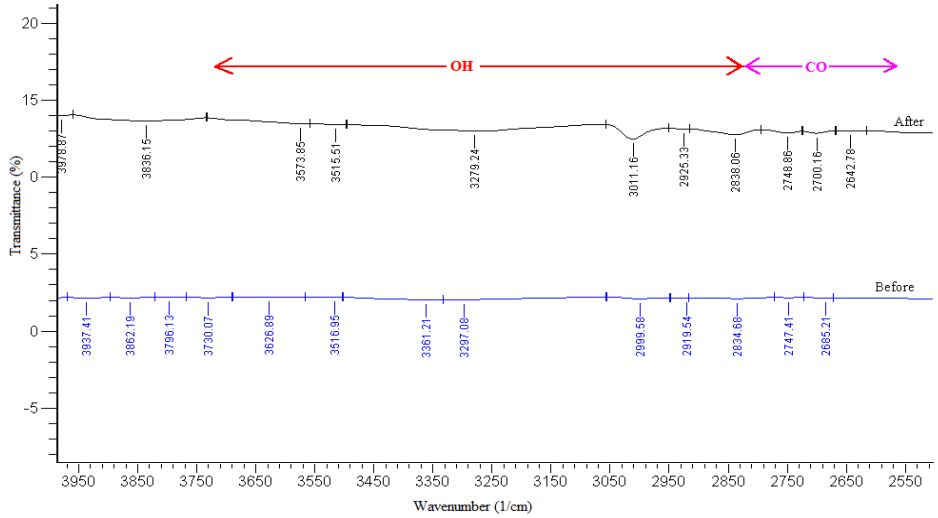

Figure 4.12: CA prepared by using sodium carbonate before and after adsorption.

Based on Figure 4.12 it is observed that 3351.09, and 2927.26 cm^{-1} had disappeared after adsorption and 3916.67, 3569.03, 3517.92, 3291.30, 2998.62, 2836.61, 2745.93, and 2698.71 cm^{-1} had shifted their initial positions to 3854.47, 3584.94, 3515.03, 3274.42, 3012.60, 2839.02, 27252.71, and 2697.75 cm^{-1} respectively.

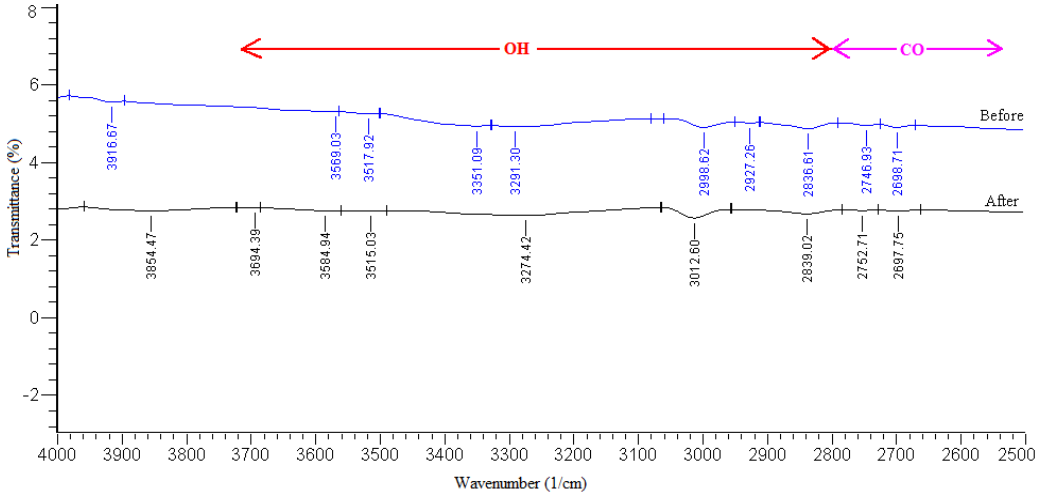

Figure 4.13: CA prepared by using sodium hydroxide before and after adsorption of chromium.

FTIR spectra of chromium adsorbed CAs showed that some hydroxyl groups had disappeared and some had shifted their initial position as shown in Figures 4.11, 4.12 and 4.13 due to chromium sorption. These are attributed to the changes in counter ions associated with hydyroxylate anions, suggesting that the acidic group, hydroxyl, was the predominant contributor in metal ion uptake.

4.5 Sorption kinetic studies

The kinetic studies of sorption processes are important because the data obtained from these studies are necessary to understand the variables that influence the sorption of solutes. The adsorption kinetics of the experiment are influenced by various factors, which include initial metal ion concentration, amount of adsorbent and pH value of solution [Pradhan, 2001]. The effects of all these factors were examined in the experiments described here.

4.5.1 Effect of initial metal ion concentration

One of the most important factors that determine the equilibrium concentration, the

uptake rate of metal ion and the kinetic character is the initial metal ion concentration [Pradhan, 2001]. The initial chromium concentration was studied to observe the influence of initial concentration of adsorbate on the sorption process using CAs. Batch experiments were conducted as reported in section 3.3.1.

Figures 4.14 to 4.16 show the relation between the removal percentages versus time. The removal percentage was calculated using equation 4.1 [Abdullah *et al*., 2006; Rahman, 2007].

$$\text{Removal percentage} = \frac{C_i - C_e}{C_i} \times 100\% \quad \text{.....} \quad (4.1)$$

Where,

C_i ≡ Initial concentration (mg/L) of the metal solution.

C_e ≡ Equilibrium concentration (mg/L) of the metal solution.

The initial chromium concentration was studied to observe the influence of the initial concentration of sorbate on the sorption process using CAs. The results showed that when the range of chromium concentration at 5, 10, 30, 40 ppm, the uptake of chromium was rapid in the first 16 min. The uptake then gave way to a much slower adsorption, which became constant at 60 min and after which no significant removal was observed as shown in Figures 4.14 to 4.16. This initial rapid uptake can be attributed to the concentration gradient created at the start of the adsorption process between solute concentration in solution and that at the CAs surface [Oladoja, 2008]. Moreover, in the beginning there is a larger surface area, which can be used for the adsorption of the chromium ion in the CAs. However, with gradual occupancy of these sites with time, the sorption becomes less efficient [Rahman, 2007].

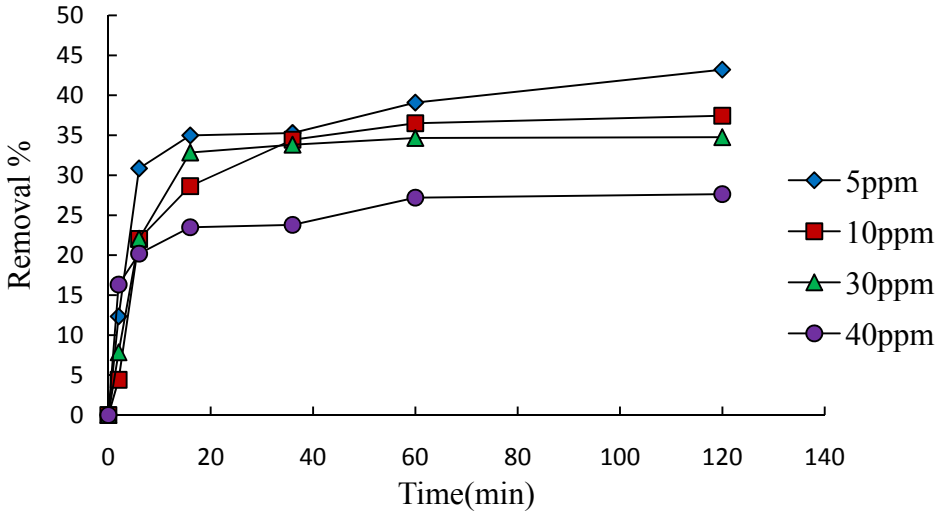

Figure 4.14: Time variation of chromium sorption on acetic acid CA at different chromium concentration (data in appendix B).

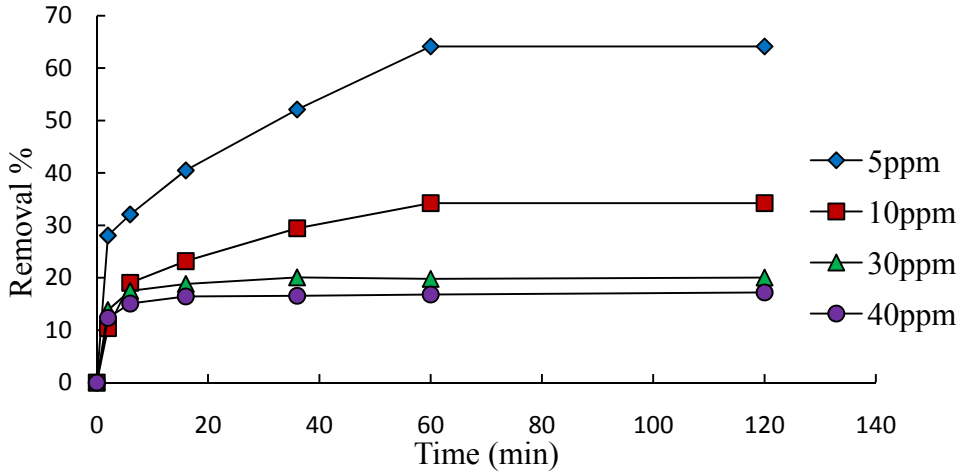

Figure 4.15: Time variation of chromium sorption on sodium carbonate CA at different chromium concentration (data in appendix B).

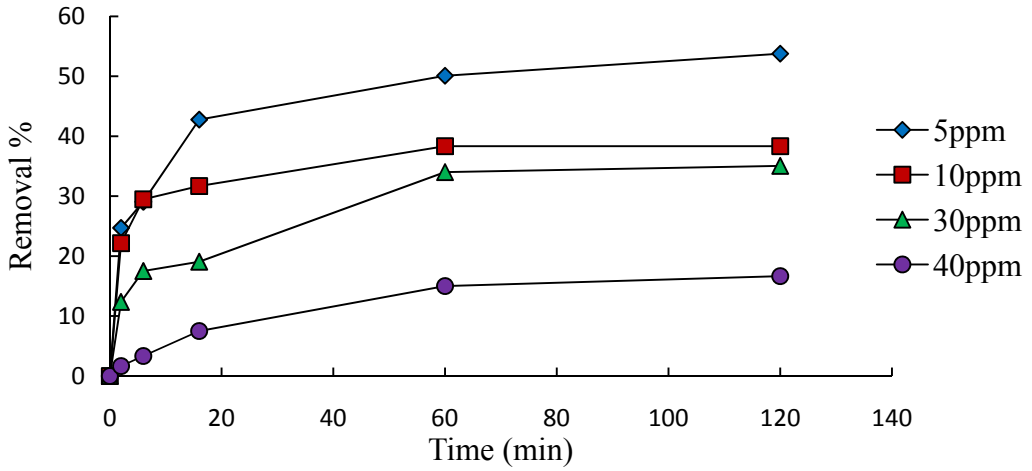

Figure 4.16: Time variation of chromium sorption on sodium hydroxide CA at different chromium concentration (data in appendix B).

Based on Figures 4.14 to 4.16 it was noted that variation in the initial concentration of chromium did not affect the time in which equilibrium was attained. The rapid uptake of chromium indicates that the sorption process could be an ion exchange in nature, where the chromium ions bind with the functional groups present on the surface of the CAs as confirmed by the FTIR results earlier (Figures 4.6 - 4.8).

It was noted that while the chromium concentration increased, the percentage of removal decreased. Several researchers have also studied the effect of initial sorbate concentration on sorption of heavy metals by using different materials and found similar results to those of this study [Meena *et al*., 2005; Rahman, 2007; Oladoja *et al*., 2007]. This agreement can be explained by the observation that when chromium concentration is lower, most of the chromium ions are able to bind with the available sites in the CAs. Consequently, when the concentration is higher, the chromium removal percentage is lower because the available sites for adsorption are already filled [Meena *et al*., 2005; Rahman, 2007].

In order to observe the sorption process of chromium onto the adsorbents, the results obtained using the three types of CAs were tested with pseudo first and second order model using equations 3.1 and 3.3 respectively.

If pseudo-first order kinetics is applicable, the plot of log (q_e-q_t) versus t should give a linear relationship, from which the pseudo-first order parameters can be determined from the slope and intercept of the plot. Figures 4.17 to 4.19 represent the plots of log (q_e-q_t) versus t for the three types of CAs.

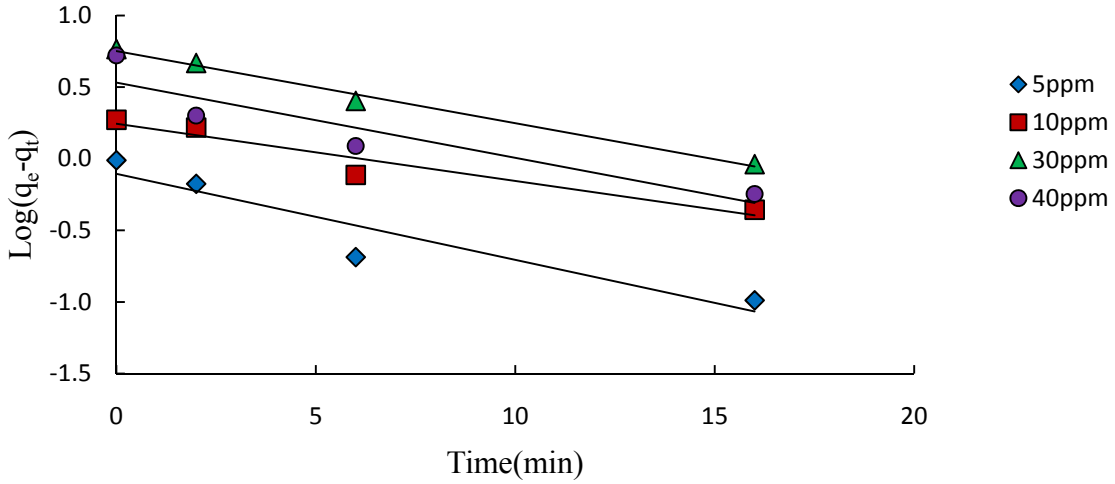

Figure 4.17: Pseudo-first order plot of sorption of chromium on CA prepared by acetic acid CA at varying initial metal concentration (data in appendix B).

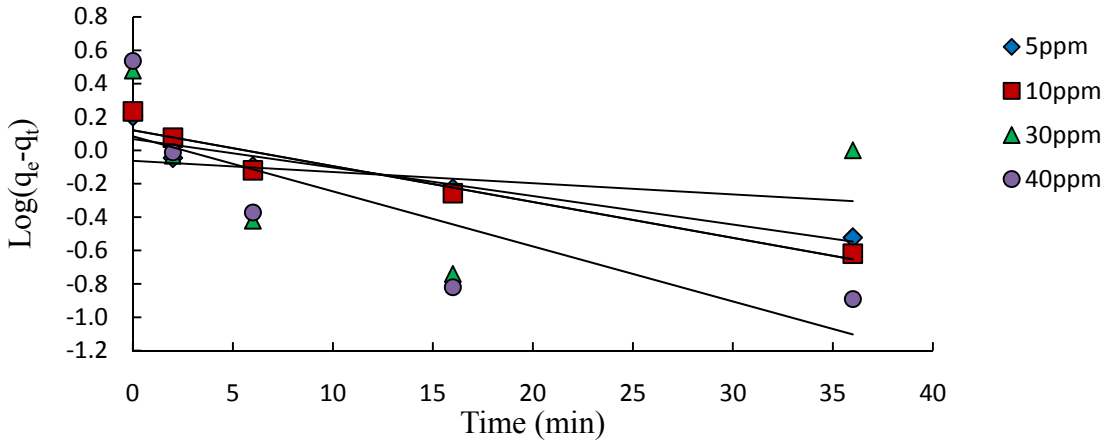

Figure 4.18: Pseudo-first order plot of sorption of chromium on CA prepared by sodium carbonate CA at varying initial metal concentration (data in appendix B).

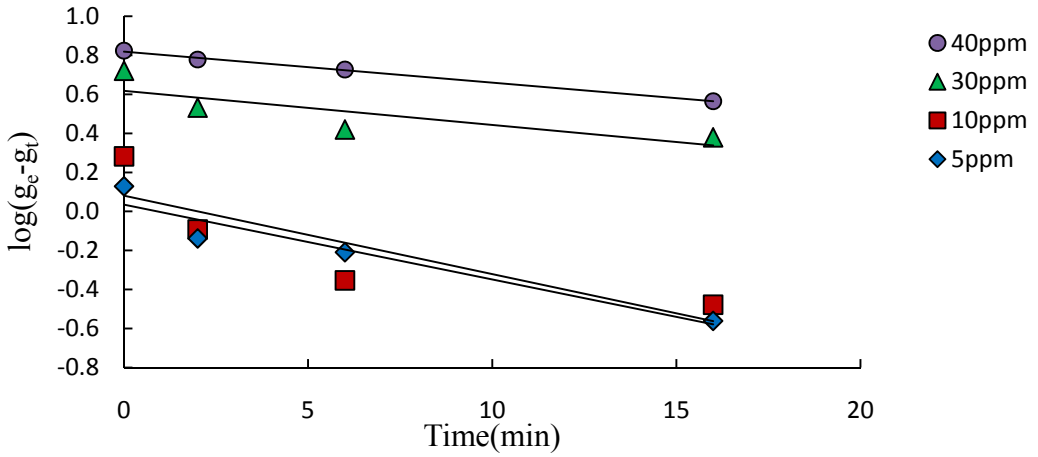

Figure 4.19: Pseudo-first order plot of sorption of chromium on CA prepared by sodium hydroxide CA at varying initial metal concentration (data in appendix B).

Figures 4.20 to 4.22 present the plots of t/qt versus t for the three types of CAs. Where pseudo-second order kinetics is applicable, the plot of t/qt against t of equation (3.3) should also give a linear relationship, where q_e and k_s can be determined from the slope and intercept of the plot.

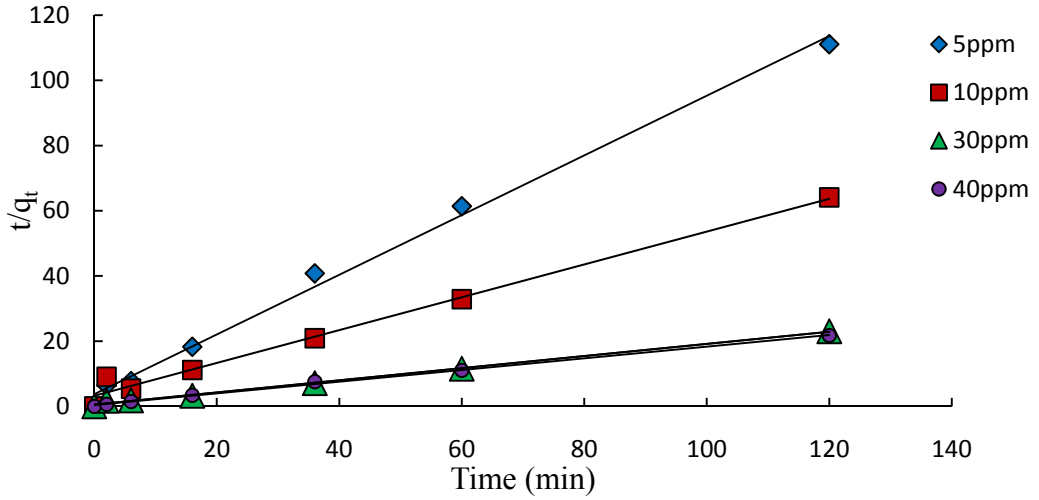

Figure 4.20: Pseudo-second order plot of sorption of chromium on CA prepared by acetic acid CA at varying initial metal concentration (data in appendix B).

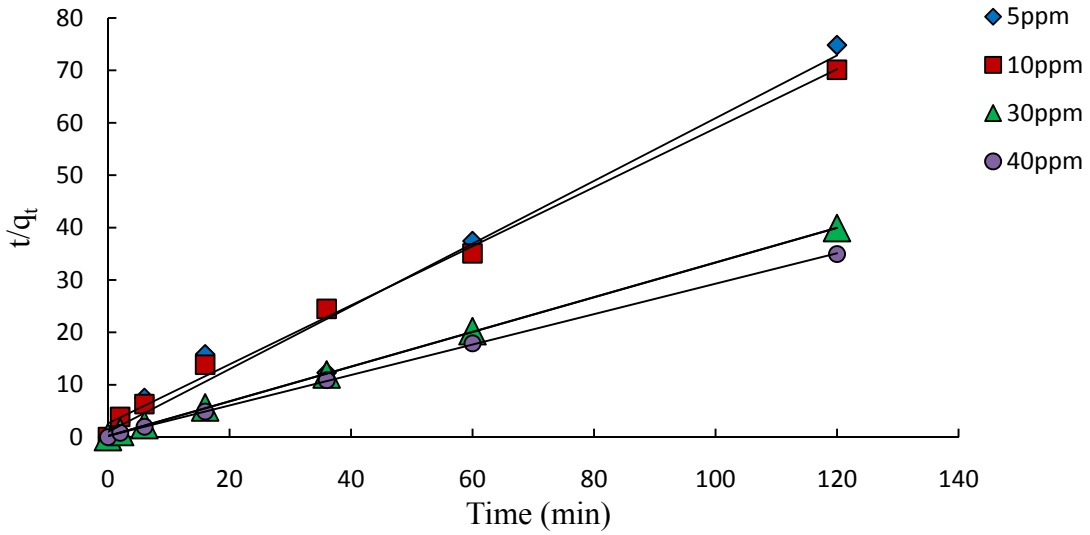

Figure 4.21: Pseudo-second order plot of sorption of chromium on CA prepared by sodium carbonate CA at varying initial metal concentration (data in appendix B).

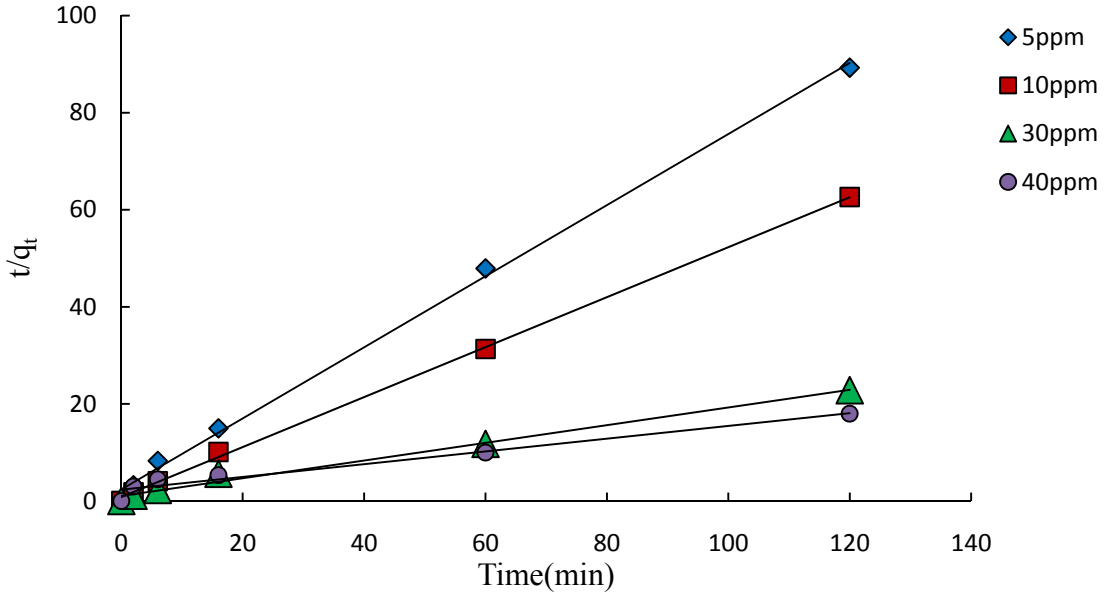

Figure 4.22: Pseudo-second order plot of sorption of chromium on CA prepared by sodium hydroxide CA at varying initial metal concentration (data in appendix B).

Tables 4.2, 4.3 and 4.4 represent the parameters of the two kinetic models using the three types of CAs. From these tables it can be observed that the two models adequately describe the sorption of chromium in to the CAs with the pseudo second order model having a higher correlation than the pseudo first order. It can also be observed from Tables 4.2 to 4.4 that the effect of initial chromium concentration was significant, the sorption capacity (q_e, i.e. mg of chromium adsorbed per g of each type of CA) values increased with increasing the initial concentration. Similar results were achieved in other studies by using CA in removing other types of heavy metals which was cadmium [Goel *et al.*, 2006].

Table 4.2: Kinetic parameters for the sorption of Cr by acetic acid CA at different initial Cr concentrations (ppm).

Chromium concentration (ppm)	Pesudo-first order parameters			Pseudo-second order parameters			
	q_{e1}	k_f	R^2	q_{e2}	k_s	h	R^2
5	0.787	0.14	0.891	1.093	0.225	0.269	0.995
10	1.754	0.09	0.927	1.9881	0.503	1.988	0.987
30	5.649	0.12	0.992	5.3763	0.186	5.376	0.997
40	7.145	0.12	0.854	5.587	0.179	5.587	0.997

k_f= min^{-1}; q_{e1}= mg/g ; k_s = $g.mg^{-1}.min^{-1}$; h = $g.mg^{-1}.min^{-1}$

Table 4.3: Kinetic parameters for the sorption of Cr by sodium carbonate CA at different initial Cr concentrations (ppm).

Chromium concentration (ppm)	Pseudo-first order parameters			Pseudo-second order parameters			
	q_{e1}	k_f	R^2	q_{e2}	k_s	h	R^2
5	1.230	0.484	0.741	1.603	0.1821	0.468	0.959
10	1.419	0.645	0.862	1.776	0.12	0.379	0.995
30	1.663	0.152	0.818	3.021	0.05	0.457	0.999
40	1.91	0.170	0.861	3.448	0.356	4.233	0.999

k_f= min^{-1}; q_{e1}= mg/g ; k_s = $g.mg^{-1}.min^{-1}$; h = $g.mg^{-1}.min^{-1}$

Table 4.4: Kinetic parameters for the sorption of Cr by sodium hydroxide CA at different initial Cr concentrations (ppm).

Chromium concentration (ppm)	Pseudo-first order parameters			Pseudo-second order parameters			
	q_{e1}	k_f	R^2	q_{e2}	k_s	h	R^2
5	1.081	0.0875	0.922	1.366	0.263	0.490	0.998
10	1.202	0.092	0.724	1.946	0.321	1.215	0.999
30	4.14	0.035	0.662	5.495	0.031	0.942	0.989
40	6.577	0.039	0.997	7.634	0.007	0.425	0.959

k_f= min^{-1}; q_{e1}= mg/g ; k_s = $g.mg^{-1}.min^{-1}$; h = $g.mg^{-1}.min^{-1}$

4.5.2 Effect of adsorbent dose on the adsorption process

The dependence of chromium on three types of CAs was studied at room temperature (23 ^oC) at fixed pH (pH=5) and chromium concentration (30 ppm). The sorbent amount was varied between 0.015, 0.025 and 0.05 g, while the volume of the metal solution and agitation rate was kept constant at 25 ml, 120rpm respectively.

The concentrations of chromium solutions before adsorption and after adsorption were measured by AAS and the percentage of metal adsorption was calculated using equation 4.1. The effects of sorbent dosage on the sorption process are presented in Figures 4.25 to 4.27.

It is observed from Figure 4.23 that the percentage of removal of the metal ions increased quickly with the increase in weight of the CA prepared by acetic acid. This is expected as an increase in the CA amount will lead to an increase in the quantity of sorption sites available for sorbent-sorbate interaction [Meena *et al*., 2005; Yu, 1995]. The same results can be drawn for CAs prepared by sodium carbonate and sodium hydroxide as appears in Figures 4.24 and 4.25.

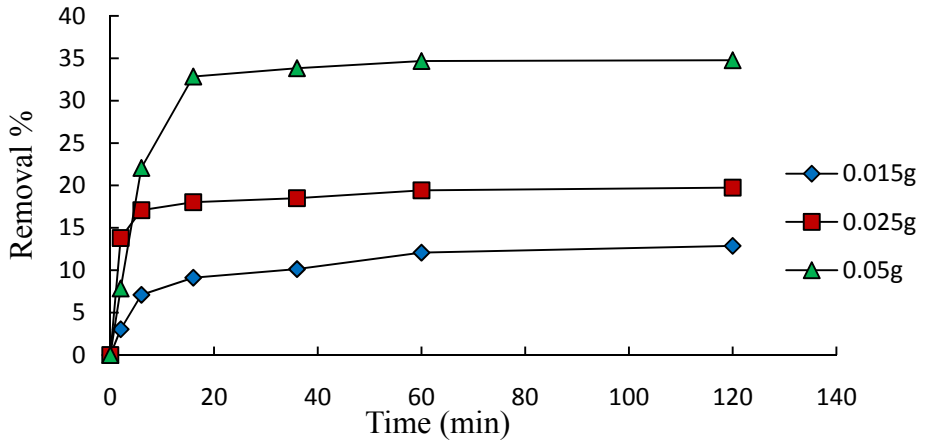

Figure 4.23: Time variation of chromium sorption on acetic acid CAs at different sorbent dosages (data in appendix B).

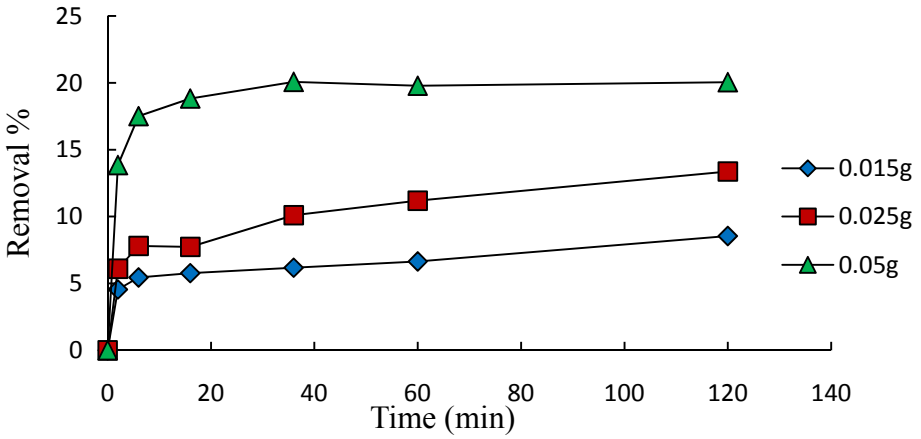

Figure 4.24: Time variation of chromium sorption on sodium carbonate CAs at different sorbent dosages (data in appendix B).

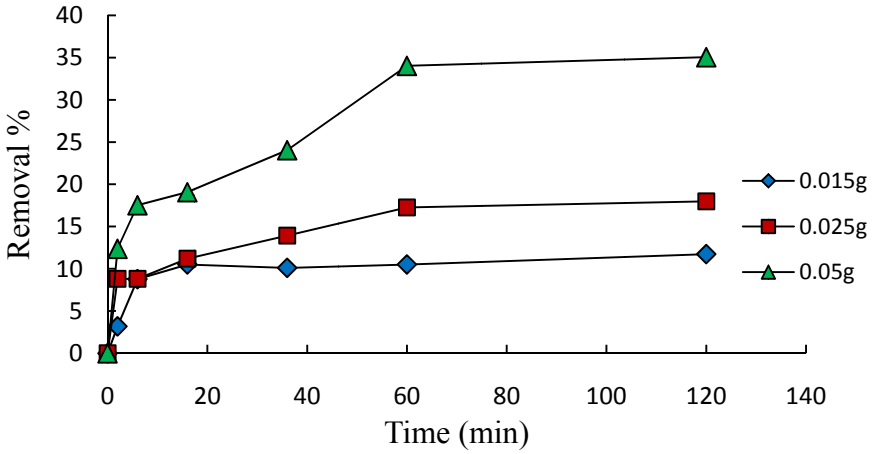

Figure 4.25: Time variation of chromium sorption on sodium hydroxide CAs at different sorbent dosages (data in appendix B).

Figure 4.26 shows a reverse trend in the loading capacity (q_t).The loading capacity decreased as the adsorbent dosage was increased. This can be explained by the fact that for a fixed amount of adsorbate the adsorption sites remain unsaturated during the adsorption reaction, whereas the number of available sites is increased by increasing the dosage [Rahman, 2007].

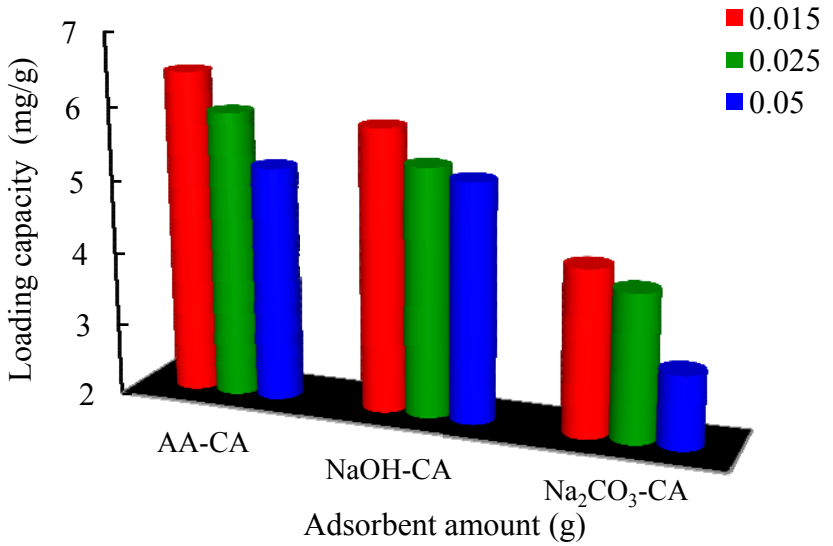

Figure 4.26: Adsorption capacity of chromium variation with different adsorbent dosages (data in appendix B).

The results obtained using the three types of CAs were tested with both pseudo first and second-order kinetic models using equations 3.1 and 3.3. Figures 4.27 to 4.32 represent the linear plots of both models.

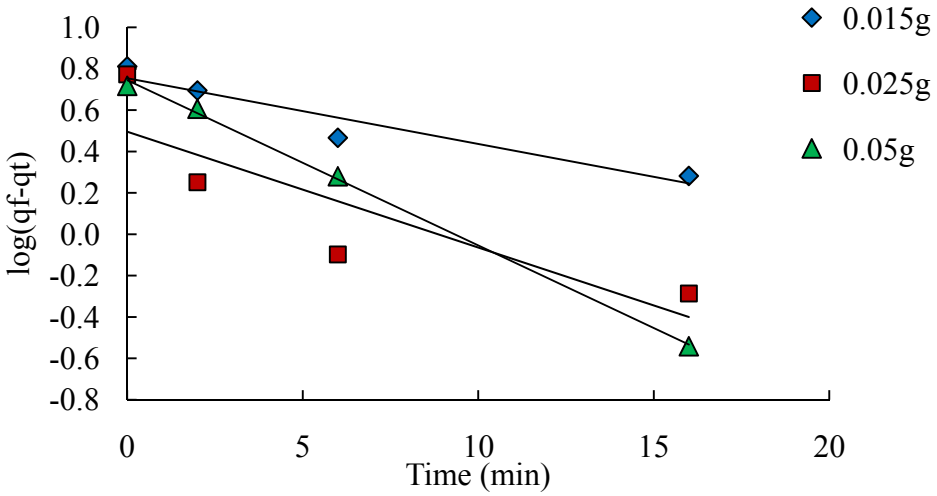

Figure 4.27: Pseudo-first order plot of sorption of chromium on acetic acid CA at varying sorbent dosages (data in appendix B).

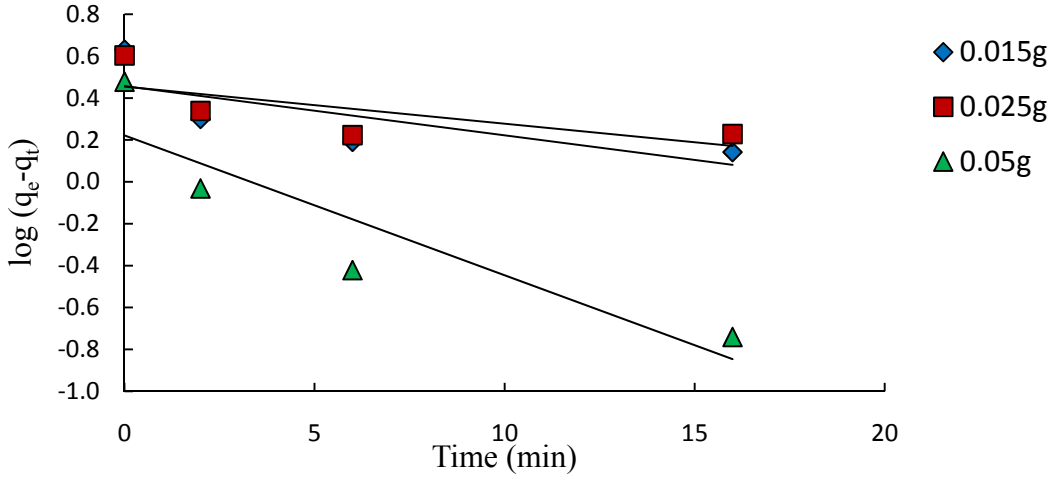

Figure 4.28: Pseudo-first order plot of sorption of chromium on sodium carbonate CA at varying sorbent dosages (data in appendix B).

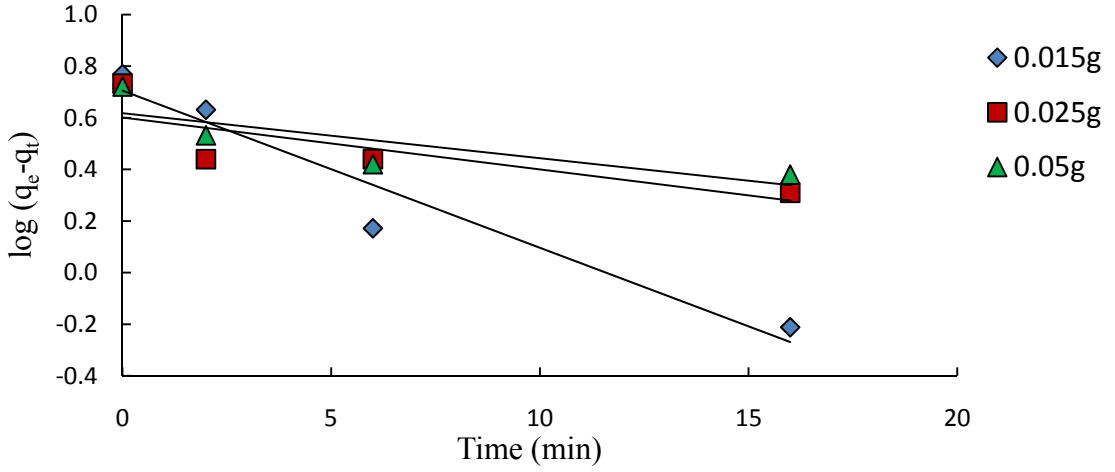

Figure 4.29: Pseudo-first order plot of sorption of chromium on sodium hydroxide CA at varying sorbent dosages (data in appendix B).

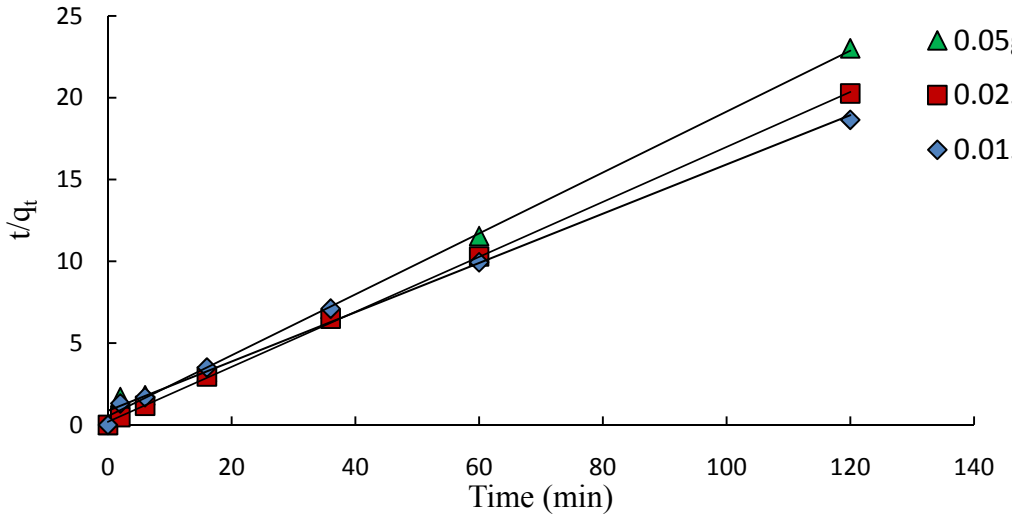

Figure 4.30: Pseudo-second order plot of sorption of chromium on acetic acid CA at varying sorbent dosages (data in appendix B).

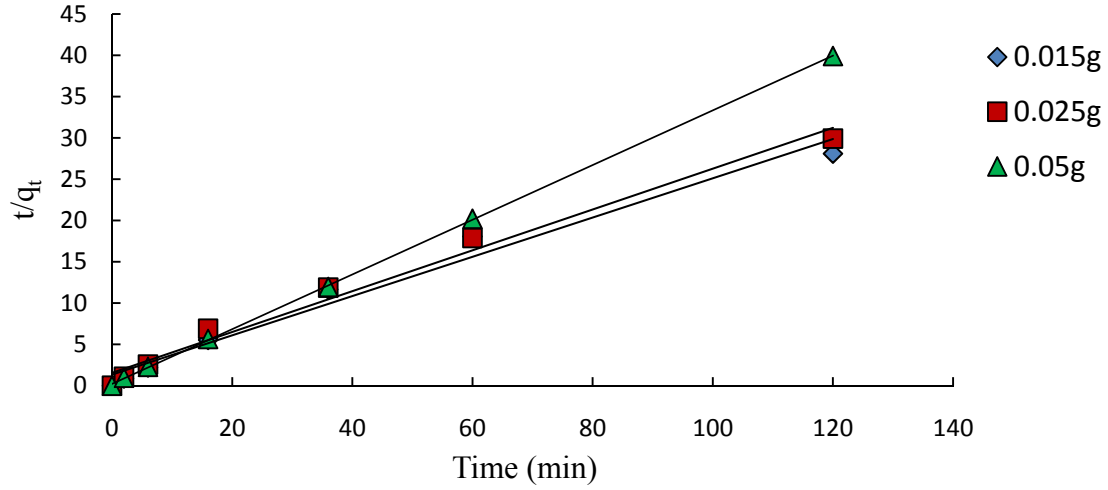

Figure 4.31: Pseudo-second order plot of sorption of chromium on sodium carbonate CA at varying sorbent dosages (data in appendix B).

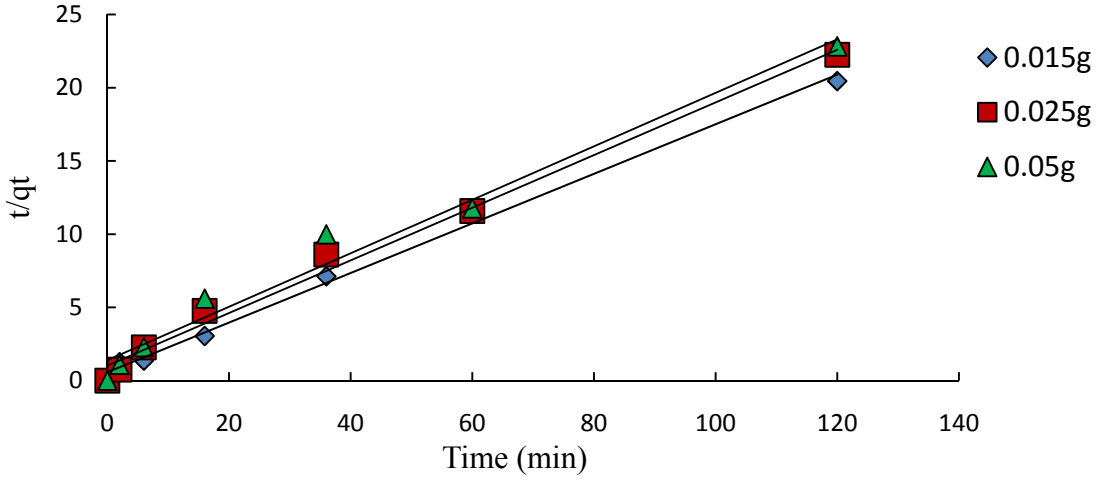

Figure 4.32: Pseudo-second order plot of sorption of chromium on sodium hydroxide CA at varying sorbent dosages (data in appendix B).

Tables 4.5 to 4.7 present the two model parameters. A comparative analysis of the linearity of the plots obtained from the test of the two kinetic models with the sorption data showed that the pseudo-second order kinetic model had better linearity (R^2) and could be said to describe the mechanism of sorption of chromium by the three types of CAs at different sorbent dosages.

Table 4.5: Kinetic parameters for the sorption of Cr at different acetic acid CA dosages.

Adsorbent amount	Pesudo-first order parameters			Pseudo-second order parameters			
	q_{e1}	k_f	R^2	q_{e2}	k_s	h	R^2
0.015	1.016	0.0046	0.006	6.667	0.026	1.1557	0.993
0.025	1.694	0.0415	0.315	5.952	0.1494	5.2927	0.999
0.05	5.649	0.1152	0.992	5.376	0.186	5.3763	0.997

k_f= min^{-1}; q_{e1}= mg/g ; k_s = $g.mg^{-1}.min^{-1}$; h = $g.mg^{-1}.min^{-1}$

Table 4.6: Kinetic parameters for the sorption of Cr at different sodium carbonate CA dosages.

Adsorbent amount	Pesudo-first order parameters			Pseudo-second order parameters			
	q_{e1}	k_f	R^2	q_{e2}	k_s	h	R^2
0.015	2.858	0.053	0.576	4.219	0.04185	0.7451	0.976
0.025	2.845	0.0392	0.5	4.049	0.0394	0.6458	0.983
0.05	1.663	0.152	0.818	3.021	0.5	4.5637	0.999

k_f= min^{-1}; q_{e1}= mg/g ; k_s = $g.mg^{-1}.min^{-1}$; h = $g.mg^{-1}.min^{-1}$

Table 4.7: Kinetic parameters for the sorption of Cr at different sodium hydroxide CA dosages.

Adsorbent amount	Pesudo-first order parameters			Pseudo-second order parameters			
	q_{e1}	k_f	R^2	q_{e2}	k_s	h	R^2
0.015	5.070	0.1382	0.937	5.917	0.050	1.739	0.995
0.025	3.981	0.0461	0.640	5.587	0.032	0.990	0.99
0.05	4.140	0.0346	0.662	5.495	0.031	0.942	0.989

k_f= min^{-1}; q_{e1}= mg/g ; k_s = $g.mg^{-1}.min^{-1}$; h = $g.mg^{-1}.min^{-1}$

4.5.3 Effect of pH on the sorption process

The term pH is used to describe the acid-base characteristics of water; it can be measured by using a pH meter. Formally, pH is the negative logarithm of the H^+ concentration, *i.e.*, pH= -log [H^+]. The following values indicate the classification of water using pH [Ayres, 1994]:

pH < 7 refers to acid solutions
pH > 7 refers to basic solutions
pH = 7 refers to neutral solutions

The study on the effect of pH was conducted at a constant initial metal ions concentration of 30 mg/l, adsorbent dose 0.05 g and a maximum agitation period of 120 min for all CAs at varying pH levels. Figure 4.35 and Table 4.8 show the effect of initial solution pH on percentage removal of chromium using three types of CAs. It can be observed from Figure 4.33, with the increase of the initial solution pH from 2.0 to 5.0, the percent removal of chromium ion for the CAs prepared using sodium hydroxide and acetic acid increased. However, a reverse trend was observed in the CA prepared by sodium carbonate, and this is attributed to the C=C substitute which is due to due meta substitute aromatic (resorcinol) as represented in Figure 4.7. This resorcinol will increase the pH of the initial solution because of the hydroxyl. It was also observed that increasing the pH above 5.0 (6.0 and 8.0), lead to a decrease in the removal percentage value in all types of adsorbents used.

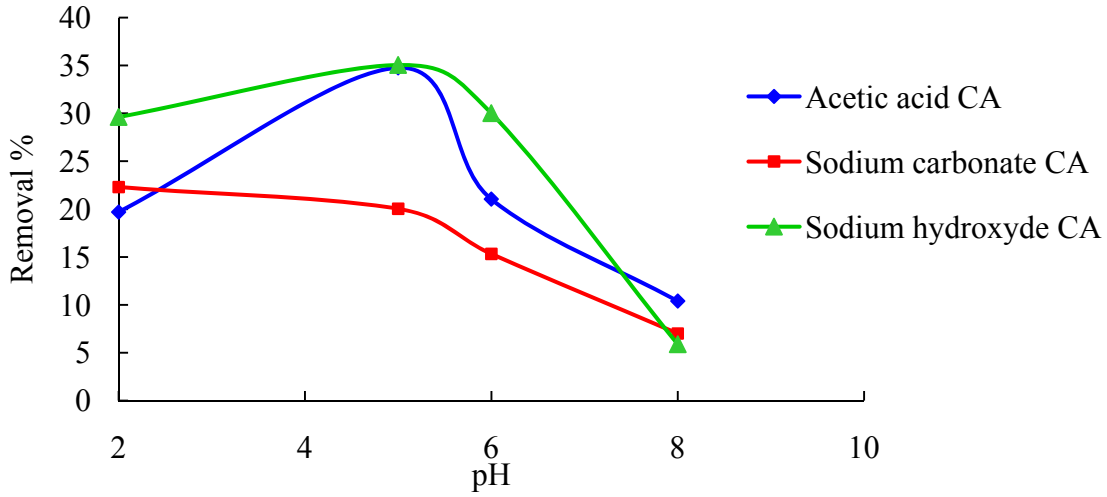

Figure 4.33: Effect of pH on chromium removal through sorption on three types of CAs (data in appendix B).

In a range of higher pH levels, precipitation of metal ions resulted in the lower efficiency of adsorption [Yu, 1995; Rahman, 2007; Meena *et al*., 2005]. According to a study made by Ayres *et al*., (1994) on pH effect on chromium solution, this hypothesis is reasonable. Figure 4.34 shows the findings from this study where the y-axis displays the concentration of dissolved chromium in the wastewater, in mg/L. A wide variation in the scale can be observed. The upper part of the scale shows a dissolved concentration of 100 mg/L. The lowest number on the scale is 0.001 mg/L. This solubility graph displays regions where the chromium is soluble or insoluble. The region above the dark line (the shaded area) signifies that the chromium should precipitate as chromium hydroxide. The region below or outside of the dark line illustrates where the chromium is dissolved in solution and no precipitation occurs.

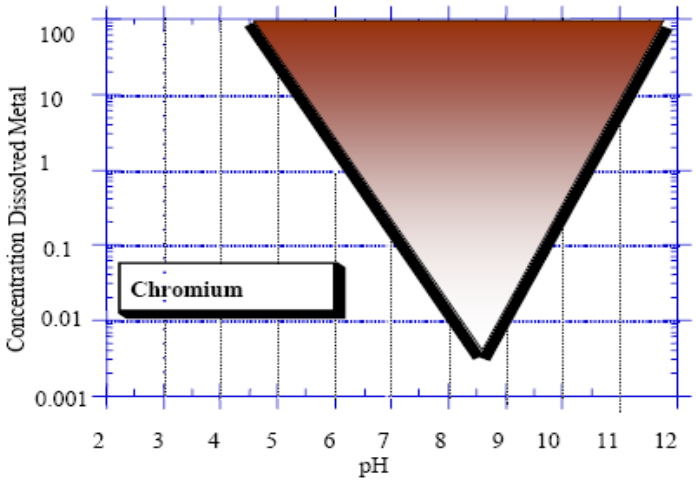

Figure 4.34: Chromium solubility under different pH values, by Ayres *et al.* (1994).

At lower pH, both the adsorbent surface and adsorbate species distribution changes are positively charged which lead to a competition between H^+ and Cr^{+6} for adsorption at the ion-exchangeable sites on the surface of the CA, leading to a low removal of metal [Rahman , 2007; Meena *et al*., 2005].

Table 4.8: The Effect of pH levels on chromium removal through sorption on three types of CAs

Contact time: 2hrs, temperature: 23^0C, chromium concentration: 30ppm								
Acetic acid CA			Sodium carbonate CA			Sodium hydroxide CA		
pH	Equili-brium conc.	Removal %	pH	Equilibri-um conc.	Removal %	pH	Equilibri-um conc.	Remo-val %
2	24.089	19.7	2	23.3086	22.304	2	24.614	17.954
5	19.571	34.763	5	23.988	20.041	5	19.485	35.051
6	23.686	21.047	6	25.402	15.327	6	20.993	30.025
8	26.883	10.389	8	27.897	7.011	8	28.235	5.884

The results obtained using the three types of CAs were tested with both pseudo first and second-order kinetic models using equations 4.2 and 4.4. Figures 4.35 to 4.37 present the linear plots of pseudo first order model, whereas Figures 4.38 to 4.40 represent the pseudo second order model.

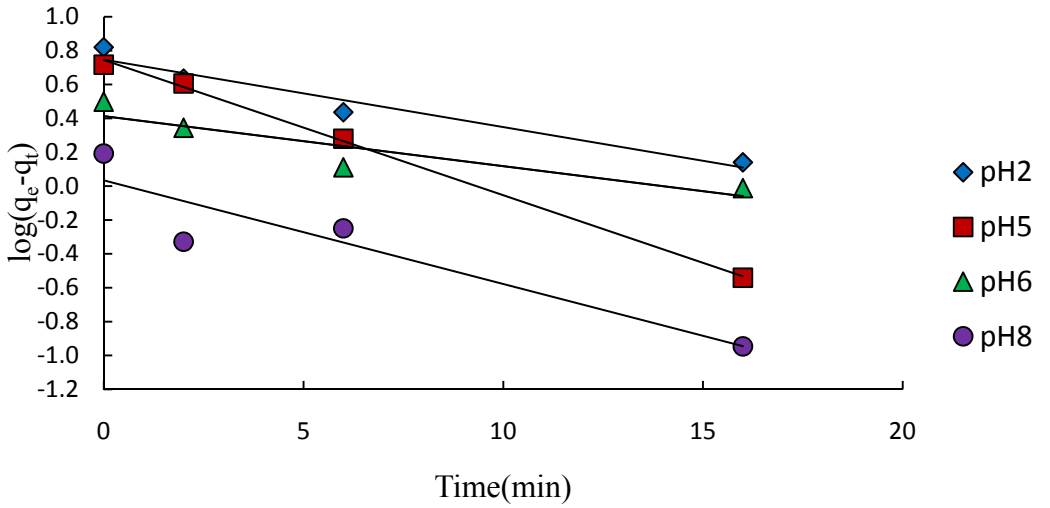

Figure 4.35: Pseudo-first order plot of sorption of chromium on acetic acid CA at different pH levels (data in appendix B).

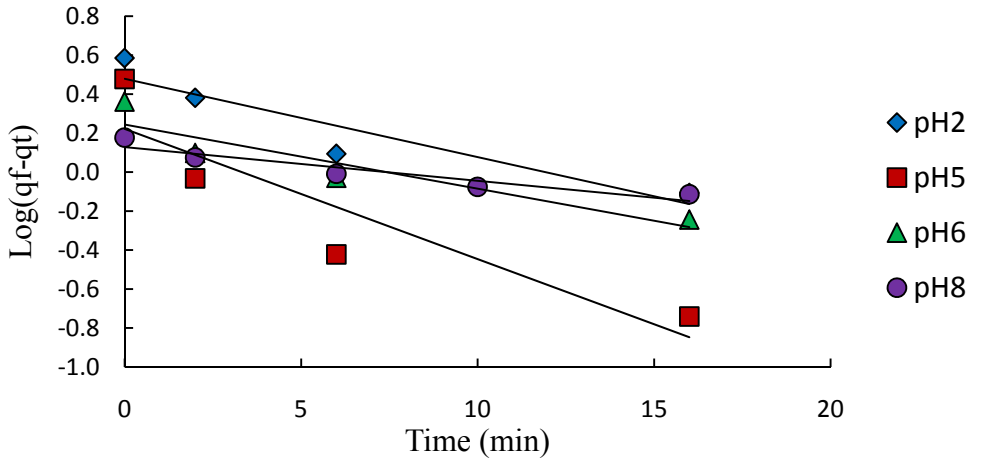

Figure 4.36: Pseudo-first order plot of sorption of chromium on sodium carbonate CA at different pH levels (data in appendix B).

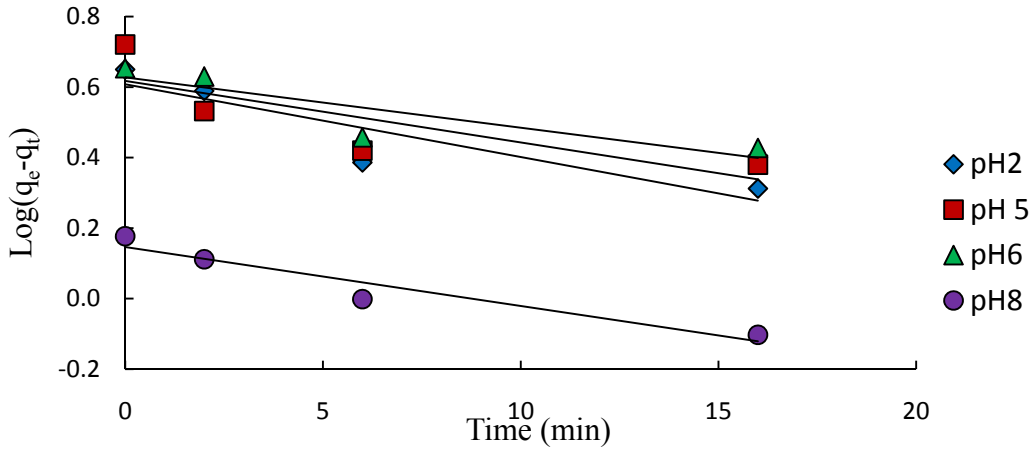

Figure 4.37: Pseudo-first order plot of sorption of chromium on sodium hydroxide CA at different pH levels.

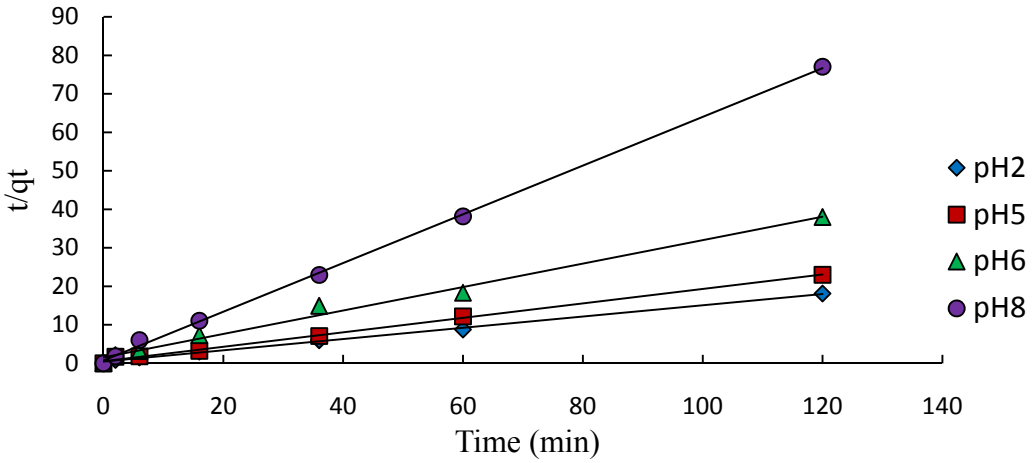

Figure 4.38: Pseudo-second order plot of sorption of chromium on acetic acid CA at different pH levels (data in appendix B).

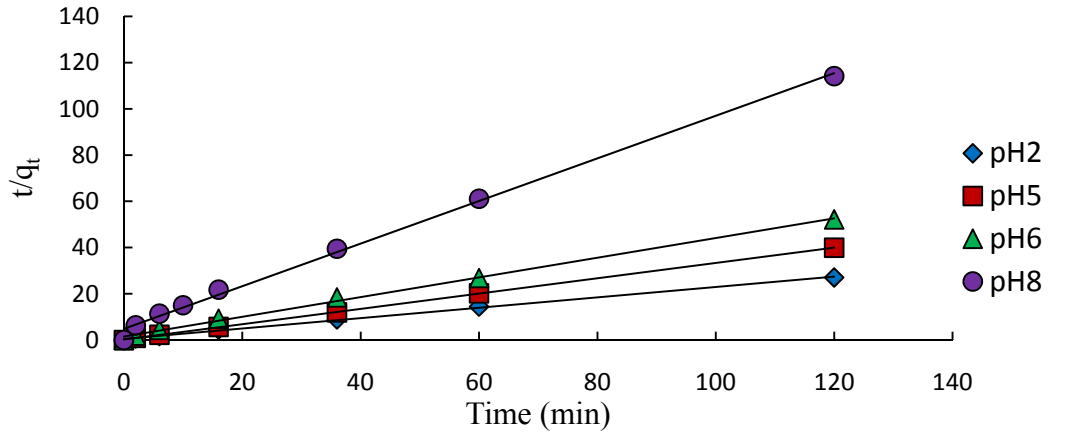

Figure 4.39: Pseudo-second order plot of sorption of chromium on sodium carbonate CA at different pH levels (data in appendix B).

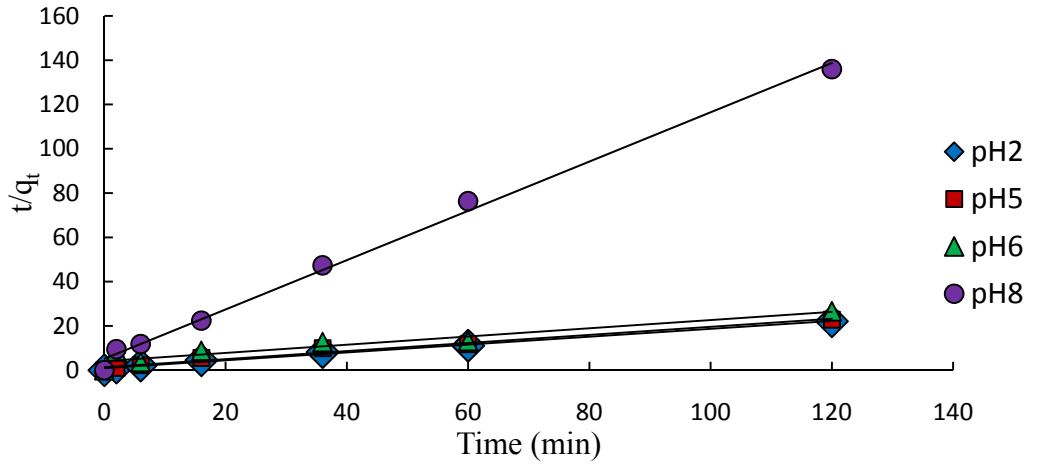

Figure 4.40: Pseudo-second order plot of sorption of chromium on sodium hydroxide CA at different pH levels (data in appendix B).

Tables 4.9 to 4.11 present the two model parameters. The kinetic study showed that Pseudo-second-order model had better linearity (R^2) and could be said to describe the mechanism of sorption of chromium by the three types of CAs under different pH levels.

Table 4.9: Kinetic parameters for the sorption of Cr using acetic acid CA under different pH levels.

Solution pH	Pseudo-first order parameters			Pseudo-second order parameters			
	q_{e1}	k_f	R^2	q_{e2}	k_s	h	R^2
2	2.655	0.065	0.966	5.348	0.0610	1.745	0.997
5	5.649	0.115	0.992	5.376	0.186	5.376	0.997
6	2.588	0.067	0.839	3.289	0.06	0.646	0.989
8	1.081	0.141	0.863	1.583	0.538	1.348	0.999

k_f= min^{-1}; q_{e1}= mg/g ; k_s = $g.mg^{-1}.min^{-1}$; h = $g.mg^{-1}.min^{-1}$

Table 4.10: Kinetic parameters for the sorption of Cr using sodium carbonate CA under different pH levels.

Solution pH	Pseudo-first order parameters			Pseudo-second order parameters			
	q_{e1}	k_f	R^2	q_{e2}	k_s	h	R^2
2	3.013	0.092	0.873	3.378	0.177	2.020	0.999
5	1.663	0.152	0.818	3.021	0.500	4.564	0.999
6	1.75	0.074	0.856	2.353	0.117	0.648	0.997
8	1.343	0.039	0.89	1.086	0.174	0.205	0.996

k_f= min^{-1}; q_{e1}= mg/g ; k_s = $g.mg^{-1}.min^{-1}$; h = $g.mg^{-1}.min^{-1}$

Table 4.11: Kinetic parameters for the sorption of Cr using sodium hydroxide CA under different pH levels.

Solution pH	Pseudo-first order parameters			Pseudo-second order parameters			
	q_{e1}	k_f	R^2	q_{e2}	k_s	h	R^2
2	4.23	0.035	0.782	5.780	0.006	0.190	0.751
5	4.14	0.0346	0.662	5.495	0.031	0.942	0.977
6	4.24	0.0322	0.763	5.405	0.008	0.243	0.894
8	1.4	0.0369	0.923	0.898	0.24	0.193	0.995

k_f= min^{-1}; q_{e1}= mg/g ; k_s = $g.mg^{-1}.min^{-1}$; h = $g.mg^{-1}.min^{-1}$

The results of chromium ion adsorption by all types of carbon aerogels using 0.025 g of adsorbent dose and 30 mg/l chromium ion solution concentration under room temperature are as shown in Figure 4.41. The results show that the carbon aerogel prepared by using acetic acid has the highest removal percentage of 19.74 %. This is followed by the carbon aerogel prepared using sodium hydroxide with a removal percentage of 17.98 % and then the one prepared by using sodium carbonate at13.37 %.

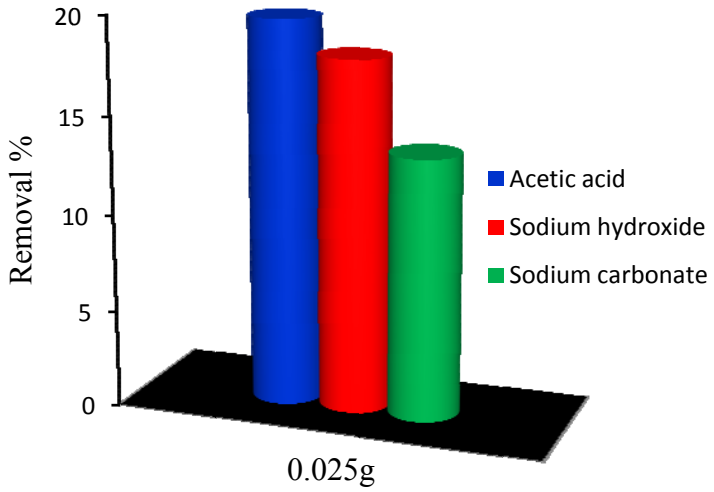

Figure 4.41: Adsorption removal percentage of chromium ion using three types of CAs.

The difference in adsorption capacity between the carbon aerogel prepared using acetic acid and those prepared using sodium carbonate and sodium hydroxide is not as high as the difference in the functional groups (hydroxyl and carboxyl groups) which mostly affect the uptake of chromium ion. These is due to the hypothesis that carboxyl groups will often lend their OH- H+ into solution and therefore act as acids that will lead to a reduction in the pH level of the solution [Shukla *et al*., 2005; Crews *et al*., 1998; Pavia *et al*., 2001; Aramata *et al*., 1991]. This in turn will reduce the adsorption capacity of the chromium ion. This was confirmed by a kinetic study using four different pH levels as shown in Figure 4.42. Based on this study the main finding was that at an acidic condition of pH=2 the chromium uptake was low compared to the uptake at pH=5; and it will decrease again with further increasing in the pH (6 and 8).

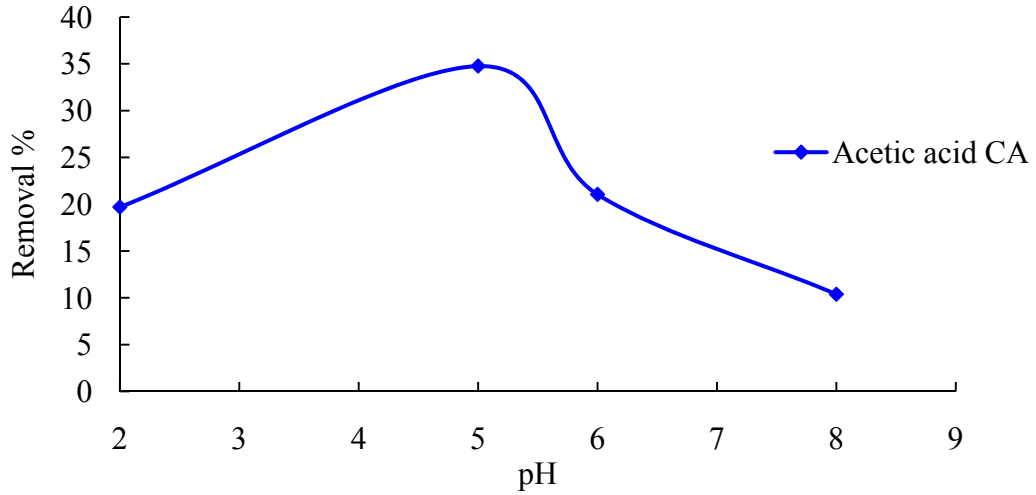

Figure 4.42: Effect of pH on chromium removal through sorption on carbon aerogel prepared using acetic acid.

4.5.4 Concluding remarks of the sorption kinetic study

The kinetic study showed that the pseudo second order equation was more suitable to describe the adsorption of the chromium ion than first order equation as established from the correlation coefficient values as well as the predicted value for q_e deviated considerably from the theoretical calculation data of q_e. It was clearly found that the sorption capacity (q_e) values increased with increasing the initial chromium concentrations, and decreased by increasing the adsorbent dosages. It is found that in a range of high pH levels, precipitation of metal ions resulted in the lower efficiency of adsorption. At lower pH, there is a competition between H^+ and Cr^{+6} for adsorption at the ion-exchangeable sites on the surface of the CAs, which leads to a low removal of chromium. .

4.6 Isotherm study

Batch isotherm studies were conducted using different concentrations of chromium. This was done in order to study the equilibrium relationship between the concentration of the chromium in the fluid phase and its concentration in the CAs at constant temperature, pH, and amount of adsorbent.

In order to understand the mechanism of chromium adsorption on CAs, the experimental data were analyzed using two of the most widely used adsorption isotherms equations (i.e. Langmuir, and Freundlich isotherm equations) [Akinbayo, 2000; Fabre *et al*., 2003; Meena *et al*., 2005; Jusoh *et al.*, 2005; Goel *et al*., 2006; Oladoja, 2007; Rahman , 2007; Aber *et al*., 2007]. The different isotherm parameters, obtained from the different plots using the CAs, are presented in Tables 4.12 and 4.13.

In order to evaluate the fitness of each isotherm equation to the experimental data obtained, an error function is required. In the present study the linear correlation coefficient of determinations, R^2, was used [Rahman, 2007].

The linerized form of Langmuir adsorption isotherm was presented in equation 3.6. The plot of $1/q_e$ versus $1/C_e$ is shown in Figure 4.43.

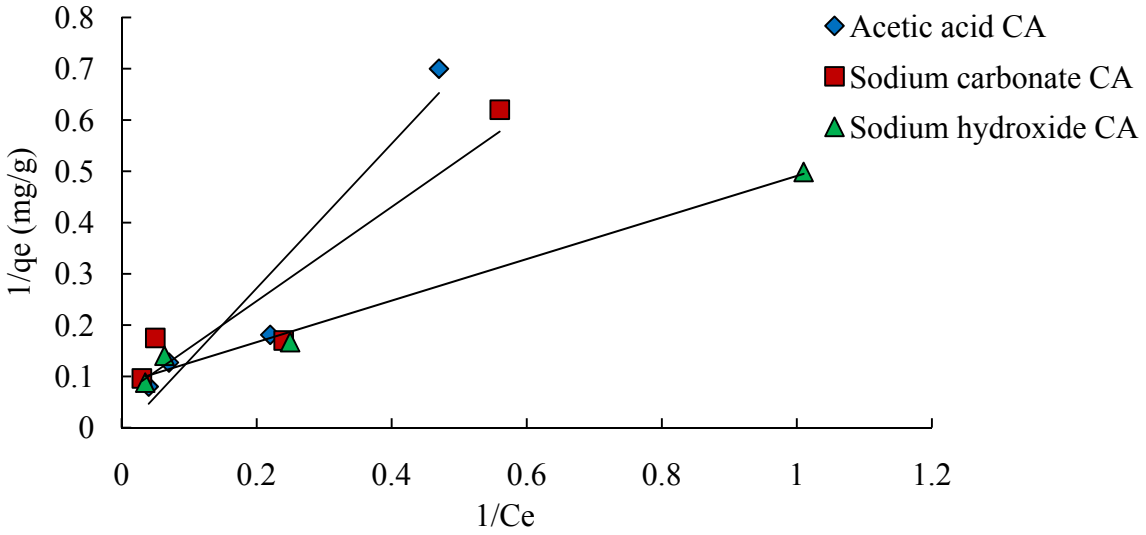

Figure 4.43: Linear plots for the sorption of chromium onto CA prepared using acetic acid, sodium carbonate and sodium hydroxide based on Langmuir (data in appendix B).

The linearized form of the Freundlich isotherm model can be written as in equation 3.8. The plot of $\log q_e$ versus $\log C_e$ is presented in Figure 4.44.

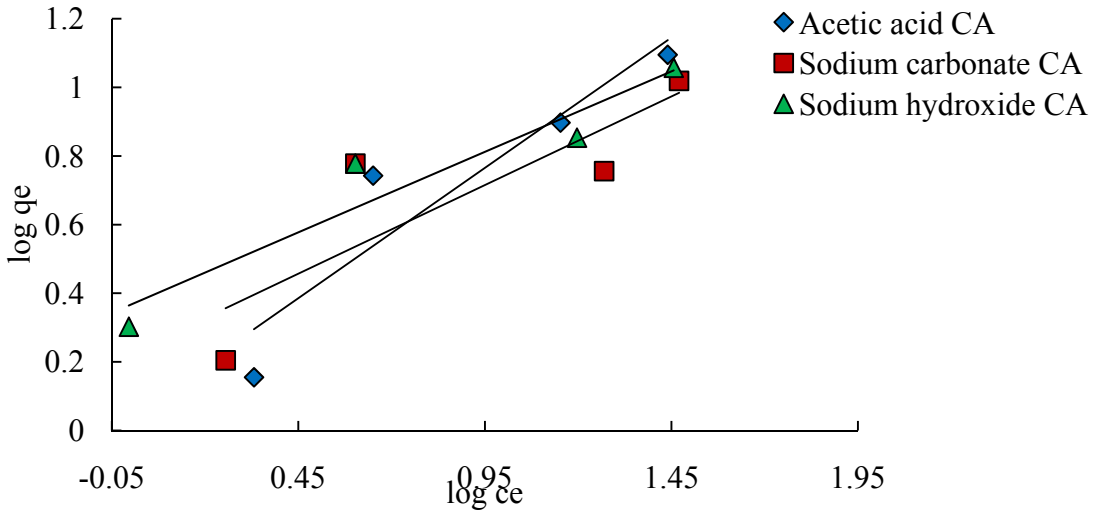

Figure 4.44: Linear plots for the sorption of chromium onto CA prepared using acetic acid, sodium carbonate and sodium hydroxide based on Freundlich (data in appendix B).

The Langmuir and Freundlich equations were used to describe the data derived from the adsorption of Cr by each adsorbent over the entire concentration range studied. The plot of $1/q_e$ versus $1/C_e$ showed that the experimental data was reasonably well fitted with the linearized equation of the Langmuir isotherm for all of the Cr concentration range studied. Linear plots of ln q_e versus ln C_e showed that the Freundlich isotherm also represented the Cr adsorption for all types of adsorbent tested. In this study, the prepared CAs showed that the Langmuir isotherm was the better fitted model than the Freundlich

as the former has higher linear correlation coefficient than the latter (Tables 4.12 and 4.13). This therefore, indicates the applicability of monolayer coverage of the Cr on the surface of the adsorbents, which is consistent with kinetic results.

Table 4.12: Langmuir parameters for the sorption of Cr at using the three types of CAs.

Adsorbent material	Equation	q_m	k	R^2
Acetic acid CA	$q_e = \frac{(0.007)(100).C_e}{1+(0.007).C_e}$	100	0.007	0.92
Sodium carbonate CA	$q_e = \frac{(0.067)(15.87)C_e}{1+(0.067)C_e}$	15.87	0.067	0.89
Sodium hydroxide CA	$q_e = \frac{(0.21)(11.76)C_e}{1+(0.21)C_e}$	11.76	0.21	0.99

q_m is estimated from the Langmuir equation.

Table 4.13: Freundlich parameters for the sorption of Cr using the three types of CAs.

Adsorbent material	Equation	n	k_l	R^2
Acetic acid CA	$q_e = 1.104C_e^{1/1.318}$	1.318	1.104	0.87
Sodium carbonate CA	$q_e = 1.675C_e^{1/1.938}$	1.938	1.675	0.72
Sodium hydroxide CA	$q_e = 2.323.C_e^{1/2.132}$	2.132	2.323	0.92

4.6.1 Concluding remarks of the sorption isotherm study

From the isotherm study it was found that the data were better fitted by the Langmuir isotherm model than the Freundlich one. This result indicates presence of chemisorptions and monolayer coverage of the chromium on the surface of CAs. This result was found to be similar for the all CAs used throughout this study.

When these adsorption results compared with the results from Okparanma and Ayotamuno (2008) (78.6%), we found their removal percentage was higher than the one achieved in this study (Acetic acid CA 52.6 %, sodium hydroxide CA 47.5%, and 37.9 %). This because they used adsorbent dosages of 10g/l, while 0.05g were used in this study using the three type of CAs.

REFERENCES

Abdullah M. A., Chiang L., Nadeem M., "Comparative evaluation of adsorption kinetics and isotherms of a natural product removal by Amberlite polymeric adsorbents," *Chemical Engineering Journal*, 2007.

Aber S., Daneshvara N., Soroureddina S. M., Chaboka A., Asadpour-Zeynalib K., "Study of acid orange 7 removal from aqueous solutions by powdered activated carbon and modeling of experimental results by artificial neural network," *Desalination*, vol. 211, pp. 87–95, 2007.

Acharya J., Sahu J.N., Sahoo B.K., Mohanty C.R., Meikap B.C., "Removal of chromium(VI) from wastewater by activated carbon developed from Tamarind wood activated with zinc chloride", *Chemical Engineering Journal*, (2008), doi:10.1016/j.cej.2008.11.035.

Akinbayo, A., "Removal of lead from aqueous solutions by adsorption using peat moss." Master's thesis, University of Regina, Canada, 2000.

Alkarkhi A. F. M. & Ahmad A., Ismail N., & Easa A. M., "Multivariate analysis of heavy metals concentrations in river estuary," *Environ Monit Assess*, vol. 143, pp. 179–186, 2008.

Allen S.J., Mckayb G., Porter J.F., "Adsorption isotherm models for basic dye adsorption by peat in single and binary component systems," *Journal of Colloid and Interface Science*, vol. 280, pp. 322–333, 2004.

Aramata A., Enyo M., Koga O., and Hori Y., "FTIR spectrometry of the reduced CO^2 at Pt electrode and anomalous of Ca^{+2} ions," *Chemisrty letters*, pp. 749-752, 1991.

Ayres D. M., Davis A. P., Gietka P. M., "Removing Heavy Metals from Wastewater," University of Maryland, Engineering Research Center Report, August 1994.

Baral S. S., Das S. N., Rath P., "Hexavalent chromium removal from aqueous solution by adsorption on treated sawdust", *Biochemical Engineering Journal*, vol. 31, pp. 216–222, 2006.

Benmaamar Z., Bengueddach A., "Correlation with Different Models for Adsorption Isotherms of m-Xylene and Toluene on Zeolites," *Journal of Applied Sciences in Environmental Sanitation*, vol. 2, pp. 43-56, 2007.

Bock V., Emmerling A., and Fricke J., "Influence of monomer and catalyst concentration on RF and carbon aerogel structure," *Journal of Non Crystalline Solids*, vol. 225, pp. 69–73, 1998.

Brandt R., and Fricke J., "Acetic-acid-catalyzed and subcritically dried carbon aerogels with a nanometer-sized structure and a wide density range," *Journal of Non-Crystalline Solids*, vol. 350, pp. 131–135. 2004

Brandt R., Petricevic R., Bstle H. P., and Fricke J., "Acetic Acid Catalyzed Carbon Aerogels," *Journal of Porous Materials*, vol. 10, pp. 171–178, 2003.

Castilla C. M., and Hodar F.J. M., "Carbon aerogel for catalysis applications: An overview," *Carbon*, vol. 43, pp. 455-465, 2005.

Castilla C. M., and Morfin I., "Nanoporous carbon materials: Comparison between information obtained by SAXS and WAXS and by gas adsorption," *Carbon*, vol. 43, pp. 3002-3039, 2005.

Cheryan M., and Rajagopalan N., "Membrane processing of oily streams. Wastewater treatment and waste reduction," Journal of Membrane Science, vol. 151, Issue 1, pp 13-28, December 1998.

Chuah T. G., Jumasiah A., Azni I., Katayon S., ChoongS.Y. T., "Rice husk as a potentially low-cost biosorbent for heavy metal and dye removal: an overview," *Desalination*, vol. 175, pp. 305-316, 2005.

Cotet L.C., Gich M., Roig A., Popescu I.C., Cosoveanu V., Molins E., and Danciu V., "Synthesis and structural characteristics of carbon aerogels with a high content of Fe, Co, Ni, Cu, and Pd," *Journal of Non-Crystalline Solids*, vol. 352, pp 2772–2777, 2006.

Crews P., Rodriguez J., and Jaspars M., "Organic structure analysis," University of California, Santa Cruz," Oxford University press, 1998.

Czakkel O., Marthi K., Geissler E., and Laszlo K., "Influence of drying on the morphology of resorcinol-formaldhyde-based gels," *Microporous and Mesoporous Materials*, vol. 86, pp 124-133, 2005.

Demirbas E., Kobya M., Senturk E., Ozkan T., "Adsorption kinetics for the removal of chromium (VI) from aqueous solutions on the activated carbons prepared from agricultural wastes," *Water SA*, vol. 30, pp. 533-539, October 2004

Demirbas A., "Heavy metal adsorption onto agro-based waste materials: A review," *Journal of Hazardous Materials*, vol. 157, pp. 220-229, 2008.

Dolle F. E., Jimenez D. F., Fabry S. B., Achard P., Bley F., Marin F. C., Djurado D., Castilla C. M. and Morfin I., "Nanoporous carbon materials: Comparison between information obtained by SAXS and WAXS and by gas adsorption," *Carbon*, vol. 43, pp. 3002–3039, 2005.

Du H., Li B., Kang F., Fu R., Zeng Y., "Carbon aerogel supported Pt–Ru catalysts for using as the anode of direct methanol fuel cells," *Carbon*, vol. 45, pp. 429–435, 2007.

Durairaj R. B., *Resorcinol: Chemistry, Technology and Applications*, Birkhauser, 2005, pp. 181.

Fabry S. B., Langohr D., Achard P., Charrier D., Djurado D., and Dolle F. E., "Anisotropic high-surface-area carbon aerogels," *Journal of Non-Crystalline Solids*, vol. 350, pp. 136–144, 2004.

Faust S. D., Aly O. M., *Chemistry of water treatment*, 2nd edition, CRC Press, 1998, pp. 135-137.

Gavalda S., Gubbins K. E., Hanzawa Y., Kaneko K., and Thomson K. T., "Nitrogen adsorption in carbon aerogels: A molecular simulation study," *Langmuir*, vol. 18, pp. 2141-2151, 2002.

Goel J., Kadirvelu K., Rajagopal C., Garg V. K., "Cadmium (II) uptake from aqueous solution by adsorption onto carbon aerogel using a response surface methodological approach," *Ind. Eng. Chem. Res*., vol. 45, pp. 6531-6537, 2006.

Goel J., Kadirvelu K., Rajagopal C., Vinod K. G.,"Investigation of adsorption of lead, mercury and nickel from aqueous solutions onto carbon aerogel," *Journal of chemical technology and biotechnology*, vol. 80, pp. 469-476, 2005.

Goel J., Kadirvelu K., Rajagopal C., Garg V.K., "Removal of mercury (II) from aqueous solution by adsorption on carbon aerogel: Response surface methodological approach," *Carbon*, vol. 43, pp. 195–213, 2005.

Goel J., Kadirvelu K., Rajagopal C., Vinod Kumar G., "Investigation of adsorption of lead, mercury and nickel from aqueous solutions onto carbon aerogel," *chemical technology and biotechnology*, vol. 80, pp. 469-476, 2005.

Guilminot E., Fischer F., Chatenet M., Rigacci A., Fabry S. B., Achard P., and Chainet E., "Uses of cellulose-based carbon aerogelas catalyst support for PEM fuel cell electrodes: Electrochemical characterization, " *Power Sources*, vol. 166, pp. 104-111, 2007.

Guyer H. H., *Industrial Processes and Waste Stream Management*, John Wiley and Sons, 1998, pp. 106.

Hanson J.R., *Functional group chemistry*, The royal society of chemistry, 2001, pp. 1.

Hanzawa Y., Kaneko K., Yoshizawa N., Pekala R.W., and Dresselhaus M.S., "The Pore Structure Determination of Carbon Aerogels," *Adsorption*, vol. 4, 1998, pp. 187–195.

Hebalkar N., Arabale G., Sainkar S. R., Pradhan S. D., Mulla I. S., Vijayamohanan k., Ayyub p., and Kulkarni S. K., "Study of correlation of structural and surface properties with electrochemical behaviour in carbon aerogels," *Journal of materials science*, vol. 40, pg 3777 – 3782, 2005.

Horikawa T., Hayashi J., and Muroyama K., "Controllability pore characteristics of resorcinol-formaldehyde carbon aerogel," *Carbon*, vol. 42, pg 1625-1633, 2004.

Horikawa T., Ono Y., Hayashi J., and Muroyama K., "Influence of surface-active agents on pore characteristics of the generated spherical resorcinol–formaldehyde based carbon aerogels," *Carbon*, vol. 42, pp. 2683–2689, 2004.

Hua B., Deng B., Thornton E. C., Yang J., and Amonette J. E., "Incorporation of chromate into calcium carbonate structure during coprecipitation," *Water Air Soil Pollut*, vol. 179, pg 381–390, 2007.

Husing N., and Schubert U., "Aerogels," Wiley-VCH Verlag GmbH & Co. KGaA, Weinheim, pp. 1-27, 2005.

Hwang S. W., and Hyun S. H., "Capacitance control of carbon aerogel electrodes," *Journal of Non-Crystalline Solids*, vol. 347, pp. 238–245, 2004.

Jimenez D. F., Marıan F. C., and Castilla C. M., "Porosity and surface area of monolithic carbon aerogels prepared using alkaline carbonates and organic acids as polymerization catalysts," *Carbon*, vol. 44, pp. 2301–2307, 2006.

Jirglov H., Cadenas A. F. P., and Hodar F. J. M., "Synthesis and properties of phloroglucinol−phenol−formaldehyde carbon aerogels and xerogels," *Langmuir*, , 25 vol. 4, pp. 2461–2466, 2009.

Job N., Thery A., Pirard R., Marien J., Kocon L., Rouzaud J. N., Beguin F., and Pirard J. P., "Carbon aerogel,s cryogels and xerogels: Influence of drying method on the textural properties of porous carbon materials," *Carbon*, vol. 43, pp. 2481-2494, 2005.

Jusoh A., Chenga W.H., Lowa W.M., Ali N., M.J. Noor M. M., "Study on the removal of iron and manganese in groundwater by granular activated carbon," *Desalination*, vol. 182, pp. 347–353, 2005.

Kadirvelu K., Goel J., and Rajagopal C., "Sorption of lead, mercury and cadmium ions in multi-component system using carbon aerogel as adsorbent," *Journal of Hazardous Materials*, vol. 153, pp. 502–507, 2008.

Karthikeyan G., Ilango S. S., "Adsorption of Cr (VI) onto Activated Carbons Prepared from Indigenous Materials," *Journal of Chemistry*, vol. 5, pp. 666-678, October 2008.

Khan N. A., Mohamad H., "Investigations on the removal of chromium (VI) from wastewater by sugarcane bagasse," *Water & Wastewater Asia*, pp. 37-41, 2007.

Kumara P. A., Ray M., Chakraborty S., "Hexavalent chromium removal from wastewater using aniline formaldehyde condensate coated silica gel", *Journal of Hazardous Materials*, vol. 143, pp. 24–32, 2007.

Kuyucak, Nural, Sheremata, Tamara, "Lime neutralization process for treating acidic waters," U.S. Patent no. 5427691, Jun. 1995.

Li W., Reichenauerc G., and Frickeb J., "Carbon aerogels derived from cresol–resorcinol–formaldehyde for supercapacitors," *Carbon*, vol. 40, pp. 2955–2959, 2002.

Liang C., Sha G., and Guo S., "Resorcinol-formaldehyde aerogels prepared by supercritical acetone drying," *Journal of Non-Crystalline Solids*, vol. 271, pp. 167-170, 2000.

Liu N., Zhang S., Fu R., and Dresselhaus M. S. D. G., "Carbon aerogel spheres prepared via alcohol supercritical drying," *Carbon*, vol. 44, pp. 2430–2436, 2006.

Lowell S., Shields J. E., Thomas M. A., Thommes M., Characterization of porous solids and powders: surface area, pore size, and density, 4th rd, Springer, 2004, pp 13-14.

Matheickal J. T., Yu Q., "Biosorption of lead (II) and copper (II) from aqueous solutions by pre-treated biomass of Australian marine algae," *Bioresource Technology*, vol. 69, pp. 223-229, 1999.

Meena A. K., Mishra G.K., Rai P.K., Rajagopal C., and Nagar P.N., "Removal of heavy metal ions from aqueous solutions using carbon aerogel as an adsorbent," *Journal of Hazardous Materials*, vol. B122, pp. 161–170, 2005.

Melaku S., Cornelis R., Vanhaecke F., Dams R., Moens L, "Method development for the speciation of chromium in river and industrial wastewater using GFAAS," *Microchim Acta*, vol. 150, pp. 225–231, 2005.

Merzbacher C. I., Meier S. R., Pierce J. R., and Korwin M. L., "Carbon aerogels broadband non-reflective materials," *Journal of non-crystalline solids*, vol. 285, pp. 210-215, 2001.

Mor S., Ravindra K., Bishnoi N.R., "Adsorption of chromium from aqueous solution by activated alumina and activated charcoal," *Bioresource Technology*, vol. 98, pp. 954–957, 2007.

Nameni M., Moghadam M. R. A., Arami M., "Adsorption of hexavalent chromium from aqueous solutions by wheat bran," *Int. J. Environ. Sci. Tech.*, vol. 5, pp. 161-168, 2008.

Malaysia environmental quality report, 2004, pp 40-43

Noyes R., *Handbook of Pollution Control Processes*, William Andrew Inc., 1991, pp. 280.

Okparanma R. N., Ayotamuno M. J., "Predicting chromium (VI) adsorption rate in the treatment of liquid-phase oil-based drill cuttings," *African Journal of Environmental Science and Technology*, vol. 2, pp. 068-074, April 2008.

Okushita H., and Shimidzu T., "Membrane separation of Ga 3+ by selective interaction of Ga3+ with N-octadecanoyl-N-phenylhydroxylamine," *Journal of Membrane Science*, vol. 116, pp. 61-65, 1996.

Oladoja N. A., Asia I. O., Aboluwoye C. O., Oladimeji Y. B., and Ashogbon A. O., "Studies on the Sorption of Basic Dye by Rubber (Hevea brasiliensis) Seed Shell," *Turkish J. Eng. Env. Sci.*, vol. 32, pp. 143 – 152, 2008.

Park D., Yun Y. S., Jo J. H., Park J. M., "Mechanism of hexavalent chromium removal by dead fungal biomass of Aspergillus niger," *Water Research*, vol. 39, pp. 533–540, 2005.

Pavia D. L., Lampman G. M., and Kriz G. S., *Introduction to spectroscopy*, 3rd ed. Western Washington University, Harcourt college publisher, 2001, pp. 13-72.

Pehlivan E., Yanık B.H., Ahmetli G., Pehlivan M., "Equilibrium isotherm studies for the uptake of cadmium and lead ions onto sugar beet pulp," *Bioresour Technol.*, vol. 99, pp. 3520–3527, 2008.

Pekala R. W. and Alviso C. T., Lu X., and Fricke J., "New organic aerogels based upon a phenolic-furfural reaction," University of California, Livermore, California 94551, 1994.

Pekala R.W., "Organic aerogels from the polycondensation of resorcinol with formaldehyde," *Journal of materials science*, vol. 24, pp. 3221-3227, 1989.

Poloa M. S., Utrillaa J. R., Salhib E., and Guntenb U., "Ag-Adoped carbon aerogels for removing halide ions in water treatment," *Water research*, vol. 41, pp. 1031-1037, 2007.

Pradhan S. V., "Removal of heavy metals from wastewater and effect of anions on their adsorption by crabshells." Master's thesis, Lamar University, August, 2001.

Qin G., and Guo S., "Preparation of RF organic aerogels and carbon aerogels by alcoholic sol–gel process," *Carbon*, vol. 39, pp. 1929 –1941, 2001.

Rahman M. S., "The prospect of natural additives in enhanced oil recovery and water purification perations." Master's thesis, Dalhousie University, March, 2007.

Rana P., Mohan N., and Rajagopal C., "Electrochemical removal of chromium from wastewater by using carbon aerogel electrodes," *Water Research*, vol. 38, pp. 2811–2820, 2004.

Rawat M., Moturi C. M. Z., Subramanian V., "Inventory compilation and distribution of heavy metals in wastewater from small-scale industrial areas of Delhi, India," *The Royal Society of Chemistry*, vol. 5, pp. 906–912, 2003.

Reichenauer G., Emmerling A., Fricke J., and Pekala R.W., "Micro porosity in carbon aerogels," *Journal of Non-Crystalline Solids*, vol. 225, pp. 210–214, 1998.

Saliger R., Bock V., Petricevic R., Tillotson T., Geis S., and Fricke J., "Carbon aerogels from dilute catalyst of resorcinol with formaldehyde," *Journal of Non-Crystalline Solids*, vol. 221, pp. 144–150, 1998.

Saliger R., Fischer U., Herta C., and Fricke J., "High surface area carbon aerogels for super capacitors," *Journal of Non-Crystalline Solids*, vol. 225, pp. 81–85, 1998.

Sandu I., Brousse T. Schleich D.M., "Effect of nickel coating on electrochemical performance of graphite anodes for lithium ion batteries", *Ionics*, vol. 9, pp. 329-335, 2003.

Shen J., Hou J., Guo Y., XuE H., WU G., and Zhou B., "Microstructure Control of RF and Carbon Aerogels Prepared by Sol-Gel Process," *Journal of Sol-Gel Science and Technology*, vol. 36, pp. 131–136, 2005.

Shukla S.R., and Pai R.S., "Removal of Pb(II) from solution using cellulose containing materials," *J. Chem. Technol. Biotechnol.*, vol. 80, pp. 176–183, 2005.

Smith L., Means J., *Recycling and reuse of material found on superfund sites*, DIANE Publishing, 1994, pp. 34-35.

Solmaz S. K. A., G. Ustun E., Birgul A., Tasdemir Y., "Treatability studies with chemical precipitation and ion exchange for an organized industrial district (OID) effluent in Bursa, Turkey," *Desalination*, vol. 217, pp. 301–312, 2007.

Tadessea I., Isoahoa S.A., Greenb F.B., and Puhakka J.A., "Lime enhanced chromium removal in advanced integrated wastewater pond system," *Bioresource Technology*, vol. 97, Issue 4, pp. 529-534, March 2006.

Tamon H., and Ishizaka H., "Influence of Gelation Temperature and Catalysts on the Mesoporous Structure of Resorcinol–Formaldehyde Aerogels," note by *Journal of Colloid and Interface Science*, vol. 223, pp. 305–307, 2000.

Tamon H., and Ishizaka H., "SAXS study on gelation process in preparation of resorcinol-formaldehyde aerogel," *Journal of colloid and interface science*, vol. 206, pp. 577–582, 1998.

Tamon H., and Ishtzaka H., "Porous characterization of carbon aerogels," *Carbon*, vol. 36, pp. 1397-1409, 1998.

Tamon H., Ishizaka H., Mikami M., and Okazaki M., "Control of mesoporous structure of organic and carbon aerogels," *Carbon*, vol. 36, pp. 1257–1262, 1998.

Tamon H., Ishizaka H., M. Mikami and M. Okazaki, "Porous structure of organic and carbon aerogels synthesized by sol-gel poly condensation of resorcinol with formaldehyde," *Carbon*, vol. 35, pp. 791-796, 1997.

Tonanon N., Wareenin Y., Siyasukh A.,Tanthapanichakoon W. , Nishihara H., Mukai S. R., and Tamon H., "Preparation of resorcinol formaldehyde (RF) carbon gels:Use

of ultrasonic irradiation followed by microwave drying," *Journal of Non-Crystalline Solids*, vol. 352, pp. 5683–5686, 2006.

Volesky B., *Biosorption of Heavy Metals*, CRC Press, 1990, pp. 374.

Wang L. H., Lin C., "Equilibrium study on chromium (III) ion removal by adsorption onto rice hull ash," *Journal of the Taiwan Institute of Chemical Engineers*, vol. 40, pp. 110–112, 2009.

Wiener M., Reichenauer G., Scherb T., and FrickeJ., "Accelerating the synthesis of carbon aerogel precursors," *Journal of Non-Crystalline Solids*, vol. 350, pp. 126–130, 2004.

Wu D., and Fu R., Zhang S., Dresselhaus M. S., and Dresselhaus G., "Preparation of low-density carbon aerogels by ambient pressure drying," *Carbon*, vol. 42, pp. 2033–2039, 2004.

Wu D., and Fu R., "Fabrication and Physical Properties of Organic and Carbon Aerogel Derived from Phenol and Furfural," *Journal of Porous Materials*, vol. 12, pp. 311–316, 2005.

Wu D., and Fu R., "Synthesis of organic and carbon aerogels from phenol–furfural by two- step polymerization," *Microporous and Mesoporous Materials*, vol. 96, pp. 115–120, 2006.

Wu D., Fu R., Yu Z., "Organic and carbon aerogels from the naoh-catalyzed polycondensation of resorcinol–furfural and supercritical drying in ethanol," *Journal of applied polymer science*, vol. 96, no4, pp. 1429-1435, 2005.

Wu D., Fu R., Dresselhaus S. M., Dresselhaus G., "Fabrication and nano-structure control of carbon aerogels via a microemulsion-templated sol–gel polymerization method," *Carbon*, vol. 44, pp. 675–681, 2006.

Xu Y., Zhao D., "Reductive immobilization of chromate in water and soil using stabilized iron nanoparticles," *Water research*, vol. 41, pp. 2101 – 2108, 2007.

Xuan Z.X., Tang Y.R., Li X.M., Liu Y.H., and Luo F., "Study on the equilibrium, kinetics and isotherm of biosorption of lead ions onto pretreated chemically modified orange peel," *Biochem. Eng. J.*, vol. 31, pp. 160–164, 2006.

Yu B., "Adsorption of copper and lead from industrlal wastewater by maple sawdust." Ph.D. diss./Master's thesis, Lamar University – Beaumont. 1995.

Zanto E. J., Al-Muhtaseb S. A. , and Ritter J. A. "Sol-Gel-Derived Carbon Aerogels and Xerogels: Design of Experiments Approach to Materials Synthesis," *Ind. Eng. Chem. Res.*, vol. 41, pp. 3151-3162, 2002.

Zhang R., Lu Y., Meng Q., Zhan L.,Wu G. , Li K., and Ling L., "On Porosity of Carbon Aerogels from Sol-Gel Polymerization of Phenolic Novolak and Furfural," *Journal of Porous Materials*, vol. 10, pp. 57–68, 2003.

Zhang S.Q., Huang C.G., Zhou Z.Y., and Li Z., "Investigation of the microwave absorbing properties of carbon Aerogels," *Materials Science and Engineering*, vol. B90, pp. 38–4, 2002.

Zielinski M., Wojcieszak R., Monteverdi S., Mercy M., Bettahar M.M., "Hydrogen storage on nickel catalysts supported on amorphous activated carbon," *Catalysis Communications*, vol. 6, pp.777–783, 2005.

http://dic.academic.ru/dic.nsf/enwiki/489938, 2009.

http://www.cdtwater.com/CDT_Technology_Summary.pdf, August 2008.

http://www.epa.gov/OGWDW/dwh/c-ioc/chromium.html, 30 March 2009.

http://www.lenntech.com/aquatic/metals.htm, 29 March 2009.

http://www.nhm.ac.uk/research-curation/projects/phosphate-recovery/Nordwijkerhout/Arnotdoc, 28 March 2009.

http://www.pollutionissues.com/Ho-Li/Industry.html, 29 March 2009.

http://vienna.bioengr.uic.edu/teaching/che396/sepProj/FinalReport.pdf, 28 March 2009.

Chapter 5

CONCLUSION AND RECOMMENDATIONS

5.1 Conclusions

The objectives of this study were to synthesize CAs, characterize the synthesized CAs and investigate the feasibility of using them for the removal of the chromium metal from aqueous solutions, as well as investigate adsorption isotherm and kinetic behaviour of chromium adsorption on synthesized CAs.

Porous CAs were successfully produced by using acetic acid, sodium carbonate and sodium hydroxide. Based on the XRD analysis it was found that all of the carbon aerogels are amorphous and reveal two peaks; a large peak at $2\theta=23^{o}$ and a small peak at $2\theta=43^{o}$. On a micrometer scale, the surface morphology of CA prepared using acetic acid was different from that of CAs prepared using sodium carbonate and sodium hydroxide. CA prepared using acetic acid showed a smoother surface, which was formed by fused small particles whilst carbon aerogels prepared using sodium carbonate and sodium hydroxide showed an open structure with large interconnected network of pores. According to BET results, CA prepared using acetic acid had the highest surface area (619.26 m^2/g) followed by the one prepared using sodium hydroxide (362.27 m^2/g) then the one prepared using sodium carbonate (209 m^2/g). The FTIR analysis showed that the synthesized CAs are rich in functional groups such as hydroxyl, which is known to strongly bind metal cations in aqueous solution.

The kinetic study showed that the adsorption equilibrium for all of the chromium ion concentrations was reached within 60 min. It was also found that the first order equation deviated considerably from the theoretical calculation data of q_e. It was clearly shown that the pseudo second order equation was more suitable to describe the adsorption of the

chromium ion as established from the correlation coefficient values as well as the predicted value for q_e. The kinetic study showed that the sorption capacity (q_e) values increased with increasing the initial chromium concentrations, and decreased by increasing the adsorbent dosages. It was clearly found that the sorption capacity (q_e) values increased with increasing the initial chromium concentrations, and decreased by increasing the adsorbent dosages. It is found that in a range of high pH levels, precipitation of metal ions resulted in the lower efficiency of adsorption. At lower pH, there is a competition between H^+ and Cr^{+6} for adsorption at the ion-exchangeable sites on the surface of the CAs, which leads to a low removal of chromium.

In this study, the Langmuir isotherm was a better fitting model than Freundlich as the former has a higher linear correlation coefficient than the latter, thus indicating the applicability of monolayer coverage of Cr on the surface of both of the adsorbents.

The removal of chromium ion by the synthesized CAs showed that the CA prepared using acetic acid gave the best removal capacity with 6.44 mg/g, followed by the CA prepared using sodium hydroxide (5.87 mg/g), and the lowest removal capacity was given by the one prepared using sodium carbonate which gave only 4.27 mg/g. These differences in the removal capacity of the CAs were mainly due to differences in micropore volume, surface area and density of the hydroxyl groups.

The main contribution of this thesis is that the CA produced can be utilized by industries that discharge high concentrations of heavy metals in their wastewater. Apart from that, this study also presents the use of CAs as a new method for removing chromium from aqueous solutions.

5.2 Recommendations and Future Work

During the course of executing this study only one temperature degree level was used for the various experimental adsorption tests. However, in order to have better understand on the adsorption behaviour, it is recommended that future study carried out at various temperatures.

Adsorption of chromium ion onto carbon aerogel is viable and technically feasible. Due to the rapid uptake between the metal solution and the adsorbent in this process, adsorption of chromium on a column filled with this carbon aerogel should be considered. Therefore a dynamic adsorption study should be conducted to optimise chromium ion removal from wastewater.

APPENDICES

APPENDIX A

Carbon aerogel preparations ratios:

No.	R/F [mole ratio]	R/C [mole ratio]	R/W [mole ratio]	Type of catalyst	Curing T [^{o}C]	Pyrolysis T [^{o}C]
1	0.5	0.3	0.027	Acetic acid	85±3	800
2	0.5	400	0.125	Sodium carbonate	85±3	800
3	0.5	400	0.125	Sodium hydroxide	85±3	800

Carbon aerogel amounts

No.	R/F [mole ratio]	Resorcinol [g]	Formaldehyde [ml]	Catalyst	Water [ml]
1	0.5	20	10.91	34.67 ml	121.5
2	0.5	20	10.91	0.0182 g	26.16
3	0.5	20	10.91	0.0481 g	26.16

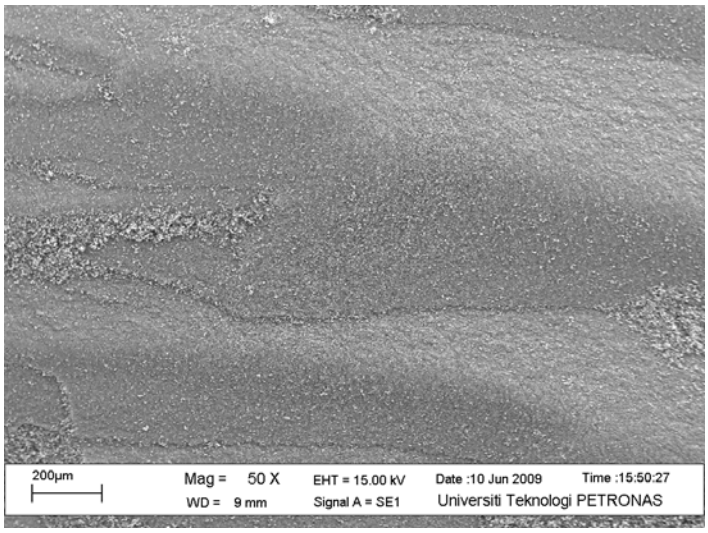

Carbon aerogel prepared using acetic acid

APPENDIX B

(1) Carbon aerogel prepared using acetic acid as a catalyst

⇒ **Effect of solution pH**

Rpm : 120
Volume : 25ml
Adsorbent Amount : 0.05 g

pH2

Time (min)	Run#1	Run#2	$C_{t.}$	C_i-C_t	$((C_i-C_t)/C_i)*100$	$q_t= [(C_i-C_t)/m]$ v (mg/g)	q_e-q_t	$\log(q_e-q_t)$	t/q_t
0	30.0	30.00	30.00	0.00	0.00	0.00	2.95	0.47	0
2	28.72	28.00	28.36	1.63	5.46	0.81	2.13	0.32	2.4412
6	27.90	27.13	27.52	2.47	8.26	1.23	1.71	0.23	4.8422
16	25.78	26.26	26.02	3.97	13.25	1.98	0.96	-0.01	8.0484
60	23.85	25.39	24.62	5.37	17.90	2.68	0.27	-0.56	22.33
120	23.19	24.98	24.08	5.91	19.70	2.95	0.00	#NUM!	40.60

pH5

Time (min)	Run#1	Run#2	$C_{t.}$	C_i-C_t	$((C_i-C_t)/C_i)*100$	$q_t= [(C_i-C_t)/m]$ v (mg/g)	q_e-q_t	$\log(q_e-q_t)$	t/q_t
0	30.00	30.00	30.00	0.00	0.00	0.00	5.21	0.7172	0
2	27.64	27.64	27.64	2.35	7.84	1.17	4.03	0.6061	1.70
6	23.38	23.38	23.38	6.61	22.05	3.30	1.90	0.2800	1.81
16	20.44	19.85	20.14	9.85	32.84	4.92	0.28	-0.5411	3.24
36	19.55	20.14	19.85	10.14	33.82	5.07	0.14	-0.8519	7.09
60	19.05	20.14	19.60	10.39	34.66	5.19	0.01	-1.8514	11.53
120	19.29	19.85	19.57	10.42	34.76	5.21	0.00	#NUM!	23.01

pH6

Time (min)	Run#1	Run#2	$C_{t.}$	C_i-C_t	$((C_i-C_t)/C_i)*100$	$q_t= [(C_i-C_t)/m]$ v (mg/g)	q_e-q_t	$\log(q_e-q_t)$	t/q_t
0	30.00	30.00	30.00	0.00	0.00	0.00	3.27	0.51	0.00
2	27.11	29.11	28.11	1.89	6.30	0.95	2.33	0.37	2.12
6	24.27	28.27	26.27	3.73	12.43	1.86	1.41	0.15	3.22
16	24.63	26.63	25.63	4.37	14.55	2.18	1.09	0.04	7.33
36	22.18	28.18	25.18	4.82	16.06	2.41	0.86	-0.07	14.94
60	22.45	24.45	23.45	6.55	21.83	3.27	0.00	#NUM!	18.32
120	22.99	24.38	23.69	6.31	21.05	3.16	0.11	-0.95	38.01

pH8

Time (min)	Run#1	Run#2	$C_{t.}$	C_i-C_t	$((C_i-C_t)/C_i)*100$	qt= [(Ci-Ct)*m] v (mg/g)	q_e-q_t	$\log(q_e-q_t)$	t/q_t
0	30.00	30.00	30.00	0.00	0.00	0.00	1.57	0.20	0.00
2	27.68	27.97	27.82	2.18	7.26	1.09	0.48	-0.32	1.84
6	28.06	27.96	28.01	1.99	6.63	0.99	0.58	-0.24	6.03
16	26.90	27.32	27.11	2.89	9.63	1.44	0.13	-0.90	11.07
36	26.55	27.17	26.86	3.14	10.47	1.57	0.00	#NUM!	22.93
60	25.35	28.35	26.85	3.15	10.49	1.57	0.00	#NUM!	38.13
120	25.77	27.99	26.88	3.12	10.39	1.56	0.01	-1.93	77.01

⇒ **Effect of initial adsorbent amount**

Rpm : 120
Volume : 25ml
pH : 5

0.015g

Time (min)	Run#1	Run#2	C_t	C_i-C_t	$((C_i-C_t)/C_i)*100$	qt= [(Ci-Ct)/m] v (mg/g)	q_e-q_t	$\log(q_e-q_t)$	t/q_t
0	30.00	30.00	30.00	0.00	0.00	0.00	6.44	0.81	0.00
2	29.03	29.14	29.09	0.91	3.04	1.52	4.92	0.69	1.32
6	27.83	27.92	27.87	2.13	7.09	3.55	2.89	0.46	1.69
16	27.14	27.39	27.26	2.74	9.12	4.56	1.88	0.27	3.51
36	26.98	26.94	26.96	3.04	10.13	5.07	1.37	0.14	7.11
60	26.25	26.50	26.38	3.62	12.08	6.04	0.40	-0.40	9.94
120	25.77	26.50	26.14	3.86	12.87	6.44	0.00	#NUM!	18.64

0.025g

Time (min)	Run#1	Run#2	C_t	C_i-C_t	$((C_i-C_t)/C_i)*100$	$q_t= [(C_i-C_t)*v]/g$ (mg/g)	q_e-q_t	$\log(q_e-q_t)$	t/q_t
0	30.00	30.00	30.00	0.00	0.00	0.00	5.92	0.77	#DIV/0!
2	25.29	26.43	25.86	4.14	13.80	4.14	1.78	0.25	0.48
6	24.36	25.39	24.87	5.13	17.08	5.13	0.80	-0.10	1.17
16	24.10	25.09	24.59	5.41	18.02	5.41	0.52	-0.29	2.96
36	23.96	24.94	24.45	5.55	18.49	5.55	0.38	-0.42	6.49
60	23.70	24.64	24.17	5.83	19.43	5.83	0.10	-1.02	10.29
120	23.51	24.64	24.08	5.92	19.74	5.92	0.00	#NUM!	20.26

0.05g

Time (min)	Run#1	Run#2	C_t	C_i-C_t	$((C_i-C_t)/C_i)*100$	qt= [(Ci-Ct)/m] v (mg/g)	q_e-q_t	$\log(q_e-q_t)$	t/q_t
0	30.00	30.00	30.00	0.00	0.00	0.00	5.20	0.72	#DIV/0!
2	27.65	27.65	27.65	2.35	0.06	1.18	4.02	0.67	1.70
6	23.38	23.38	23.38	6.62	0.17	3.31	1.89	0.40	1.81
16	20.44	19.85	20.15	9.85	0.25	4.93	0.27	-0.04	3.25
36	19.56	20.15	19.85	10.15	0.25	5.07	0.13	-0.11	7.10
60	19.05	20.15	19.60	10.40	0.26	5.20	0.00	#NUM!	11.54
120	19.29	19.85	19.57	10.43	0.26	5.21	-0.01	-0.20	23.01

⇒ **Effect of initial chromium concentration**

Rpm : 120
Volume : 25ml
Adsorbent Amount : 0.05g

5ppm

Time (min)	Run#1	Run#2	$C_{t.}$	C_i-C_t	$((C_i-C_t)/C_i)*100$	qt= [(Ci-Ct)/m] v (mg/g)	q_e-q_t	$\log(q_e-q_t)$	t/q_t
0	5.00	5.00	5.00	0.00	0.00	0.00	1.08	0.03	#DIV/0!
2	4.71	4.06	4.38	0.62	12.34	0.31	0.77	-0.11	6.48
6	3.41	3.50	3.46	1.54	30.86	0.77	0.31	-0.51	7.78
16	3.12	3.38	3.25	1.75	34.98	0.87	0.21	-0.69	18.30
36	3.30	3.17	3.24	1.76	35.29	0.88	0.20	-0.70	40.81
60	3.13	2.96	3.05	1.95	39.09	0.98	0.10	-0.99	61.40
120	2.81	2.87	2.84	2.16	43.21	1.08	0.00	#NUM!	111.08

10ppm

Time (min)	Run#1	Run#2	$C_{t.}$	C_i-C_t	$((C_i-C_t)/C_i)*100$	qt= [(Ci-Ct)/m] v (mg/g)	q_e-q_t	$\log(q_e-q_t)$	t/q_t
0	10.00	10.00	10.00	0.00	0.00	0.00	1.87	0.27	#DIV/0!
2	9.19	9.93	9.56	0.44	4.41	0.22	1.65	0.22	9.07
6	7.49	8.10	7.80	2.20	22.02	1.10	0.77	-0.11	5.45
16	6.86	7.41	7.14	2.86	28.64	1.43	0.44	-0.36	11.17
36	6.35	6.77	6.56	3.44	34.43	1.72	0.15	-0.82	20.91
60	6.20	6.50	6.35	3.65	36.50	1.82	0.05	-1.33	32.88
120	6.01	6.50	6.26	3.74	37.44	1.87	0.00	#NUM!	64.10

3ppm

Time (min)	Run#1	Run#2	C_t	C_i-C_t	$((C_i-C_t)/C_i)*100$	qt= [(Ci-Ct)/m] v (mg/g)	q_e-q_t	$\log(q_e-q_t)$	t/q_t
0	30.00	30.00	30.00	0.00	0.00	0.00	5.21	0.72	#DIV/0!
2	27.65	27.65	27.65	2.35	7.84	1.18	4.04	0.61	1.70
6	23.38	23.38	23.38	6.62	22.06	3.31	1.91	0.28	1.81
16	20.44	19.85	20.15	9.85	32.84	4.93	0.29	-0.54	3.25
36	19.56	20.15	19.85	10.15	33.82	5.07	0.14	-0.85	7.10
60	19.05	20.15	19.60	10.40	34.67	5.20	0.01	-1.84	11.54
120	19.29	19.85	19.57	10.43	34.76	5.21	0.00	#NUM!	23.01

40ppm

Time (min)	Run#1	Run#2	C_t	C_i-C_t	$((C_i-C_t)/C_i)*100$	qt= [(Ci-Ct)/m] v (mg/g)	q_e-q_t	$\log(q_e-q_t)$	t/q_t
0	40.00	40.00	40.00	0.00	0.00	0.00	5.44	0.74	#DIV/0!
2	32.35	34.61	33.48	6.52	16.31	3.26	2.18	0.34	0.61
6	28.78	35.07	31.93	8.07	20.19	4.04	1.40	0.15	1.49
16	26.37	34.84	30.60	9.40	23.49	4.70	0.74	-0.13	3.41
36	26.93	34.04	30.48	9.52	23.80	4.76	0.68	-0.17	7.56
60	24.57	33.67	29.12	10.88	27.19	5.44	0.00	#NUM!	11.03
120	24.22	33.67	28.95	11.05	27.63	5.27	0.17	-0.76	21.71

(2) Carbon aerogel prepared using sodium carbonate as a catalyst

⇒ **Effect of solution pH**

Rpm : 120
Volume : 25ml
Adsorbent Amount : 0.05 g

pH2

Time (min)	Run#1	Run#2	C_t	C_i-C_t	((C_i-C_t)/C_i)*100	qt= [(Ci-Ct)/m] v (mg/g)	q_e-q_t	log(q_e-q_t)	t/q_t
0	30.00	30.00	30.00	0.00	0.00	0.00	3.35	0.52	#DIV/0!
2	28.14	26.09	27.12	2.88	9.61	1.44	1.90	0.28	1.39
6	25.14	24.44	24.79	5.21	17.37	2.61	0.74	-0.13	2.30
16	23.99	23.75	23.87	6.13	20.43	3.06	0.28	-0.55	5.22
36	23.71	23.44	23.58	6.42	21.41	3.21	0.13	-0.87	11.21
60	23.71	23.36	23.53	6.47	21.55	3.23	0.11	-0.95	18.56
120	23.39	23.23	23.31	6.69	22.30	3.35	0.00	#NUM!	35.87

pH5

Time (min)	Run#1	Run#2	C_t	C_i-C_t	((C_i-C_t)/C_i)*100	qt= [(Ci-Ct)/m] v (mg/g)	q_e-q_t	log(q_e-q_t)	t/q_t
0	30.00	30.00	30.00	0.00	0.00	0.00	3.01	0.48	0.00
2	25.10	26.60	25.85	4.15	13.84	2.08	0.93	-0.03	0.96
6	23.52	25.97	24.75	5.25	17.52	2.63	0.38	-0.42	2.28
16	23.45	25.25	24.35	5.65	18.83	2.82	0.18	-0.74	5.67
36	23.15	24.81	23.98	6.02	20.07	3.01	0.00	#NUM!	11.96
60	23.89	24.24	24.06	5.94	19.79	2.97	0.04	-1.42	20.22
120	23.86	24.12	23.99	6.01	20.04	3.01	0.00	#NUM!	39.92

pH6

Time (min)	Run#1	Run#2	$C_{t.}$	C_i-C_t	((C_i-C_t)/C_i)*100	qt= [(Ci-Ct)/m] v (mg/g)	q_e-q_t	log(q_e-q_t)	t/q_t
0	30.00	30.00	30.00	0.00	0.00	0.00	2.30	0.36	0.00
2	28.22	27.60	27.91	2.09	6.97	1.05	1.25	0.10	1.91
6	27.57	26.97	27.27	2.73	9.10	1.36	0.93	-0.03	4.40
16	26.84	26.25	26.54	3.46	11.52	1.73	0.57	-0.24	9.26
36	26.39	25.81	26.10	3.90	13.00	1.95	0.35	-0.46	18.45
60	25.81	25.24	25.53	4.47	14.91	2.24	0.06	-1.20	26.83
120	25.68	25.12	25.40	4.60	15.33	2.30	0.00	#NUM!	52.19

pH8

Time (min)	Run#1	Run#2	$C_{t.}$	C_i-C_t	((C_i-C_t)/C_i)*100	qt= [(Ci-Ct)/m] v (mg/g)	q_e-q_t	log(q_e-q_t)	t/q_t
0	30.00	30.00	30.00	0.00	0.00	0.00	1.05	0.02	0.00
2	29.33	29.41	29.37	0.63	2.10	0.31	0.74	-0.13	6.35
6	29.33	28.57	28.95	1.05	3.50	0.52	0.53	-0.28	11.44
10	29.83	27.51	28.67	1.33	4.43	0.66	0.39	-0.41	15.05
16	28.60	28.46	28.53	1.47	4.90	0.73	0.32	-0.50	21.78
36	28.75	27.60	28.18	1.82	6.08	0.91	0.14	-0.85	39.48
60	28.03	28.05	28.04	1.96	6.55	0.98	0.07	-1.16	61.10
120	27.96	27.83	27.90	2.10	7.01	1.05	0.00	#NUM!	114.11

⇒ **Effect of initial adsorbent amount**

Rpm : 120
Volume : 25ml
pH : 5

0.015g

Time (min)	Run#1	Run#2	C_t	C_i-C_t	$((C_i-C_t)/C_i)*100$	qt= [(Ci-Ct)/m] v (mg/g)	q_e-q_t	$\log(q_e-q_t)$	t/q_t
0	30.00	30.00	30.00	0.00	0.00	0.00	4.27	0.63	0.00
2	28.24	29.03	28.63	1.37	4.55	2.28	1.99	0.30	0.88
6	27.77	28.97	28.37	1.63	5.44	2.72	1.55	0.19	2.21
16	27.95	28.59	28.27	1.73	5.78	2.89	1.38	0.14	5.54
36	28.08	28.21	28.15	1.85	6.18	3.09	1.18	0.07	11.65
60	27.86	28.16	28.01	1.99	6.64	3.32	0.95	-0.02	18.06
120	26.78	28.10	27.44	2.56	8.54	4.27	0.00	#NUM!	28.09

0.025g

Time (min)	Run#1	Run#2	C_t	C_i-C_t	$((C_i-C_t)/C_i)*100$	qt= [(Ci-Ct)/m] v (mg/g)	q_e-q_t	$\log(q_e-q_t)$	t/q_t
0	30.00	30.00	30.00	0.00	0.00	0.00	4.01	0.60	0.00
2	28.12	28.22	28.17	1.83	6.11	1.83	2.18	0.34	1.09
6	27.79	27.52	27.66	2.34	7.81	2.34	1.67	0.22	2.56
16	27.70	27.65	27.68	2.32	7.74	2.32	1.69	0.23	6.89
36	27.57	26.36	26.97	3.03	10.11	3.03	0.98	-0.01	11.87
60	27.21	26.08	26.64	3.36	11.19	3.36	0.66	-0.18	17.87
120	26.41	25.57	25.99	4.01	13.37	4.01	0.00	#NUM!	29.91

0.05g

Time (min)	Run#1	Run#2	C_t	C_i-C_t	((C_i-C_t)/C_i)*100	qt= [(Ci-Ct)/m] v (mg/g)	q_e-q_t	log(q_e-q_t)	t/q_t
0	30.00	30.00	30.00	0.00	0.00	0.00	3.01	0.48	0.00
2	25.10	26.60	25.85	4.15	13.84	2.08	0.93	-0.03	0.96
6	23.52	25.97	24.75	5.25	17.52	2.63	0.38	-0.42	2.28
16	23.45	25.25	24.35	5.65	18.83	2.82	0.18	-0.74	5.67
36	23.15	24.81	23.98	6.02	20.07	3.01	0.00	#NUM!	11.96
60	23.89	24.24	24.06	5.94	19.79	2.97	0.04	-1.42	20.22
120	23.86	24.12	23.99	6.01	20.04	3.01	0.00	#NUM!	39.92

⇒ **Effect of initial chromium concentration**

Rpm : 120
Volume : 25ml
Adsorbent Amount : 0.05 g

5ppm

Time (min)	Run#1	Run#2	C_t	C_i-C_t	((C_i-C_t)/C_i)*100	qt= [(Ci-Ct)/m] v (mg/g)	q_e-q_t	log(q_e-q_t)	t/q_t
0	5.00	5.00	5.00	0.00	0.00	0.00	1.60	0.20	0.00
2	3.42	3.77	3.60	1.40	28.05	0.70	0.90	-0.04	2.85
6	3.56	3.23	3.40	1.60	32.08	0.80	0.80	-0.10	7.48
16	3.56	2.39	2.98	2.02	40.48	1.01	0.59	-0.23	15.88
36	2.75	2.04	2.39	2.61	52.11	1.30	0.30	-0.52	27.28
60	2.24	1.36	1.80	3.20	64.00	1.60	0.00	#NUM!	37.50
120	2.33	1.27	1.80	3.20	64.02	1.60	0.00	#NUM!	74.98

10ppm

Time (min)	Run#1	Run#2	C_t	C_i-C_t	$((C_i-C_t)/C_i)*100$	qt= [(Ci-Ct)/m] v (mg/g)	q_e-q_t	$\log(q_e-q_t)$	t/q_t
0	10.00	10.00	10.00	0.00	0.00	0.00	1.71	0.23	0.00
2	8.18	9.74	8.96	1.04	10.38	0.52	1.19	0.08	3.85
6	7.73	8.47	8.10	1.90	19.03	0.95	0.76	-0.12	6.31
16	7.27	8.10	7.68	2.32	23.15	1.16	0.55	-0.26	13.82
36	6.97	7.15	7.06	2.94	29.42	1.47	0.24	-0.62	24.48
60	6.40	6.76	6.58	3.42	34.22	1.71	0.00	#NUM!	35.07
120	6.21	6.95	6.58	3.42	34.22	1.71	0.00	#NUM!	70.14

30ppm

Time (min)	Run#1	Run#2	C_t	C_i-C_t	$((C_i-C_t)/C_i)*100$	qt= [(Ci-Ct)/m] v (mg/g)	q_e-q_t	$\log(q_e-q_t)$	t/q_t
0	30.00	30.00	30.00	0.00	0.00	0.00	3.01	0.48	0.00
2	25.10	26.60	25.85	4.15	13.84	2.08	0.93	-0.03	0.96
6	23.52	25.97	24.75	5.25	17.52	2.63	0.38	-0.42	2.28
16	23.45	25.25	24.35	5.65	18.83	2.82	0.18	-0.74	5.67
36	23.15	24.81	23.98	6.02	20.07	3.01	0.00	#NUM!	11.96
60	23.89	24.24	24.06	5.94	19.79	2.97	0.04	-1.42	20.22
120	23.86	24.12	23.99	6.01	20.04	3.01	0.00	#NUM!	39.92

40ppm

Time (min)	Run#1	Run#2	C_t	C_i-C_t	$((C_i-C_t)/C_i)*100$	qt= [(Ci-Ct)/m] v (mg/g)	q_e-q_t	$\log(q_e-q_t)$	t/q_t
0	40.00	40.00	40.00	0.00	0.00	0.00	3.43	0.54	0.00
2	39.08	31.08	35.08	4.92	12.31	2.46	0.97	-0.01	0.81
6	37.33	30.63	33.98	6.02	15.05	3.01	0.42	-0.37	1.99
16	36.87	30.00	33.43	6.57	16.42	3.28	0.15	-0.82	4.87
36	35.99	30.78	33.39	6.61	16.53	3.31	0.12	-0.89	10.89
60	34.24	32.34	33.29	6.71	16.78	3.36	0.08	-1.10	17.88
120	33.99	32.28	33.13	6.87	17.17	3.43	0.00	#NUM!	34.94

(3) Carbon aerogel prepared using sodium hydroxide a catalyst

⇒ **Effect of solution pH**

Rpm	:	120
Volume	:	25ml
Adsorbent Amount	:	0.05

pH2

Time (min)	Run#1	Run#2	$C_{t.}$	C_i-C_t	((C_i-C_t)/C_i)*100	qt= [(Ci-Ct)/m] v (mg/g)	q_e-q_t	log(q_e-q_t)	t/q_t
0	30.00	30.00	30.00	0.00	0.00	0.00	4.47	0.65	#DIV/0!
2	29.53	28.14	28.83	1.17	3.89	0.58	3.89	0.59	3.43
6	26.73	25.14	25.93	4.07	13.56	2.03	2.43	0.39	2.95
16	26.34	23.99	25.17	4.83	16.11	2.42	2.05	0.31	6.62
60	20.87	21.71	21.29	8.71	29.05	4.36	0.11	-0.96	13.77
120	20.99	21.13	21.06	8.94	29.79	4.47	0.00	#NUM!	26.86

pH5

Time (min)	Run#1	Run#2	$C_{t.}$	C_i-C_t	((C_i-C_t)/C_i)*100	qt= [(Ci-Ct)/m] v (mg/g)	q_e-q_t	log(q_e-q_t)	t/q_t
0	30.00	30.00	30.00	0.00	0.00	0.00	5.26	0.72	0.00
2	27.73	24.85	26.29	3.71	12.37	1.86	3.40	0.53	1.08
6	24.74	24.75	24.74	5.26	17.52	2.63	2.63	0.42	2.28
16	24.05	24.50	24.28	5.72	19.07	2.86	2.40	0.38	5.59
36	22.30	23.27	22.79	7.21	24.04	3.61	1.65	0.22	9.98
60	16.59	23.00	19.79	10.21	34.02	5.10	0.15	-0.81	11.76
120	16.10	22.87	19.48	10.52	35.05	5.26	0.00	#NUM!	22.82

pH6

Time (min)	Run#1	Run#2	$C_{t.}$	C_i-C_t	$((C_i-C_t)/C_i)*100$	qt= [(Ci-Ct)/m] v (mg/g)	q_e-q_t	$\log(q_e-q_t)$	t/q_t
0	30.00	30.00	30.00	0.00	0.00	0.00	4.57	0.65	0.00
2	29.91	29.15	29.53	0.47	1.58	0.24	4.33	0.63	8.47
6	27.27	26.18	26.73	3.27	10.92	1.64	2.93	0.46	3.66
16	26.54	26.14	26.34	3.66	12.19	1.83	2.74	0.43	8.75
36	25.10	23.59	24.34	5.66	18.86	2.83	1.74	0.22	12.73
60	23.53	18.20	20.87	9.13	30.45	4.57	0.00	#NUM!	13.14
120	23.40	18.58	20.99	9.01	30.02	4.50	0.07	-3.51	26.64

pH8

Time (min)	Run#1	Run#2	$C_{t.}$	C_i-C_t	$((C_i-C_t)/C_i)*100$	qt= [(Ci-Ct)/m] v (mg/g)	q_e-q_t	$\log(q_e-q_t)$	t/q_t
0	30.00	30.00	30.00	0.00	0.00	0.00	0.88	-0.06	0.00
2	28.60	30.55	29.58	0.42	1.41	0.21	0.67	-0.17	9.49
6	28.75	29.22	28.99	1.01	3.38	0.51	0.37	-0.43	11.83
16	29.83	27.31	28.57	1.43	4.77	0.71	0.17	-0.78	22.38
36	28.03	28.93	28.48	1.52	5.07	0.76	0.12	-0.92	47.35
60	29.33	27.53	28.43	1.57	5.24	0.79	0.09	-1.03	76.34
120	29.33	27.14	28.23	1.77	5.88	0.88	0.00	#NUM!	135.96

⇒ **Effect of initial adsorbent amount**

Rpm : 120
Volume : 25ml
pH : 5

0.015g

Time (min)	Run#1	Run#2	C_t	C_i-C_t	((C_i-C_t)/C_i)*100	qt= [(Ci-Ct)/m] v (mg/g)	q_e-q_t	log(q_e-q_t)	t/q_t
0	30.00	30.00	30.00	0.00	0.00	0.00	5.87	0.77	#DIV/0!
2	28.45	29.63	29.04	0.96	3.19	1.60	4.27	0.63	1.25
6	26.47	28.27	27.37	2.63	8.77	4.39	1.48	0.17	1.37
16	26.43	27.27	26.85	3.15	10.51	5.26	0.61	-0.21	3.04
36	26.79	27.15	26.97	3.03	10.11	5.06	0.81	-0.09	7.12
60	26.91	26.78	26.85	3.15	10.51	5.26	0.61	-0.21	11.42
120	26.18	26.78	26.48	3.52	11.74	5.87	0.00	#NUM!	20.45

0.025g

Time (min)	Run#1	Run#2	C_t	C_i-C_t	((C_i-C_t)/C_i)*100	qt= [(Ci-Ct)/m] v (mg/g)	q_e-q_t	log(q_e-q_t)	t/q_t
0	30.00	30.00	30.00	0.00	0.00	0.00	5.40	0.73	#DIV/0!
2	26.54	28.17	27.35	2.65	8.82	2.65	2.75	0.44	0.76
6	26.84	27.88	27.36	2.64	8.81	2.64	2.75	0.44	2.27
16	26.21	27.08	26.64	3.36	11.19	3.36	2.04	0.31	4.77
36	25.56	26.08	25.82	4.18	13.94	4.18	1.21	0.08	8.61
60	24.55	25.09	24.82	5.18	17.27	5.18	0.21	-0.67	11.58
120	24.13	25.08	24.60	5.40	17.98	5.40	0.00	#NUM!	22.24

0.05g

Time (min)	Run#1	Run#2	C_t	C_i-C_t	((C_i-C_t)/C_i)*100	qt= [(Ci-Ct)/m] v (mg/g)	q_e-q_t	log(q_e-q_t)	t/q_t
0	30.00	30.00	30.00	0.00	0.00	0.00	5.26	0.72	#DIV/0!
2	27.73	24.85	26.29	3.71	12.37	1.86	3.40	0.53	1.08
6	24.74	24.75	24.74	5.26	17.52	2.63	2.63	0.42	2.28
16	24.05	24.50	24.28	5.72	19.07	2.86	2.40	0.38	5.59
36	22.30	23.27	22.79	7.21	24.04	3.61	1.65	0.22	9.98
60	16.59	23.00	19.79	10.21	34.02	5.10	0.15	-0.81	11.76
120	16.10	22.87	19.48	10.52	35.05	5.26	0.00	#NUM!	22.82

⇒ **Effect of initial chromium concentration**

Adsorbate	:	Chromium
Temp	:	24C
Rpm	:	120
Volume	:	25ml
Adsorbent Amount	:	0.05

5ppm

Time (min)	Run#1	Run#2	$C_{t.}$	C_i-C_t	$((C_i-C_t)/C_i)*100$	qt= [(Ci-Ct)/m] v (mg/g)	q_e-q_t	$\log(q_e-q_t)$	t/q_t
0	5.00	5.00	5.00	0.00	0.00	0.00	1.34	0.13	0.00
2	3.93	3.60	3.76	1.24	24.71	0.62	0.73	-0.14	3.24
6	3.70	3.40	3.55	1.45	29.07	0.73	0.62	-0.21	8.26
16	3.33	2.39	2.86	2.14	42.78	1.07	0.27	-0.56	14.96
60	3.20	1.79	2.50	2.50	50.09	1.25	0.09	-1.04	47.91
120	2.83	1.79	2.31	2.69	53.78	1.34	0.00	#NUM!	89.26

10ppm

Time (min)	Run#1	Run#2	$C_{t.}$	C_i-C_t	$((C_i-C_t)/C_i)*100$	qt= [(Ci-Ct)/m] v (mg/g)	q_e-q_t	$\log(q_e-q_t)$	t/q_t
0	10.00	10.00	10.00	0.00	0.00	0.00	1.92	0.28	0.00
2	7.61	7.96	7.79	2.21	22.14	1.11	0.81	-0.09	1.81
6	7.01	7.10	7.05	2.95	29.46	1.47	0.44	-0.35	4.07
16	6.91	6.75	6.83	3.17	31.67	1.58	0.33	-0.48	10.10
60	5.94	6.40	6.17	3.83	38.33	1.92	0.00	#NUM!	31.31
120	6.10	6.24	6.17	3.83	38.33	1.92	0.00	#NUM!	62.62

30ppm

Time (min)	Run#1	Run#2	$C_{t.}$	C_i-C_t	$((C_i-C_t)/C_i)*100$	qt= [(Ci-Ct)/m] v (mg/g)	q_e-q_t	$\log(q_e-q_t)$	t/q_t
0	30.00	30.00	30.00	0.00	0.00	0.00	6.01	0.78	0.00
2	27.73	24.85	26.29	3.71	12.37	1.86	4.15	0.62	1.08
6	24.74	24.75	24.74	5.26	17.52	2.63	3.38	0.53	2.28
16	24.05	24.50	24.28	5.72	19.07	2.86	3.15	0.50	5.59
60	18.59	20.00	19.29	10.71	35.69	5.35	0.65	-0.18	11.21
120	17.10	18.87	17.98	12.02	40.05	6.01	0.00	#NUM!	19.97

40ppm

Time (min)	Run#1	Run #2	$C_{t.}$	C_i-C_t	$((C_i-C_t)/C_i)*100$	qt= [(Ci-Ct)/m] v (mg/g)	q_e-q_t	$\log(q_e-q_t)$	t/q_t
0	40.00	40.00	40.00	0.00	0.00	0.00	6.67	0.82	0.00
2	39.59	39.08	39.33	0.67	1.67	0.67	6.00	0.78	3.00
6	39.00	38.33	38.67	1.33	3.34	1.33	5.33	0.73	4.50
16	37.13	36.87	37.00	3.00	7.50	3.00	3.67	0.56	5.33
60	33.01	34.99	34.00	6.00	15.00	6.00	0.67	-0.18	10.00
120	32.43	34.24	33.33	6.67	16.67	6.67	0.00	#NUM!	18.00

Isotherm study data at pH=5, sorbent dosage=0.05g, rpm=120, Temperature=23^{o}C.

(1) Carbon aerogel prepared using acetic acid as a catalyst

5ppm

Time (hr)	Run#1	Run #2	C_t	C_i-C_t	(C_i-C_t)/C_i*100	(C_i-C_t)*v (mg)	qt= [(Ci-Ct)/m] v (mg/g)
0	5.00	5.00	5.00	0.00	0.00	0.00	0.00
1	3.13	2.96	3.05	1.95	39.09	0.05	0.98
2	2.81	2.87	2.84	2.16	43.21	0.05	1.08
24	2.26	2.17	2.21	2.79	55.76	0.07	1.39
48	2.26	1.96	2.11	2.89	57.80	0.07	1.45
72	2.32	1.97	2.14	2.86	57.14	0.07	1.43

10ppm

Time (hr)	Run#1	Run #2	C_t	C_i-C_t	(C_i-C_t)/C_i*100	(C_i-C_t)*v (mg)	qt= [(Ci-Ct)/m] v (mg/g)
0	10.00	10.00	10.00	0.00	0.00	0.00	0.00
1	6.20	6.50	6.35	3.65	36.50	0.09	3.65
2	6.01	6.50	6.26	3.74	37.44	0.09	3.74
24	4.22	5.04	4.63	5.37	53.73	0.13	5.37
48	4.57	4.69	4.63	5.37	53.73	0.13	5.37
72	4.38	4.57	4.47	5.53	55.28	0.14	5.53

30ppm

Time (hr)	Run#1	Run #2	C_t	C_i-C_t	(C_i-C_t)/C_i*100	(C_i-C_t)*v (mg)	qt= [(Ci-Ct)/m] v (mg/g)
0	30.00	30.00	30.00	0.00	0.00	0.00	0.00
1	19.05	20.15	19.60	10.40	34.67	0.26	5.20
2	19.29	19.85	19.57	10.43	34.76	0.26	5.21
24	16.14	16.59	16.36	13.64	45.45	0.34	6.82
48	13.87	14.56	14.22	15.78	52.61	0.39	7.89
72	13.95	14.49	14.22	15.78	52.61	0.39	7.89

40ppm

Time (hr)	Run#1	Run #2	$C_{t.}$	C_i-C_t	$(C_i-C_t)/C_i*100$	$(C_i-C_t)*v$ (mg)	qt= [(Ci-Ct)/m] v (mg/g)
0	40.00	40.00	40.00	0.00	0.00	0.00	0.00
1	24.57	33.67	29.12	10.88	27.19	0.27	10.88
2	24.22	33.67	28.95	11.05	27.63	0.28	11.05
24	23.48	32.56	28.02	11.98	29.94	0.30	11.98
48	23.20	32.15	27.67	12.33	30.82	0.31	12.33
72	22.87	32.24	27.55	12.45	31.12	0.31	12.45

(2) Carbon aerogel prepared using Sodium carbonate as a catalyst

5ppm

Time (hr)	Run#1	Run #2	$C_{t.}$	C_i-C_t	$(C_i-C_t)/C_i*100$	$(C_i-C_t)*v$ (mg)	qt= [(Ci-Ct)/m] v (mg/g)
0	5.00	5.00	5.00	0.00	0.00	0.00	0.00
1	1.69	1.90	1.79	3.21	64.13	0.08	1.60
2	1.93	1.66	1.79	3.21	64.13	0.08	1.60
24	2.30	1.36	1.83	3.17	63.36	0.08	1.58
48	2.24	1.36	1.80	3.20	64.00	0.08	1.60
72	2.33	1.27	1.80	3.20	64.02	0.08	1.60

10ppm

Time (hr)	Run#1	Run #2	$C_{t.}$	C_i-C_t	$(C_i-C_t)/C_i*100$	$(C_i-C_t)*v$ (mg)	qt= [(Ci-Ct)/m] v (mg/g)
0	10.00	10.00	10.00	0.00	0.00	0.00	0.00
1	6.40	6.76	6.58	3.42	34.22	0.09	3.42
2	6.21	6.95	6.58	3.42	34.22	0.09	3.42
24	4.70	5.02	4.86	5.14	51.40	0.13	5.14
48	3.67	4.75	4.21	5.79	57.90	0.14	5.79
72	3.52	4.50	4.01	5.99	59.94	0.15	5.99

30ppm

Time (hr)	Run#1	Run #2	C_t	C_i-C_t	$(C_i-C_t)/C_i*100$	$(C_i-C_t)*v$ (mg)	qt= [(Ci-Ct)/m] v (mg/g)
0	30.00	30.00	30.00	0.00	0.00	0.00	0.00
1	23.89	24.24	24.06	5.94	19.79	0.15	2.97
2	23.86	24.12	23.99	6.01	20.04	0.15	3.01
24	22.96	22.64	22.80	7.21	24.02	0.18	3.60
48	19.13	20.04	19.59	10.41	34.71	0.26	5.21
72	16.99	20.21	18.60	11.40	37.99	0.29	5.70

40ppm

Time (hr)	Run#1	Run #2	C_t	C_i-C_t	$(C_i-C_t)/C_i*100$	$(C_i-C_t)*v$ (mg)	qt= [(Ci-Ct)/m] v (mg/g)
0	40.00	40.00	40.00	0.00	0.00	0.00	0.00
1	34.24	32.34	33.29	6.71	16.78	0.17	6.71
2	33.99	32.28	33.13	6.87	17.17	0.17	6.87
24	32.78	31.27	32.02	7.98	19.94	0.20	7.98
48	30.08	29.27	29.67	10.33	25.82	0.26	10.33
72	29.97	29.13	29.55	10.45	26.12	0.26	10.45

(2) Carbon aerogel prepared using sodium hydroxide as a catalyst

5ppm

Time (hr)	Run#1	Run #2	C_t	C_i-C_t	$(C_i-C_t)/C_i*100$	$(C_i-C_t)*v$ (mg)	qt= [(Ci-Ct)/m] v (mg/g)
0	5.00	5.00	5.00	0.00	0.00	0.00	0.00
1	3.20	1.79	2.50	2.50	50.09	0.06	1.25
2	2.83	1.79	2.31	2.69	53.78	0.07	1.34
24	1.96	1.01	1.48	3.52	70.34	0.09	1.76
48	1.06	0.99	1.02	3.98	79.52	0.10	1.99
72	0.97	1.01	0.99	4.01	80.20	0.10	2.01

10ppm

Time (hr)	Run#1	Run #2	$C_{t.}$	C_i-C_t	(C_i-C_t)/C_i*100	(C_i-C_t)*v (mg)	qt= [(Ci-Ct)/m] v (mg/g)
0	10.00	10.00	10.00	0.00	0.00	0.00	0.00
1	5.94	6.40	6.17	3.83	38.33	0.10	3.83
2	6.10	6.24	6.17	3.83	38.33	0.10	3.83
24	4.48	4.04	4.26	5.74	57.40	0.14	5.74
48	3.20	4.65	3.93	6.07	60.72	0.15	6.07
72	3.69	4.33	4.01	5.99	59.94	0.15	5.99

30ppm

Time (hr)	Run#1	Run #2	$C_{t.}$	C_i-C_t	(C_i-C_t)/C_i*100	(C_i-C_t)*v (mg)	qt= [(Ci-Ct)/m] v (mg/g)
0	30.00	30.00	30.00	0.00	0.00	0.00	0.00
1	18.59	20.00	19.29	10.71	35.69	0.27	5.35
2	17.10	18.87	17.98	12.02	40.05	0.30	6.01
24	16.55	17.04	16.80	13.21	44.02	0.33	6.60
48	14.63	16.54	15.59	14.41	48.05	0.36	7.21
72	14.98	16.50	15.74	14.26	47.54	0.36	7.13

40ppm

Time (hr)	Run#1	Run #2	$C_{t.}$	C_i-C_t	(C_i-C_t)/C_i*100	(C_i-C_t)*v (mg)	qt= [(Ci-Ct)/m] v (mg/g)
0	40.00	40.00	40.00	0.00	0.00	0.00	0.00
1	33.01	34.99	34.00	6.00	15.00	0.15	6.00
2	32.43	34.24	33.33	6.67	16.67	0.17	6.67
24	28.66	29.39	29.02	10.98	27.44	0.27	10.98
48	27.98	29.37	28.67	11.33	28.32	0.28	11.33
72	28.01	29.18	28.60	11.40	28.51	0.29	11.40

APPENDIX C

Materials properties

- **Resorcinol**

Resorcinol crystallizes from benzene as colorless needles which are readily soluble in water, alcohol and ether, but insoluble in chloroform and carbon disulfide. Resorcinol (or resorcin) is a chemical compound from the dihydroxy phenols. It is the 1,3-isomer of benzenediol. It is also known with a variety of other names, including: m-dihydroxybenzene, 1,3-benzenediol, 1,3-dihydroxybenzene, 3-hydroxyphenol, m-hydroquinone, m-benzenediol, and 3-hydroxycyclohexadien-1-one.

Table 3. 1 Resorcinol properties.

Properties	Value
Density and phase	1.28 g/cm3, solid
Solubility in water	1.4 g/ml
Melting point	110 °C
Molar mass	110.1 g/mol
Boiling point	280 °C

- **Formaldehyde**

Formaldehyde is a colorless, strong-smelling gas (H_2CO). The commercial name is either Formalin, or Formol. In water, formaldehyde mostly converts to the hydrate CH_2OH or methanediol. Formaldehyde is an important industrial chemical used to make other chemicals, building materials, and household products.

Table 3. 2 Formaldehyde properties.

Properties	Value
Density and phase	1000 g/·m^3, gas
Solubility in water	1g/ml
Melting point	-117 ^oC
Molar mass	30.03g/·mol
Boiling point	-19.3°C

- **Sodium carbonate**

Sodium carbonate (Na_2CO_3) also known as washing soda or soda ash, is a sodium salt of carbonic acid. It most commonly occurs as a crystalline heptahydrate, which readily effloresces to form a white powder, the monohydrate. It has a cooling alkaline taste, and can be extracted from the ashes of many plants. It is synthetically produced in large quantities from table salt in a process known as the Solvay process. It is used as a relatively strong base in various settings.

Table 3. 3 Sodium carbonate properties.

Properties	Value
Density and phase	2.5 g/cm³, solid
Solubility in water	0.30 g/ ml
Melting point	851 °C
Molar mass	105.99 g/mol
Boiling point	Decomposes

- **Sodium hydroxide**

Sodium hydroxide (NaOH), also known caustic soda, is a caustic metallic base. Sodium hydroxide forms a strong alkaline solution when dissolved in a solvent such as water. It is used in many industries, mostly as a strong chemical base in the manufacture of pulp and paper, textiles, drinking water, soaps and detergents and as a drain cleaner. Pure sodium hydroxide is a white solid. It is very soluble in water with liberation of heat. It also dissolves in ethanol and methanol. It is insoluble in ether and other non-polar solvents.

Table 3. 4 Sodium hydroxide properties.

Properties	Value
Density and phase	2.1 g/cm³, solid
Solubility in water	1.11 g/ml
Melting point	318°C
Molar mass	39.99 g/mol
Boiling point	1390°C

- **Acetic Acid**

Acetic acid (CH_3COOH) is one of the simplest carboxylic acids (the second-simplest, next to formic acid). It is an important chemical reagent and industrial chemical that is used in the production of polyethylene terephthalate mainly used in soft drink bottles. Concentrated acetic acid is corrosive and must therefore be handled with appropriate care, since it can cause skin burns, permanent eye damage, and irritation to the mucous membranes. These burns or blisters may not appear until hours after exposure.

Table 3. 5 Acetic acid properties.

Properties	Value
Density and phase	1.049 g/cm^{-3}, liquid
Solubility in water	Fully miscible
Melting point	16.5 °C
Molar mass	60.05 g/mol
Boiling point	118.1 °C

- **Acetone**

Acetone (CH_3COCH_3), also known as propanone, dimethyl ketone, 2-propanone, propan-2-one and β-ketopropane is a colorless, mobile, flammable liquid. Acetone is miscible with water, ethanol, ether, etc., and itself serves as an important solvent. Acetone is used to make plastic, fibers, drugs, and other chemicals. In addition to being manufactured as a chemical, acetone is also found naturally in the environment, including in small amounts in the human body.

Table 3. 8 Acetone properties.

Properties	Value
Density and phase	0.79 g/cm³, liquid
Solubility in water	miscible
Melting point	−94.9 °C
Molar mass	58.08 g/mol
Boiling point	56.4 °C

- **Sodium dichromate 2-hydrate**

Sodium dichromate 2-hydrate ($Na_2Cr_2.2H_2O$) was provided from HmbG Chemicals Company. It is a toxic and dangerous for the environment material. It molecular weight is 298 g/mol.